



A STOCHASTIC BUCKLEY-LEVERETT MODEL

Simon. J. Carter

Supervisor: Dr John van der Hoek

Thesis submitted for the degree of Doctor of Philosophy
15 June 2010

SCHOOL OF MATHEMATICAL SCIENCES
DISCIPLINE OF APPLIED MATHEMATICS

To Sunrui

Abstract

Even while numerical simulation methods dominate reservoir modeling, the Buckley-Leverett equation provides important insight into the physical processes behind enhanced oil recovery. The interest in a stochastic Buckley-Leverett equation, the subject of this thesis, arises because uncertainty is at the heart of petroleum engineering. Stochastic differential equations, where one modifies a deterministic equation with a stochastic perturbation or where there are stochastic initial conditions, offers one possible way of accounting for this uncertainty. The benefit of examining a stochastic differential equation is that mathematically rigorous results can be obtained concerning the behavior of the solution.

However, the Buckley-Leverett equation belongs to a class of partial differential equations called first order conservation equations. These equations are notoriously difficult to solve because they are non-linear and the solutions frequently involve discontinuities. The fact that the equation is being considered within a stochastic setting adds a further level of complexity. A problem that is already particularly difficult to solve is made even more difficult by introducing a non-deterministic term.

The results of this thesis were obtained by making the fractional flow curve the focus of attention, rather than the relative permeability curves. Reservoir conditions enter the Buckley-Leverett model through the fractional flow function. In order to derive closed form solutions, an analytical expression

for fractional flow is required. In this thesis, emphasis is placed on modeling fractional flow in such a way that most experimental curves can readily be approximated in a straightforward manner, while keeping the problem tractable. Taking this approach, a range of distributional results are obtained concerning the shock front saturation and position over time, breakthrough time, and even recovery efficiency.

Acknowledgement

I would like to thank friends and family that have helped me along the way. To the Department of Applied Mathematics at the University of Adelaide, I greatly value the support I have received over the years. Thank you also to the School of Petroleum Engineering at the University of Adelaide for the helpful advice.

There are two people to whom I am eternally grateful. My supervisor, mentor and friend, Dr John van der Hoek, has given me many, many years of unqualified encouragement. I owe this PhD to you, and without your guidance it never would have happened. Thank you one-thousand times over. To my dear wife Sunrui, I am sorry to have put you through this process. Words cannot express my appreciation or my affection.

Statement of Originality

This work contains no material which has been accepted for the award of any other degree or diploma in any university or other tertiary institution and, to the best of my knowledge and belief, contains no material previously published or written by another person, except where due reference has been made in the text. The work can be divided broadly into two parts. The first, comprising Chapter One to Chapter Four, is largely background information in which the work of others is explained and accounted for. Chapter Five onwards, which details the stochastic approach, is for the most part original material, with the exception of the derivation of the equations for recovery in Chapter Seven and Annex B (which is appropriately attributed to Welge [169]).

I give consent to this copy of my thesis, when deposited in the University Library, being made available for loan and photocopying, subject to the provisions of the Copyright Act 1968. I also give permission for the digital version of my thesis to be made available on the website, via the University's digital research repository, the Library catalogue, the Australasian Digital Thesis Program (ADTP) and also through web search engines.

Simon J. Carter

15 June 2010

Preface

One of the most distinguished contributors to reservoir engineering, Laurie Dake [44], has made a call: *for the revival of fractional flow of water which seems to have ‘gone missing’ since the advent of simulation and, it is argued, is the key to understanding any form of displacement process.*¹ This thesis firmly belongs to the “Dakian” school of thought. From the first line until the last page, the emphasis will be on closed form, analytical solutions. The reader will appreciate that solutions of this kind are significantly more difficult to obtain than numerical ones. This approach is taken in the belief that increased insight is thereby gained into the physical processes behind the model.

¹Dake [43] page 311.

Contents

1	Introduction	1
1.1	The Model	4
1.2	The Continuum Approach	5
1.3	State and Field Equations	8
1.4	Relative Permeability	10
1.5	Buckley-Leverett and Welge	11
1.6	Riemann Problems	13
1.7	Stochastic Buckley-Leverett	15
1.8	What's New?	18
1.9	Conclusion	19
2	The Mathematical Formulation of Multiphase Flow	20
2.1	Darcy's Law	20
2.2	Two Fluids	23
2.3	One Dimensional Displacement	26
2.3.1	Conservation Equations	27
2.3.2	Reducing the differential system to a single PDE	28
2.4	The Buckley-Leverett Equation	30
2.5	Conclusion	31
3	Riemann Problems and the Solution of the Buckley-Leverett Equation	33
3.1	Introduction	34
3.2	Several Examples	36

3.3	Weak Solutions	39
3.4	Rankine-Hugoniot	43
3.5	Entropy Conditions	46
3.6	Solving Buckley-Leverett	48
3.7	Welge Tangent Method	51
3.8	Conclusion	53
4	Relative Permeability	55
4.1	Introduction	56
4.2	Wettability	57
4.3	Permeability: Absolute, Effective and Relative	58
4.4	Laboratory Measurements	62
4.4.1	Steady-state experiments	62
4.4.2	Unsteady-state experiments	63
4.5	Other Factors Influencing Relative Permeability Measurements - of which there are many.	65
4.6	Two-Phase Analytical Models	75
4.6.1	Corey and Brooks	76
4.6.2	MBC	76
4.6.3	Carman-Kozeny	77
4.6.4	Other Models	80
4.7	The Relative Permeability Ratio	80
4.8	Conclusion	82
5	A Stochastic Version	85
5.1	Introduction	85
5.2	Incorporating Uncertainty	87
5.3	The Problem	88
5.3.1	Assumptions	90
5.4	Analytical Solution	91
5.4.1	Distribution of a Function of a Random Variable	93

5.4.2	Expectation	94
5.4.3	Stochastic Velocity and the Position of the Shock Front	96
5.5	Conclusion	99
6	Numerical Results	101
6.1	Introduction	101
6.2	Example Reservoir	101
6.3	Deterministic Calculations	109
6.4	Stochastic Calculations	110
6.4.1	Stochastic Shock Front Saturation	110
6.4.2	Stochastic Velocity	111
6.4.3	Stochastic Position	114
6.5	Extensions and Considerations	115
6.5.1	Non-Linear Semi-Log Relationships	115
6.5.2	Generalized and Weighted Least Squares	117
6.5.3	Uncertainty is an Open Issue	118
6.6	Conclusion	118
7	Break Through and Beyond	120
7.1	Introduction	120
7.2	Breakthrough Time	122
7.3	Average Saturation and Recovery	123
7.4	Production with Uncertainty	127
7.5	Conclusion	132
8	Achievements, Future Research and Concluding Comments	133
8.1	Overview	133
8.2	Limitations and Improvements	134
8.3	Further Work	137
8.4	One Alternative Approach	138
8.5	Concluding Comments	142

A	Properties of the Normal and Log-Normal Distribution	143
B	Geometric Method for Finding Average Saturation	145

Nomenclature

S saturation (without subscripts it refers to the displacing fluid), fraction of pore volume

S_L displacing saturation at end of core/reservoir

S_c connate displacing fluid saturation, fraction of pore volume

\bar{S} average saturation, fraction of pore volume

S^* shock front saturation, fraction of pore volume

k permeability, darcy

k_r relative permeability, fraction

f fractional flow (without subscripts it refers to the displacing fluid), fraction

ϕ porosity, fraction

μ viscosity, cp

ρ density, kg/m³

p pressure, Pa

P oil production, pore volumes

q_{total} total flow rate (oil + water), m³/day

q_i water injection rate, m³/day

Q_i cumulative injected water volume, m³/day

Q_{dim} dimensionless cumulative injected water, in pore volumes

Subscriptes may be added to specify a number of quantities.

1, 2 fluid 1 or 2

d, nd displacing or non-displacing fluid

w, nw wetting or non-wetting fluid

w, o, g water, oil or gas (it is clear by context whether water or wetting fluid is intended)

c connate or critical (depending on the phase)

ir irreducible

dim dimensionless

Note on Subscripts and Connate Saturation

It would simplify matters greatly if the entire thesis could be written in terms of a single set of subscripts, but this is impractical. Generally, fluid 1 versus fluid 2 is used to present the flow equations, wetting fluid versus non-wetting is used when discussing relative permeability, and displacing fluid versus non-displacing is used for Buckley-Leverett. Other subscripts are used to be consistent with original sources, or when formulas only apply to specific phases. Throughout the examination of Buckley-Leverett, the initial saturation corresponds to the connate saturation.

PART I - Background

Chapter 1

Introduction

“In its operational sense the principle of uncertainty, which is usually considered as a limit to the realm of microscopic physics, constitutes the very essence of applied reservoir engineering as a science.” (Morris Muskat)

This chapter will provide an overview of the thesis. The motivation for developing a stochastic formulation of the Buckley-Leverett equation will be examined. Before making an original contribution to the field, it is necessary to first review the work of others, and this will be done. By the end of the chapter, it will be clear what other people have contributed, and the new area of research will be specified.

This thesis is concerned with the Buckley- Leverett equation in a stochastic setting. The Buckley Leverett equation belongs to a class of partial differential equations called first order conservation equations. These equations are difficult to solve because they are non-linear and the solutions frequently involve discontinuities. The fact that the equation is being considered within a stochastic setting adds a further level of complexity.

There are at least two solid reasons for focusing on the Buckley Leverett equation within a stochastic setting. Firstly, such a formulation is relevant to petroleum engineering. Secondly, the problem belongs to a wider class of problems that are of more general interest. Let us consider each of these points in turn.

Touching on the first point, the equation is certainly still relevant. Understanding the solution of the Buckley-Leverett equation provides a wealth of insight into the physical processes behind enhanced oil recovery, even while numerical simulation methods dominate reservoir modeling. The Buckley-Leverett equation represents the simplest statement of material balance for water-drive.¹ Water-drive was one of the first methods of enhanced oil recovery, and in places like the North Sea, water-drive has been central to the recovery process. The Buckley-Leverett equation helps us to understand this mechanism. Furthermore, the model has also proven to be quite accurate, despite its simplicity.

One might question the use of analytical models when numerical simulation dominates reservoir engineering. Analytical models provide information about the structure of solutions. These methods are still, in the words of Bedrikovetsky [14], *important in the initial stages when decisions are being taken on the technology and in optimization studies when the geological and physical studies are inadequate.*² In order to obtain analytical solution, it may be necessary to impose strong assumptions. In comparison, numerical models have the advantage that they are more general, and are able to cover situations and details not possible with analytical methods. However, that is not to suggest numerical simulation is perfect. To quote Carlson [27], *Simulator technology is not nearly as mature as most petroleum engineers would believe.*³

¹as stated in the foreword to Dake [44].

²page xix.

³page 38.

In terms of relevance, a number of recent publications, including Lie and Juanes [108], Terez and Firoozabadi [157], Guzmán and Fayers [69], and Kaasschieter [86], demonstrates that there is still a great deal of interest in the Buckley-Leverett equation in various modified forms. One should not have the idea that the study of two-phase flow in porous media is confined to petroleum engineering. It is also important for the study of soil physics and groundwater hydrology (see Bear [13]). However, in this thesis, the application to reservoir engineering is the focus.

But why should we be interested in a stochastic Buckley Leverett equation? The short answer is, uncertainty is at the heart of petroleum engineering. Flow in porous media, as it applies to areas such as the modeling of groundwater flow or petroleum reservoirs, occurs under conditions of uncertainty. To start with, there are many different scales of rock behavior that must be represented, ranging from core plugs through to large scale faults. The core sample that adequately represents a particularly porous and well interconnected area will be inadequate at representing that part of the reservoir occupied by shale. Not only are there a number of different scales operating within a reservoir, but at each of these scales different physical processes may be prominent. The microscopic level is dominated by capillary forces. At larger scales viscous and gravity forces tend to dominate. While some of the unknown factors can be partially offset by taking many samples and by integrating a range of geological information into the model, it will still only result in a representative picture. Significant uncertainty will always be present.

Stochastic differential equations, where a deterministic equation is modified with a stochastic perturbation, or where stochastic initial conditions are assumed, offers one possible way of accounting for this uncertainty. The great benefit of examining a stochastic differential equation is that mathematically

rigorous results can be obtained concerning issues such as the physical characteristics of shock waves and the asymptotic behavior of solutions. Such results do not have to be taken in isolation, but can be used to calibrate and validate numerical models of the system.

The second major reason for studying our stochastic version of the Buckley Leverett equation is that it provides a tractable but physically relevant problem within an otherwise very difficult class of problems. Over the last thirty years there have been enormous developments in stochastic differential equations. However, these uses have mostly involved second order equations with relatively well behaved solutions. First order conservation equations, in comparison, often have discontinuous solutions and stochastic methods are more difficult to apply to these equations.

In the next few chapters, we will consider the following subjects:

- The Mathematical Formulation of Multiphase Flow.
- Riemann problems and the solution of the Buckley Leverett equation.
- Relative permeability.

This will lay the foundations for posing and solving a stochastic version of the the Buckley-Leverett equation. We will now examine how each of these subjects has evolved.

1.1 The Model

What could be called a standard macroscopic description of multiphase flow can be found in any number of text books: Amyx et al. [8], Collins [34], Bear [13], Peaceman [137], Marle [112], Lake [96], Dake [44] [43], Fanchi [56], Ahmed [2] and Craig [39]. The sense in which there is a *standard* description

comes down to each text taking a common approach with regards to three shared key ingredients. First, the porous medium is treated as a continuum. Second, mass conservation equations are developed. Third, the multiphase extension of Darcy's Equation is employed, which requires relative permeability curves.

Each of the inputs, that is the continuum approach, the multiphase extension of Darcy's equation and relative permeability curves, raises separate questions. Is it appropriate to approximate the medium as a continuum? Is Darcy's equation suitable for describing multiphase flow? Are the relative permeability curves suitable and accurate descriptors of fluid behavior? Despite the limitation, this approach is ubiquitous within the literature concerning multi-phase flow through porous media.

1.2 The Continuum Approach

The effort to develop governing laws for the flow of fluid through porous media, on a par with those typical of other physical sciences, commenced with Darcy. In the approach of Darcy and those that follow, the concept of a continuum is implied simply by *introducing the term porous medium, and by considering flow of fluids through a porous medium.*⁴ The continuum approach focuses on macroscopic behavior that arises from regarding the medium as a statistical average of properties. To quote from Wyckoff and Botset, *the problem should be attacked essentially from a statistical angle which involves the study of large aggregates of pores.*⁵ This is done out of necessity since it is evidently impossible to describe perfectly the infinitely complex internal geometry of the solid or completely describe the motion of the fluid across the pore surface. Nearly all the theories relating to porous me-

⁴Bear [13] page 13.

⁵[174] page 326.

dia result in macroscopic laws that apply to volumes that are large compared to the pores. To describe macroscopic behavior this is usually an acceptable approach, and this kind of treatment is common to all macroscopic physical theories, electric charge being a good example. Indeed, the analogy between fluid flow in porous media and the study of thermal and electrical conduction in metals was recognised early by Richards [142].⁶

In the case of electric charge, there is uniformity due to the enormous number of charged particles in even a cubic centimeter of charged matter, this being in the order of Avagadro's number. In the same volume of porous media there will generally be a relatively small number of pore spaces. Furthermore, these pore spaces are unlikely to be uniform. It is therefore harder to derive an accurate theory that will be true in all situations. While we might achieve an accurate result in a large sample of uniform porous media, it is likely that the description will be poor for a non-homogeneous small sample of material.

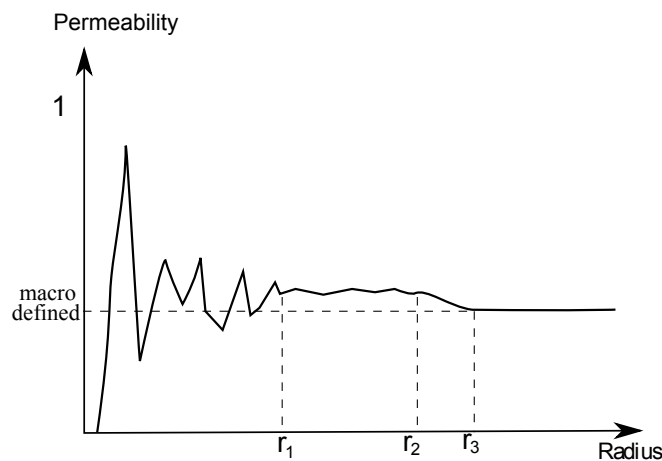


Figure 1.2.1: Macroscopic Quantities

⁶page 319. Richards credits Buckingham [22] and Gardner et al. [63] as early pioneers in the application of potential theory to liquid flow through porous material.

Consider the effort of finding permeability for a rock sample. We isolate a point we wish to consider with a ball of fixed radius r . Around this point the permeability is measured. The situation is illustrated in the Figure 1.2.1.⁷ Below r_1 the volume element is too small for an average to have meaning and permeability varies in an irregular fashion. It will be 0 if the point considered is within the solid and large otherwise. Between r_1 and r_2 permeability has local characteristics. Above r_2 any local behavior is lost as the sample takes on the characteristics of the block. Above r_3 the sample can be said to have macroscopic behavior. To quote from Dullien [53] *the sample is said to be macroscopic whenever the macroscopic pore structure parameter (e.g., k or ϕ) studied is not fluctuating any more when including more material around the initial sampling point, but its variation can be represented by a smooth line. When this smooth line runs parallel to the abscissa, the medium is said to be macroscopically, or statistically averaged.*⁸ This simple example shows that the macroscopic properties are more closely tied to the size and nature of the porous material than are the physical theories that govern examples such as electrostatics or the kinetic theory of gases, even though the general approach is similar.

Alternatives to the continuum assumption do exist. Theories have been devised that attempt to relate the macroscopic properties of porous materials to the statistical properties of the microscopic structure. Burdine et al. [25] attempted to relate the pore size distribution to the macroscopic properties of the material, while Krumbien et al. [94] endeavored to relate the grain size distribution of unconsolidated materials to macroscopic properties. A different approach is to start with the elementary laws of viscous flow in a pore then using statistical methods derive macroscopic laws (Matheron [113]). Similar attempts to derive the macroscopic constitutive equations from the microscopic equations through averaging techniques were made by Hassanizadeh

⁷After Whitaker [170].

⁸page 86.

and Gray [70], and Bachmat and Bear [11]. Yet another approach is to employ statistical mechanics (Sposito [152]). All these approaches have been restricted to simple flow systems. Despite these efforts, the continuum approach is far and away the most universal, and the most general in scope.

1.3 State and Field Equations

Darcy’s law was developed through experimentation. It describes saturated, single phase, seeping flow through a uniform porous column. It is expressed by the formula:

$$u = KA \frac{h_1 - h_2}{L} \quad (1.3.1)$$

where u is rate at which water flows down a vertical sand pack of uniform cross-sectional area A , length is given by L , and where K is the constant of permeability (this material will be covered in Chapter Two). Regarding permeability as a constant rock property, regardless of the nature of the fluid, is a strong assumption. After all, there are a number of forces that might reasonably be expected to influence the flow regime, including gravity, capillary and viscous forces - the last two of which vary with flow rate.

To describe multiphase flow, a large number of equations are required. In the seminal paper by Muskat and Meres [121], they are denoted as a) statements for viscosity and solubility, b) the “laws of flow” for the two phases, c) an empirical relation for the permeabilities of the two phases (as functions of saturation), and d) continuity equations for the two phases. Somehow this complex system of equation must be solved. To achieve this analytically, simplifying assumptions are invariably required.

Multiphase Extension of Darcy’s Law

If two immiscible fluids flow simultaneously through a porous medium then each fluid has its own permeability which depends on the saturation of each

fluid. This was studied by Wyckoff and Botset [174], who gave the first experimental relative permeability curves for the case of gas-liquid mixtures through unconsolidated sands. Since then, a number of studies have supported the assumption that, within limits, relative permeability is independent of viscosity and fluid flow rate, so that saturation can be used as the independent variable.

A giant step forward in petroleum engineering occurred with the publication of *Flow Through Porous Media* by Muskat and Meres [121]. Using the results of Wyckoff and Botset, published in the preceding article of the journal *Physics*, the authors proposed a straightforward extension of Darcy's Law by assigning individual flow equations to each fluid,⁹

$$\bar{v}_g = -\frac{k_g}{\mu_g} \nabla p \quad (1.3.2)$$

$$\bar{v}_l = -\frac{k_l}{\mu_l} \nabla p \quad (1.3.3)$$

where \bar{v}_g and \bar{v}_l are the macroscopic velocities of each phases, k_g and k_l are the permeabilities and μ_g and μ_l are the viscosities of the gas and liquid respectively. As the authors point out, *the effective permeability of a porous medium cannot be constant when the flow of fluid mixtures is involved.*¹⁰ This was alluded to by Richards [142] in 1931, who pointed out that in an unsaturated porous medium (water and air being the gas and liquid) capillary forces would dominate and the moisture content would determine conductivity.¹¹ The permeabilities in Muskat and Meres [121] are based on an empirical relationship for the gas and liquid phases as proposed by Wyckoff and Botset [174], and are functions of saturation divided by porosity (which is given the symbol ρ), so that

⁹Muskat and Meres [121] page 349.

¹⁰page 326.

¹¹page 323.

$$k_g = k_o F_g(\rho) \quad (1.3.4)$$

$$k_l = k_o F_l(\rho) \quad (1.3.5)$$

After applying equations of continuity (conservation) for the gas and liquid, Muskat and Meres obtain two *fundamental equations which will govern the flow of heterogeneous fluids through porous media*¹²:

$$\frac{c}{\mu_g} \nabla \cdot \{p F_g(\rho) \nabla p\} + \frac{s}{\mu_l} \nabla \cdot \{p F_l(\rho) \nabla p\} = \frac{f}{k_o} \frac{\partial}{\partial t} p \{s\rho + c(1 - \rho)\} \quad (1.3.6)$$

$$\nabla \cdot \{F_l(\rho) \nabla p\} = \frac{f \mu_l}{k_o} \frac{\partial p}{\partial t} \quad (1.3.7)$$

where c is the constant of proportionality for the law describing the density γ of the gas ($\gamma = c\rho$), s is the constant of proportionality for the dissolved gas ($S = sp$) and f is the porosity. These *fundamental equations* are quite general, with gas density variable and a portion of the gas dissolved in the liquid. As the authors are the first to point out, *the non-linear and complex character of these equations makes it impossible to treat or solve them generally*.¹³ Muskat and Meres consider linear, radial and spherical flow for the steady state case, that is the right side is set to zero. For a full treatment of the derivation of these equation one should consult the originally paper, or better still Muskat [120].

1.4 Relative Permeability

There is a large body of literature on relative permeability. Wyckoff and Botset, the first researchers to publish relative permeability curves, include results for four different unconsolidated sands, so that the permeability is different in each case. Leverett [105] conducted a laboratory investigation into

¹²page 349.

¹³page 349

a number of factors affecting relative permeability curves. Tests involving changes in viscosity, interfacial tension, liquid density and permeability were undertaken in a number of experiments. Leverett reports that relative permeability is largely independent of the viscosity, but is affected by *pore size distribution, and to the displacement pressure, pressure gradient and water saturation*.¹⁴ Since the publication of Leverett [105], there has been seventy years of continuous research into the factors that influence the form and accuracy of relative permeability curves.

Relative permeability is probably the single most important concept in petroleum engineering. There are two broad areas of interest: methods of measurement and factors that alter the curves. Experimental measurement of relative permeability is broken up into steady state and unsteady-state methods, however there are also methods that utilize capillary pressure and calculations made on the basis of field data. A complete overview of these methods is given in Honarpour et al. [80]. The second area of interest concerns the many various factors that effect the behavior of relative permeability. We will consider relative permeability fully in Chapter Four, which will including a review of the major contributions to the subject. In Chapter Four, the emphasis is less on the exceedingly difficult task of accounting for every factor that can influence relative permeability, and rather more centered on the virtual hopelessness of such an effort. This will lead us to consider a stochastic approach.

1.5 Buckley-Leverett and Welge

Buckley and Leverett [23] examined the waterflooding of a reservoir. In doing this, they considered the simultaneous flow of two fluids that were immiscible, incompressible and possessed constant viscosities. Furthermore,

¹⁴page 169.

they assumed capillary forces were negligible, so that a simplified fractional flow expression could be used. The authors examined the rate of advance of a plane of constant saturation, and in so doing developed the equation that bears their name. In one-dimension:

$$\left. \frac{\partial S}{\partial t} \right|_x + \frac{q_{total}}{\phi A} \left. \frac{\partial f}{\partial x} \right|_t = 0 \quad (1.5.1)$$

where t is time, x is distance along the flow path, S is the saturation of the displacing fluid, q_{total} is the total rate of flow through a uniform section, ϕ is porosity, A is cross-sectional area and f is the fractional flow (or in the words of the authors, *fraction of flowing stream comprising displacing fluid*¹⁵). If capillary forces are assumed to be negligible, the expression for fractional flow takes the form:

$$f = \frac{1}{1 + \frac{k_{rd}\mu_d}{k_d\mu_{nd}}} \quad (1.5.2)$$

where k_{rnd} , k_{rd} , μ_{nd} , and μ_d are the relative permeabilities and viscosities for the non-displacing and displacing fluids respectively. As was the case for Musket and Meres, k_{rnd} and k_{rd} are determined from relative permeability experiments.

Initial conditions are required to make the problem complete. This takes the form of a fixed saturation to the left of the origin (flow entering the reservoir) and saturation to the right of the origin, representing the initial state of the reservoir. While equations (1.3.6) and (1.3.7) could only be solved for the steady state case (using numerical methods), Buckley and Leverett were able to provide a complete solution to the model they proposed.

¹⁵Buckley and Leverett [23] pages 109-110. The equation above differs only marginally from the form in the original paper.

Buckley and Leverett calculated the saturation profile for a waterflood model. In their results, the physically impossible triple valued solution is replaced with a discontinuity. The position of the discontinuity is determined by material balance. The same result can be obtained using the Rankine-Hugoniot condition for a jump discontinuity. This is no surprise, given the Buckley-Leverett equation is a Riemann problem. The derivation of the Buckley-Leverett equation will be covered in Chapter Two, and solution will be examined in Chapter Three.

Welge [169] generalized the results of Buckley and Leverett. The author calculated the average water saturation behind the shock front, which could be used to calculate water saturation at the moment of breakthrough and beyond. This permits the calculation of oil recovery. Welge observed that the correct shock front saturation could be determined by drawing a tangent line from the initial saturation to the fractional flow curve, providing a simple graphical method for solving the system. This will be covered in Chapter Three. Oil recovery is covered in Chapter Seven.

1.6 Riemann Problems

The mathematical modeling of multiphase flow in porous media is still an open issue due to the complexity of the system being studied. Anyone who has examined these problems will be acutely aware of the mathematical difficulties in obtaining solutions for all but the most elementary cases. By making a number of the simplifying assumptions meaningful results can be obtained. In the case of the Buckley-Leverett equation, it is taken that the medium is a continuum, that Darcy's equation can be extended to cover multiphase flow, that the essential fluid properties can be captured by relative permeability curves, and finally it is assumed not merely that capillarity effects are small, but they are sufficiently small that it is possible to drop capillarity effects entirely from the formulation. We leave behind the complex physical world

and focus on a simplified mathematical abstraction. By choosing constant initial condition, the system is reduced to a Riemann Problem. In its simplest form, solve for $u \equiv u(x, t)$:

$$u_t + f(u)_x = 0 \tag{1.6.1}$$

and

$$u(x, 0) = \begin{cases} u_l & \text{if } x < 0 \\ u_r & \text{if } x > 0 \end{cases} \tag{1.6.2}$$

Riemann problems and first order conservation equations are not mentioned specifically in Buckley and Leverett [23]. The authors calculated the shock front saturation using simple material balance. However, the solutions, which may involve shocks or rarefaction waves, are better understood by studying them in terms of first order conservation equations. This subject will be covered in Chapter Three.

The subject of Riemann problems in particular and first order conservation equations in general is far too large to cover in detail here, and our needs are quite small. Courant and Friedrichs [36] provided an exposition of material within the context of gas dynamics gathered from the physics and engineering literature since 1800. A rigorous theory developed from 1950, through papers by Hopf [81], Lax [101] [102] and Oleinik [128]. These references include important contributions concerning entropy conditions, which are relevant to this thesis. These ideas were given a general presentation in Lax [103]. The mathematical theory of first order conservation equations is explored in many standard books on partial differential equations such as John [83], Thomas [160] and Evans [55]. The material is given a self contained treatment by Leveque [104]. The second half of [104] focusses on numerical methods for solving first order conservation equations. The theory of nonlinear first order conservation equations is examined Whitham [171]. The mathematical theory of hyperbolic systems is comprehensively treated by Dafermos [41] and Smoller [151]. The book by Holden and Risebro [77] is one of the more

recent contribution to the subject, providing a systematic and self-contained presentation of the theory of hyperbolic first order conservation equations. These are the main sources that were consulted when writing on this subject.

1.7 Stochastic Buckley-Leverett

There are only a few papers that consider the Buckley Leverett equation in a stochastic setting, of which two in particular stand out. Holden and Risebro [75] examine the scalar Buckley-Leverett equation with a stochastic flux function or stochastic initial data. The flux function is measured at certain points u_1, u_2, \dots, u_N , with piecewise linear interpolation between points. The condition on the flux function $f(s, x)$ is that it is piecewise constant in x and piecewise linear in s . The benefit of this formulation is the solution to the problem is simple, according to the authors. The flux function at each u_i is assumed to belong to a uniform distribution. By examining the slope of the linear interpolation between points, the expectation under certain assumptions on f is calculated. The first assumption ensures f is always convex, while the second assumptions allows some realizations to be non-convex. The authors also examine the case in which the relative permeability is given by a power law, so that the flux function has the form:

$$f(u) = \frac{u^a}{u^a + (1 - u)^a} \quad (1.7.1)$$

Since the parameter a is obtained by curve fitting, *it is natural to regard a as equipped with a certain uncertainty, i.e., to model a as a stochastic parameter.*¹⁶ The parameter a is assumed to be uniformly distributed. Finally, the case in which f is a known continuous function and the initial data is random is also examined.

¹⁶Holden and Risebro [75] page 1482.

Lars Holden [78] considers the Buckley-Leverett equation with a spatially stochastic flux function. As for Holden and Risebro [75], the condition on the flux function $f(s, x)$ is that it is piecewise constant in x and piecewise linear in s . This form of flux function is covered by Holden, Holden and Høegh-Krohn [74], and exploits the observation by Dafermos [41] that *with f piecewise linear and the initial value piecewise constant, then the solution is piecewise constant*.¹⁷ Despite the strong assumptions on f , a more general flux function can be approximated with a function of this form.¹⁸ L. Holden assumes that on each x interval $f(s, x)$ is a stochastic function of s and independent and identically distributed for each x interval. The aim of this work is to derive a convergence result based up the spatial average of $f(s, x)$, which is denoted $\bar{f}(s)$. The definition of the spatial average of $f(s, x)$ is rather specific:¹⁹

- (1) Define $g_1(y, x)$ as the inverse of s by $g_1(f(s, x), x) = s$.
- (2) Define $g_2(y)$ as the spatial average of $g_1(y, x)$ by
$$g_2(y) = \frac{1}{\bar{x}} \int_0^{\bar{x}} g_1(y, x) dx$$
- (3) Define $\bar{f}(s)$ as the inverse of $g_2(y)$ by $\bar{f}(g_2(y)) = y$

Using these definitions, the author shows that for the Buckley-Leverett equation in one dimension with Riemann initial data and spatially stochastic flux function (that is $f(s, x)$ varies randomly with position), the solution is equivalent to the solution of:

$$s(x, t)_t + \bar{f}(s(x, t))_x = 0 \tag{1.7.2}$$

This mathematically confirms the result demonstrated by Tjølsen and Damsleth [163] who used intensive reservoir simulation to show that *a spatially varying relative permeability can be replaced by the average relative permeability*

¹⁷Holden Holden and Høegh-Krohn [74] page 481.

¹⁸L. Holden [78] page 1450.

¹⁹Ibid. page 1447.

*without changing the reservoir performance considerably.*²⁰

When it comes to first order conservation equations in general, few known closed form solutions exist. Burgers' equation is a notable exception to this rule since the Hopf-Cole [81] [33] substitution allows Burgers' equation to be transformed into the heat equation. For this reason there is a reasonably complete understanding of the solution. Burgers' equation is appreciably simpler than the Buckley-Leverett equation since the flux term is $1/2u^2$. The inviscid form of Burgers' equation (the right side term εu_{xx} set to zero) has been examined with Brownian motion initial data by Sinai [149] with numerical results provided in the companion paper by She et al. [146]. Wehr and Xin [166] examine Burgers' equation with initial data of the form $u(x, 0) = u_s + V_x$, where V_x is *white noise*. They obtain a result on the distribution of the shock front, which is known to propagate at the same speed as the unperturbed front. Wehr and Xin [167] also examine the inviscid Burgers' equation for the case of a spatially random flux function. Stochastic scalar first order conservation equations are examined by King [89], and King and Scher [90], where the function $(ds/dt).dx$ is interpreted as a probability density since the integral from 0 to infinity is 1 and $ds/dt > 0$. Holden and Risebro [76] study the scalar first order conservation equation with a noisy nonlinear source, $u_t + f(u)_x = h(u, x, t) + g(u)W(t)$, where $W(t)$ is *white noise*. This paper employ a splitting up method to reduce the stochastic differential equation to two simpler problems, following the method of Bensoussan et al 1990 [16]. In the numerical examples, they examine the Buckley-Leverett equation with a random source.

²⁰Ibid. page 1444.

1.8 What's New?

It is certainly the case that a general form of the flux function does not exist for the Buckley-Leverett equation. The flux function, which is usually referred to as the fractional flow function for this problem, is determined experimentally. That is what makes the problem interesting, and leads to considering the problem from a stochastic perspective. Even without a general form, it is possible to approximate the flux function using piecewise stochastic function. This has been done for example in [75] and [78] and these authors have obtained a number of impressive general mathematical results.

The aim of this thesis is more modest. Although there is not a general form for the flux function that can be used in all cases, fortunately in many (and perhaps even most) cases, the logarithm of the ratio of relative permeabilities have a functional relationship. In this case the flux function may be given the form:

$$f(s) = \frac{1}{1 + \frac{\mu_w}{\mu_o} e^{g(s)+\varepsilon}} \quad (1.8.1)$$

where $e^{g(s)}$ models the ratio of the relative permeability curves and is determined by regression. The error term ε arises from the regression analysis. The log-linear case appears frequently in the literature, and covers a wide range of situations. While this cannot cover all situations, on the positive side, the problem becomes manageable. The function $g(s)$ is not limited to the linear case, and can be generalized. For most examples, the linear case provides an acceptable approximation. We are dealing with probability models, and approximating functions to the n^{th} degree of accuracy is not usually warranted.

The aim of this thesis is to obtain distribution and expected values of a number of quantities of interest, using a stochastic version of (1.8.1). The Buckley-Leverett equation is not just about the shock front saturation. The

spread of the saturation profile, the time to breakthrough and recovery efficiency are also fall out of the solution in what might be called an embarrassment of riches. These quantities will naturally have distributions too.

1.9 Conclusion

The motivation for developing a stochastic formulation of the Buckley Leverett equation should by now be clear. From a modeling level, the reservoir conditions enter the system through the fractional flow expression, which is determined by the relative permeability curves. These curves are experimentally determined and there are many factors that contribute to errors and uncertainty in accurately reflecting reality. This uncertainty, as Muskat points out, *constitutes the very essence of applied reservoir engineering as a science*. It is an issue that will receive considerable attention in the coming chapters.

From the time of Darcy, researchers have struggled to balance what might seem straightforward principles of hydrodynamics with the infinitely complex, multiply connected media through which the flow takes place. In every case, assumption are made so as to obtain results that would be impossible otherwise. The assumptions that underpin Buckley-Leverett theory are quite strong, but the model has stood up well over the last seventy years. This is why, even today, the equation attracts academic interest.

Chapter 2

The Mathematical Formulation of Multiphase Flow

Stigler's Law of Eponymy: "No scientific discovery is named after its original discoverer." (attributed to Robert K. Merton by Stephen Stigler)

In this chapter, we will present the standard model of multiphase flow. We will start with Darcy's law, and from there we will progress to the case of multiphase flow. Taking the assumption of Buckley and Leverett into account, the multiphase equations will be modified to obtain the Buckley-Leverett equation.

2.1 Darcy's Law

Since derivations of multiphase flow rely on an extension of Darcy's equation, it is with Henry Darcy that we will begin. Henry Darcy was employed as a government engineer in the French city of Dijon. In 1856 he conducted a series of experiments on vertical homogeneous sand filters using an apparatus constructed along the lines of the set up described in the following diagram,

which is Plate 24, Figure 3 of Darcy [46].¹ Darcy observed that the rate of flow Q is directly proportional to a) the constant area A and b) the difference in piezometric head $\Delta h = h_1 - h_2$, and inversely proportional to the length of the filter L . The result is Darcy's formula.

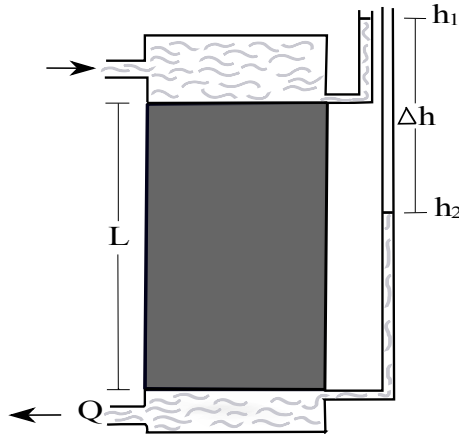


Figure 2.1.1: Darcy's Apparatus

$$Q = \frac{KA\{h_1 - h_2\}}{L} \quad (2.1.1)$$

where K is a constant of proportionality called hydraulic conductivity and the lengths h_1 and h_2 are measured with respect to an arbitrary datum level. The term $(h_1 - h_2)/L$ is called the hydraulic gradient.

Darcy's law was derived under the conditions of homogeneous incompressible flow and was limited to the one-dimensional case. All Darcy's experiments were carried out with water and the cylinder was maintained in the vertical position. Experimentation with different fluids leads to a more general result. Taking into account fluid viscosity, K can be replaced by k/μ , where μ is the viscosity of the fluid.

¹This simplified diagram owes more to Chapman [30] page 126 than Darcy's original paper.

It is important to note² that flow is from higher piezometric head to lower not from higher pressure to lower. Only for horizontal flow can we write

$$Q = -\frac{kA}{\mu} \frac{(p_b - p_a)}{L} \quad (2.1.2)$$

This says that the total discharge Q is equal to the product of the area, permeability and the pressure difference, divided by the product of viscosity and length. The SI units of Q are m^3/s , k is in m^2 , pressure is measured in Pa and the unit of μ are Pascal seconds ($Pa \cdot s$) equal to $1 \text{ kg}/(ms)$. The negative sign is required to account for flow being from high to low pressure. Extending to three dimension is as simple as replacing the derivative of p with the gradient. Upon dividing both sides by area, we obtain:

$$\mathbf{u} = -\frac{k}{\mu} \nabla p \quad (2.1.3)$$

where \mathbf{u} is the vector flow rate per unit area. If we now include body forces \mathbf{B} (in particular gravity), then assuming the porous media is isotropic and the permeability is uniform:

$$\mathbf{u} = -\frac{k}{\mu} (\nabla p - \mathbf{B}) \quad (2.1.4)$$

It is possible to write \mathbf{u} in terms of a velocity potential. Suppose that \mathbf{B} has a potential Ψ , so that $\mathbf{B} = -\nabla\Psi$. If we define the function

$$\Phi = \frac{k}{\mu} (p + \Psi) \quad (2.1.5)$$

then equation (2.1.4) can be written

$$\mathbf{u} = -\nabla\Phi \quad (2.1.6)$$

²Bear [13] page 120

In this form, the analogy between fluid flow in porous media the study of thermal and electrical conduction, recognised by Richards [142], is obvious.

It would seem reasonable to take the viscosity μ as a known, quantifiable constant, certainly in the experimental case of a fluid such as water passing through a sand filter. After all, viscosity is a property of the fluid and since the fluid is homogeneous there is no variability. However, even determining viscosity is not without problems in a real reservoir, since viscosity depends upon pressure and temperature. This problem can be circumvented by assuming that flow is isothermal and pressure drops small, as is done by Buckley and Leverett. Furthermore, when it comes to describing the solid we are far from being in an ideal situation. Even in the most homogeneous of sandstones there is considerable variability. It is therefore normal to question whether it is appropriate to capture the innate, fluid transporting property of a porous solid in the single constant k .

The elegant simplicity of the approach taken by Darcy is that he bypassed the impossibly complex microscopic description of flow through porous media by focusing on the macroscopic level. The media is treated as a continuum and the term k is a statistically averaged property taken over a large number of pores. Finding the macroscopic equivalent of the microscopic behavior turns into an experimental problem. [120] [13] [112] [97] [96] [44]

2.2 Two Fluids

Suppose we have a block of porous material and at one end we inject two fluids, 1 and 2. This was studied by Wyckoff and Botset [174], who gave the first experimental relative permeability curves for the case of gas-liquid mixtures through unconsolidated sands. Muskat and Meres [121] used the work of Wyckoff and Botset to propose a straightforward extension of Darcy's

Law by assigning individual flow equations to each fluid. We will use a more modern notations consistent with the rest of the thesis, although we are in no doubt concerning the origin of this approach in [121]. The two flow equations may be written,

$$\mathbf{u}_1 = -\frac{k_1}{\mu_1}(\nabla \mathbf{p}_1 - \rho_1 \mathbf{g}) \quad (2.2.1)$$

$$\mathbf{u}_2 = -\frac{k_2}{\mu_2}(\nabla \mathbf{p}_2 - \rho_2 \mathbf{g}) \quad (2.2.2)$$

where \mathbf{u}_1 and \mathbf{u}_2 are the filtration velocities of fluid 1 and 2 respectively. The filtration velocity is related to the velocity a tracer would experience moving through the formation by taking account of the effect of saturation and porosity. They are the flow rates per unit of surface area at right angles to the flow direction,³ so they are less than the actual velocity of each fluid. If \mathbf{v}_1 and \mathbf{v}_2 are the true average velocities,

$$\mathbf{u}_1 = \phi S_1 \mathbf{v}_1 \quad (2.2.3)$$

$$\mathbf{u}_2 = \phi S_2 \mathbf{v}_2 \quad (2.2.4)$$

where S_1 and S_2 are the saturations of each fluid and ϕ is the porosity. The driving force is a combination of the fluid pressure gradient and the gravitational gradient. The terms k_1 and k_2 are called the effective permeabilities and depend upon the true permeability and the saturation of the two fluids. Effective permeabilities are difficult to calculate and it is more common to consider the relative permeabilities, given by

$$k_{r1} = \frac{k_1}{k} \quad (2.2.5)$$

$$k_{r2} = \frac{k_2}{k} \quad (2.2.6)$$

The extension of Darcy's law to cover the multiphase case is acceptable provided the effective permeabilities at a given saturation are independent of

³Marle [112] page 31.

pressure gradients.⁴ Apart from Muskat and his fellow-workers, this approach has been validated by a wide range of experimental evidence over the years, including the pioneering work of Hassler et al. [71], Botset [18], and Terwilliger and Yuster [159].

There are many parameters upon which the relative permeabilities might be expected to depend - the fluid densities, viscosities, interfacial tension, wetting angle, pore characteristics and flow rate for example. We will consider this in greater detail in Chapter Four. Experimentally, the most significant variable is the saturation and to good accuracy we can assume that the relative permeabilities are functions of this variable. Figure 2.2.1 gives a typical example of relative permeability curves.

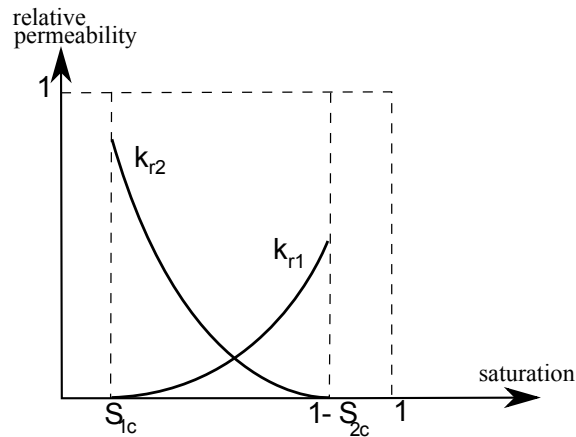


Figure 2.2.1: Typical Relative Permeability Curves

Note the saturation limits. The connate saturation S_{1c} for fluid 1 (assuming fluid 1 is wetting⁵) is the minimum saturation under reservoir conditions, as compared to the irreducible saturation which is the minimum under labora-

⁴Dullien [53] page 255.

⁵The angle between the tangent to the two fluids and the pore surface is less than 90 deg for the wetting fluid and greater than 90 deg for the non-wetting fluid i.e., the wetting fluid has a stronger propensity to cover the surface of the pore space. See Chapter Four.

tory conditions. The maximum saturation is $1 - S_{2c}$, where S_{2c} is the critical saturation of fluid 2 (the minimum saturation fluid 2 will attain). Below S_{1c} there will be no change in the saturation of fluid 1, despite a large change in pressure. Similarly for fluid 2, whatever the change in pressure, S_{2c} will always remain. This means the simultaneous flow of the two fluids will only take place if the saturation of fluid 1 is greater than S_{1c} and less than $1 - S_{2c}$.

Muskat and Meres obtained two fundamental equations that govern the flow of heterogeneous fluids through porous media, already introduced as (1.3.6) and (1.3.7). In deriving these equations, they included the capacity of the gas to dissolve in the liquid, and density was also variable. As the authors are the first to point out, *the non-linear and complex character of these equations makes it impossible to treat or solve them generally.*⁶

2.3 One Dimensional Displacement

In three dimensional two phase flow, there are 15 dependent variables, which would require 15 equations to obtain a complete solution.⁷ If we consider two inviscid, incompressible fluids with constant viscosities, many of the mathematical difficulties vanish. By neglecting capillary forces, relatively simple analytical solutions are even possible. This was first presented by Buckley and Leverett in 1942 [23], who modeled a plane of water (fluid 1) displacing oil (fluid 2). In this section we will follow the elegant presentation of Bear [13], also shown in Marle [112] with minor variations.

We already have equations to describe flow velocity. In one-dimension (which is all we require), using relative permeability the filtration velocities become:

⁶Muskat and Meres [121] page 349.

⁷Bear [13] page 466.

$$u_1 = -\frac{kk_{r1}}{\mu_1} \left(\frac{\partial p_1}{\partial x} - \rho_1 g \cos \alpha \right) \quad (2.3.1)$$

$$u_2 = -\frac{kk_{r2}}{\mu_2} \left(\frac{\partial p_2}{\partial x} - \rho_2 g \cos \alpha \right) \quad (2.3.2)$$

The angle α is measured counterclockwise from the vertical downward direction to the positive x -direction. The displacement of oil by water will be reflected in the change in saturation of the two fluids. Since the porous space is occupied by either oil or water we naturally must have:

$$S_1 + S_2 = 1 \quad (2.3.3)$$

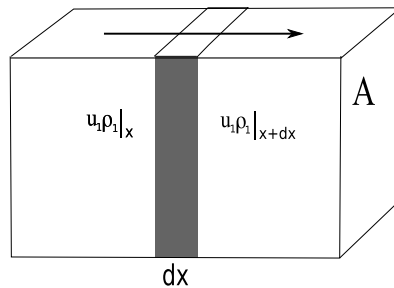
We will assume that capillary pressure is only a function of saturation, so that

$$p_2 - p_1 = p_c(S_1) \quad (2.3.4)$$

Following Buckley and Leverett, the density and viscosity of each fluid is assumed to be constant.

2.3.1 Conservation Equations

We wish to derive an equation that expresses the conservation of mass of a fluid with density ρ flowing through a volume element dx with porosity ϕ and cross section A . The situation can be visualized in the following diagram.



The difference between the *mass flow rate in* and the *mass flow rate out* is equal the *rate of increase of mass in the volume element*. This is expressed as:

$$Au_1\rho_1|_x - Au_1\rho_1|_{x+dx} = \phi A dx \frac{\partial}{\partial t}(\rho_1 S_1) \quad (2.3.5)$$

or

$$u_1\rho_1|_x - \left[u_1\rho_1|_x + \frac{\partial}{\partial x}(u_1\rho_1)dx \right] = \phi dx \frac{\partial}{\partial t}(\rho_1 S_1) \quad (2.3.6)$$

which gives,

$$\frac{\partial}{\partial x}(u_1\rho_1) = -\phi \frac{\partial}{\partial t}(\rho_1 S_1) \quad (2.3.7)$$

Assuming incompressible displacement, so that the density of each fluid is constant, we can write:

$$\frac{\partial u_1}{\partial x} + \phi \frac{\partial S_1}{\partial t} = 0 \quad (2.3.8)$$

and since we could just as well have tracked a volume element of the displaced fluid,

$$\frac{\partial u_2}{\partial x} + \phi \frac{\partial S_2}{\partial t} = 0 \quad (2.3.9)$$

2.3.2 Reducing the differential system to a single PDE

We will now reduce the system to a single partial differential equation. Together with suitable boundary condition, the partial differential equation (PDE) will capture the essential properties of one-dimensional displacement. We commence by taking a new variable

$$u = u_1 + u_2 \quad (2.3.10)$$

the sum of the filtration velocities. We will assume that u is never zero, which will allow us to define the *fraction of flowing stream*⁸ or more commonly the fractional flow of each fluid by,

$$f_1 = \frac{u_1}{u} \quad (2.3.11)$$

⁸Buckley and Leverett [23] pages 109-110.

$$f_2 = 1 - f_1 = \frac{u_2}{u} \quad (2.3.12)$$

These expressions give the portion of each fluid velocity as a fraction of the total. Equations (2.3.1) and (2.3.2) become,

$$\frac{\partial p_1}{\partial x} = \rho g \cos \alpha - \frac{\mu_1 f_1 u}{k k_{r1}} \quad (2.3.13)$$

$$\frac{\partial p_2}{\partial x} = \rho g \cos \alpha - \frac{\mu_2 (1 - f_1) u}{k k_{r2}} \quad (2.3.14)$$

Using these last two equations together with the partial derivative of (2.3.4), we obtain

$$f_1(S_1) = \frac{\frac{\mu_1}{k_{r1}(S_1)} + \frac{k(\rho_1 - \rho_2)g \cos \alpha}{u}}{\frac{\mu_1}{k_{r1}(S_1)} + \frac{\mu_2}{k_{r2}(S_1)}} + \frac{k}{u} \frac{1}{\frac{\mu_1}{k_{r1}(S_1)} + \frac{\mu_2}{\mu_2}} \frac{\partial p_c(S_1)}{\partial x} \quad (2.3.15)$$

so that $f_1(S_1)$ can be expressed as

$$f_1(S_1) = B(S_1) + C(S_1) \frac{\partial S_1}{\partial x} \quad (2.3.16)$$

where

$$B(S_1) = \frac{\frac{\mu_1}{k_{r1}(S_1)} + \frac{k(\rho_1 - \rho_2)g \cos \alpha}{u}}{\frac{\mu_1}{k_{r1}(S_1)} + \frac{\mu_2}{k_{r2}}} \quad (2.3.17)$$

and

$$C(S_1) = \frac{k}{u} \frac{1}{\frac{\mu_1}{k_{r1}(S_1)} + \frac{\mu_2}{\mu_2}} \frac{\partial p_c(S_1)}{\partial S_1} \quad (2.3.18)$$

The functional dependence on $S_1 \equiv S_1(x, t)$, the saturation of fluid 1, is indicated, while all other terms in (2.3.15) to (2.3.18) are constants. Both $B(S_1)$ and $C(S_1)$ are function of S_1 only. Returning to (2.3.8), by replacing u_1 with $f_1(S_1)u$ we obtain,

$$\frac{\partial S_1}{\partial t} + \frac{u}{\phi} \frac{\partial f_1(S_1)}{\partial x} + \frac{f_1(S_1)}{\phi} \frac{\partial u}{\partial x} = 0 \quad (2.3.19)$$

However, adding (2.3.8) and (2.3.9),

$$\phi \frac{\partial S}{\partial t} + \frac{\partial u}{\partial x} = 0 \quad (2.3.20)$$

and since $S = S_1 + S_2 = 1$ this implies,

$$\frac{\partial u}{\partial x} = 0 \quad (2.3.21)$$

This is a consequence of the assumption of incompressibility: u can be a function of time, but not a function of position. Substituting (2.3.16) into (3.4.8) and using (2.3.21),

$$\frac{\partial S_1}{\partial t} + \frac{u}{\phi} \left[\frac{dB(S_1)}{dS_1} \frac{\partial S_1}{\partial x} + \frac{\partial}{\partial x} \left(C(S_1) \frac{\partial S_1}{\partial x} \right) \right] = 0 \quad (2.3.22)$$

This equation⁹ is a function of S_1 only, and its partial derivatives.

2.4 The Buckley-Leverett Equation

We have reduced the system to the partial differential equation (2.3.22), and for given boundary conditions it should be possible to solve this and completely describe saturation for all x and t . Unfortunately, the equation is difficult to solve. The problem can be greatly simplified by neglecting the term representing the effect of capillary forces, which was the approach taken by Buckley and Leverett.

Since equation (2.3.18) includes p_c , the term involving C represents the action of capillary forces. If we assume that capillary forces are negligible then the system reduces to the Buckley Leverett equation:

$$\frac{\partial S_1}{\partial t} + \frac{u}{\phi} \frac{df_1(S_1)}{dS_1} \frac{\partial S_1}{\partial x} = 0 \quad (2.4.1)$$

where

$$f_1(S_1) = \frac{\frac{\mu_1}{k_{r1}(S_1)} + \frac{k(\rho_1 - \rho_2)g \cos \alpha}{u}}{\frac{\mu_1}{k_{r1}(S_1)} + \frac{\mu_2}{k_{r2}(S_1)}} \quad (2.4.2)$$

If we consider only horizontal flow, then the gravity term can be neglected too, and the expression for fractional flow may be written,

$$f_1(S_1) = \frac{1}{1 + \frac{\mu_1 k_{r2}(S_1)}{\mu_2 k_{r1}(S_1)}} \quad (2.4.3)$$

⁹Equation (14.15) of Marle [112] and (9.3.40) of Bear [13].

If we use the fluid injection rate, rather than the total filtration velocity, equation (2.4.1) is simply,

$$\frac{\partial S_1}{\partial t} + \frac{q_i}{\phi A} \frac{df_1(S_1)}{dS_1} \frac{\partial S_1}{\partial x} = 0 \quad (2.4.4)$$

Dimensionless Buckley-Leverett

Simplifying still further, the Buckley-Leverett equation can be expressed in dimensionless form,¹⁰ which may be useful when exploring numerical methods to derive a solution.

$$\frac{\partial S_1}{\partial t_{dim}} + \frac{df_1(S_1)}{dS_1} \frac{\partial S_1}{\partial x_{dim}} = 0 \quad (2.4.5)$$

$$S_1(x_{dim}, 0) = S_r$$

$$S_1(0, t_{dim}) = S_l \quad (2.4.6)$$

The variables x_{dim} and t_{dim} will have values between 0 and 1 and are given by:

$$x_{dim} = \frac{x}{L} \quad (2.4.7)$$

where L is the total length of the one-dimensional porous element and

$$t_{dim} = \int_0^t \frac{u dt}{\phi L} \quad (2.4.8)$$

By making these substitutions, the number of parameters is reduced from four to two.

2.5 Conclusion

In this chapter, the standard model of multiphase flow was derived, starting with Darcy's law and from there progressing to the case of multiphase flow via the extension of Darcy's law proposed by Muskat and Meres. Buckley

¹⁰Dake [44]

and Leverett considered the simultaneous flow of two fluids that were immiscible, incompressible and possessed constant viscosities, while assuming negligible capillary forces. The equation that results from this approach will be examined in the next chapter.

Chapter 3

Riemann Problems and the Solution of the Buckley-Leverett Equation

On two occasions I have been asked, ‘Pray, Mr. Babbage, if you put into the machine wrong figures, will the right answers come out?’ I am not able rightly to apprehend the kind of confusion of ideas that could provoke such a question. (Charles Babbage)

In this chapter the mathematics for solving first order conservation equations will be introduced. We will consider some simple examples to explain the concepts of characteristics, weak solutions, and the Rankine-Hugoniot and other and entropy conditions. The Buckley-Leverett equation is not an isolated problem, rather it is a Riemann problem which can be solved, and interpreted, within the context of first order conservation equations.

3.1 Introduction

Now that we have derived a formula that describes two-phase immiscible flow, we turn to finding the solution. The Buckley–Leverett Equation belongs to the class of partial differential equations known as first order conservation equations. Conservation equations commonly arise in situations where the conservation laws of physics are modeled, such as conservation of mass, momentum or energy.

For the one-dimensional case, consider some material over an interval $[a, b]$ of the independent variable x . If this material is to be conserved, then the rate of change of the material must equal the flux of the material over the boundary. If we do not consider the possibility that the material is either created or destroyed in the region, we have

$$\frac{d}{dt} \int_a^b u(x, t) dx = F_a - F_b \quad (3.1.1)$$

where $u \equiv u(x, t)$ is a conserved quantity such as mass, momentum or energy, and $F \equiv F(u(x, t))$ is the rate of flow or *flux*. If the flux is greater at boundary x_a than at x_b then material will build up in the interval and the rate of change of material u will be positive. Assuming differentiation and integration can be interchanged,

$$\int_a^b (u_t + F_x) dx = 0 \quad (3.1.2)$$

Since the interval is arbitrary, we have

$$u_t + F_x = 0 \quad (3.1.3)$$

More generally a first order conservation equation, as defined for example in Smoller [151],¹ is a quasi-linear system of the form

$$u_t + F_x = 0 \quad (3.1.4)$$

¹page 239.

where $u = (u_1, u_2, \dots, u_n) \in \mathcal{R}^n, n \geq 1$, and $(x, t) \in \mathcal{R} \times \mathcal{R}_+$. It is usually assumed that in some open subset $\Omega \subset \mathcal{R}^n$, the vector valued function F is C^2 , the set of twice-differentiable functions with continuous second derivatives.

A partial differential equation (PDE) of this form, together with piecewise initial constant data having a single discontinuity, is called a Riemann Problem. For example,

$$u_t + F(u)_x = 0 \tag{3.1.5}$$

and

$$u(x, 0) = \begin{cases} u_l & \text{if } x < 0 \\ u_r & \text{if } x > 0 \end{cases} \tag{3.1.6}$$

In the case of the Buckley-Leverett Equation, the flux function $F(u)$ is a non-linear (and non-convex) function of u . Such PDEs are generally difficult to solve exactly and numerical methods are often required to find the approximate solution. In particular, shock formation is associated with non-linear first order conservation equations and this heavily influences the techniques that can be used to find the solution. Although there are significant difficulties in determining exact solutions, a great deal is known about the mathematical structure of the equations, and this can be used to shape the methods employed. It should be noted that these ideas are common knowledge within the study of first order conservation equations and we are not including anything new. The material is covered in a number of text books such as Smoller [151], Dafermos [42], Holden and Risebro [77], Evans [55], Leveque [104], Whitham [171], Taylor [156], Lax [103] and Thomas [160].

3.2 Several Examples

Before examining the Buckley-Leverett Equation, we will begin by studying a simple equation of the form:

$$u_t(x, t) + cu_x(x, t) = 0 \quad (3.2.1)$$

where $c \geq 0$ is a constant. This can be written as the directional derivative $(c, 1) \cdot \nabla u = 0$. Thus, in the direction $[c, 1]$ (or along $x - ct = x_0$) the function $u(x, t)$ is constant. The restriction of u to these lines, called characteristic lines, is given by $u(ct + x_0, t)$. If $u(x, t)$ is a solution of (3.2.1), then it will be constant for all t since,

$$\frac{d}{dt}u(ct + x_0, t) = cu_x(ct + x_0, t) + u_t(ct + x_0, t) = 0 \quad (3.2.2)$$

Therefore, $u(ct + x_0, t) = u(x_0, 0)$, so that

$$u(x, t) = u(x - ct, 0) \quad (3.2.3)$$

$$= \begin{cases} u_l & \text{if } \frac{x}{t} < c \\ u_r & \text{if } \frac{x}{t} > c \end{cases} \quad (3.2.4)$$

Since u is constant for all (x, t) on some set C , the set of characteristics, the value of u along characteristics is determined by the initial values on C .

Consider the problem

$$u_t + c(u)u_x = 0 \quad (3.2.5)$$

$$u(x, 0) = f(x) \quad (3.2.6)$$

so that, in terms of (3.1.5), $c(u) = F'(u)$. The expression $u_t + c(u)u_x$ is the total derivative of u along curves which have slope $\frac{dx}{dt} = c(u(x, t))$ because,

$$\frac{du}{dt} = \frac{\partial u}{\partial t} + \frac{dx}{dt} \frac{\partial u}{\partial x} \quad (3.2.7)$$

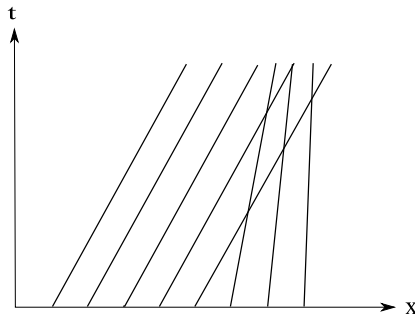


Figure 3.2.1: Multi-valued Solution

We construct the set of characteristics C , which will be straight lines with slopes given by $\frac{dx}{dt} = c(u)$. The value of u along one such curve will be $u = f(x_0)$ and the slope of a characteristic will be $c(f(x_0))$, for some x_0 . The equation of a typical characteristic is then:

$$x = c(f(x_0))t + x_0 \quad (3.2.8)$$

We can construct a whole set of such curves and on each of these, and for some x_0 , we have $u(x, t) = f(x_0)$.

The question arises, can the characteristics overlap? Since the characteristics have different slopes this could occur. This is shown in Figure 3.2.1, which plots the characteristic curves (lines in this case) of time versus distance. On each line u takes constant values. Evidently, at a point where the characteristics overlap u is multi-valued (the fact that this is physically impossible if u is fluid saturation will be dealt with later). This behavior can be described in terms of breaking waves. To visualize this situation, consider Figure 3.2.2,² which shows a possible plot of u against x at three different fixed points in time. We see that $u(x, t)$ move to the right with increasing time. At the moment corresponding to overlapping characteristics, u breaks and then has multiple values for a fixed x and t . Burgers' equation provides a specific

²After Figure 2.1 of Whitham [171]

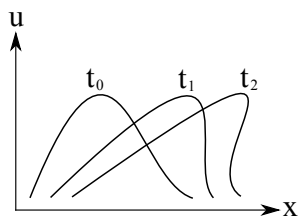


Figure 3.2.2: Breaking Waves

example of this type of behavior.

Burgers' Equation

Suppose that $F(u) = \frac{1}{2}u^2$ so that we have Burgers' equation:

$$u_t + \left(\frac{1}{2}u^2\right)_x = 0 \quad (3.2.9)$$

This is probably the most famous first order conservation equation. Notice that the flux function can also be written $u \cdot u_x$. Breaking will occur when the initial conditions has a discontinuous step with the value of $c(u) = u$ behind the discontinuity greater than the value ahead. Take the case

$$u(x, 0) = f(x) = \begin{cases} u_l & \text{if } x < 0 \\ u_r & \text{if } x > 0 \end{cases}$$

and

$$c(f(x_0)) = \begin{cases} c_l & \text{if } x_0 < 0 \\ c_r & \text{if } x_0 > 0 \end{cases}$$

If $c_l > c_r$ breaking occurs immediately, as shown in Figure 3.2.3.

If the initial step function has $c_l < c_r$ then there is a straightforward continuous solution. Let the characteristics that pass through the origin take all the values between c_l and c_r . This corresponds to a set of lines that fan out from the origin, shown in Figure 3.2.4. When breaking arises the solution is no longer physically acceptable. However, these solutions can be modified by

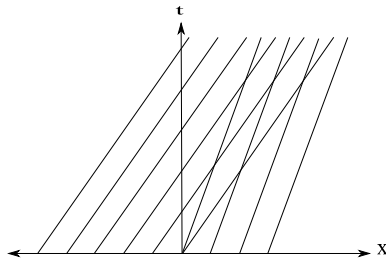


Figure 3.2.3: Immediate Breaking

including discontinuities, and changing the definition of what it means for a solution to be acceptable. This gives rise to the concept of a weak solution, which will be covered in the next section.

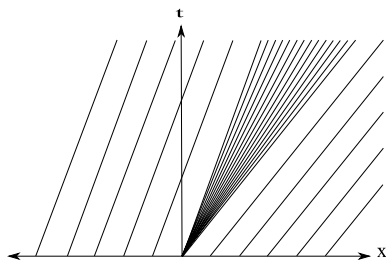


Figure 3.2.4: Wave Fan

3.3 Weak Solutions

It should be clear from the previous discussion and examples that equation (3.1.3) does not always have a smooth solution for all time $t > 0$. The classical idea of a solution requires that the partial derivatives of that solution are continuous. However, consider the following simple first order partial differential equation,

$$u_t + cu_x = 0 \tag{3.3.1}$$

where c is a constant. This equation is satisfied by $u(x, t) = f(x - ct)$. This solution is still valid even if f is not differentiable. The concept of a weak solution is motivated by the need to relax the requirement of differentiability and even continuity for a solution.

We shall start with the initial value problem for a one dimensional scalar first order conservation equation:

$$u_t + F(u)_x = 0 \quad x \in \mathbb{R}, t \geq 0 \quad (3.3.2)$$

$$u(x, 0) = u_0(x) \quad x \in \mathbb{R} \quad (3.3.3)$$

Define the class of test functions as those $\phi \in C_0^1(\mathbb{R}^2)$. Here C_0^1 is the space of functions that are continuously differentiable with compact support in $\mathbb{R} \times [0, \infty]$. This means $\phi = 0$ outside a finite rectangle $[a, b] \times [0, \tau]$. Multiply (3.3.2) by ϕ and integrate:

$$0 = \int_0^\infty \int_{-\infty}^\infty (u_t + F(u)_x) \phi dx dt \quad (3.3.4)$$

$$= \int_a^b [u\phi]_0^\tau - \int_0^\tau u\phi_t dx + \int_0^\tau [F(u)\phi]_a^b - \int_a^b F(u)\phi_x dt \quad (\text{integration by parts}) \quad (3.3.5)$$

On the boundary, $\phi(x, \tau) = \phi(a, t) = \phi(b, t) = 0$, however, $\phi(x, t)$ is not necessarily zero. Using these boundary condition, we obtain the desired result,

$$0 = \int_0^\infty \int_{-\infty}^\infty (u\phi_t + F(u)\phi_x) dx dt + \int_{-\infty}^\infty u_0\phi_0 dx \quad (3.3.6)$$

Definition

A weak solution of (3.3.2) and (3.3.3) is a piecewise continuous function $u(x, t)$ such that (3.3.6) holds for each test function ϕ .

The basic idea is explained neatly in Leveque³: “take the PDE, multiply by a smooth ‘test function’, integrate one or more times over some domain, and

³[104] page 27.

then use integration by parts to move derivatives off the function u and onto the smooth test function. The result is an equation involving fewer derivatives on u , and hence requiring less smoothness.” However, there will now be a greater number of solutions. Selection of an appropriate solution can be justified as the limit of an equations with some dissipation as that dissipation goes to zero. This will be covered in Section 3.5.

Burgers’ Equation Revisited

With the benefit of test functions and weak solutions, we take another look at Burgers’ Equation (3.2.9). There are two cases to consider.

Case One, ($u_l > u_r$)

$$u(x, 0) = \begin{cases} 1 & \text{if } x \leq 0 \\ 0 & \text{if } x > 0 \end{cases} \quad (3.3.7)$$

This has a weak solution shown in Figure 3.3.1 and given by

$$u(x, t) = \begin{cases} 1 & \text{if } x \leq t/2 \\ 0 & \text{if } x > t/2 \end{cases} \quad (3.3.8)$$

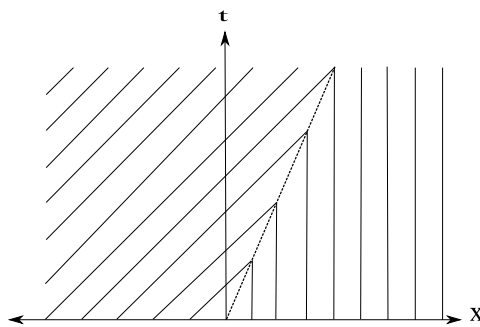


Figure 3.3.1: Case One

Using the definition of weak solutions,

$$\begin{aligned}
& \int_0^\infty \int_{-\infty}^\infty (u\phi_t + F(u)\phi_x) dx dt + \int_{-\infty}^\infty u_0\phi_0 dx \\
= & \int_0^\infty \int_{-\infty}^\infty u\phi_t + \frac{u^2}{2}\phi_x dx dt + \int_{-\infty}^\infty u_0\phi_0 dx \\
= & \int_0^\tau \int_a^{t/2} \phi_t + \frac{1}{2}\phi_x dx dt + \int_a^0 u_0\phi_0 dx \\
= & \int_a^0 \int_0^\tau \phi_t dt dx + \int_0^{\tau/2} \int_{2x}^\tau \phi_t dt dx + \frac{1}{2} \int_0^\tau \int_a^{t/2} \phi_x dx dt + \int_a^0 u_0\phi_0 dx
\end{aligned}$$

Noting that $\phi(x, \tau) = \phi(a, \tau) = 0$, canceling terms and setting $y = 2x$,

$$\begin{aligned}
& = -\frac{1}{2} \int_0^\tau \phi(y/2, y) dy + \frac{1}{2} \int_0^\tau \phi(t/2, 2) dt \\
& = 0
\end{aligned}$$

Case Two, ($u_l < u_r$)

$$u(x, 0) = \begin{cases} 0 & \text{if } x \leq 0 \\ 1 & \text{if } x > 0 \end{cases} \quad (3.3.9)$$

This has a weak solution shown in Figure 3.3.2 and given by,

$$u(x, t) = \begin{cases} 0 & \text{if } x \leq t/2 \\ 1 & \text{if } x > t/2 \end{cases} \quad (3.3.10)$$

This can be shown using an almost identical argument to the previous case. However, this is not the only weak solution. Another valid solution shown in Figure 3.3.3 is,

$$u(x, t) = \begin{cases} 0 & \text{if } x < 0 \\ x/t & \text{if } 0 \leq x \leq t \\ 1 & \text{if } x > t \end{cases} \quad (3.3.11)$$

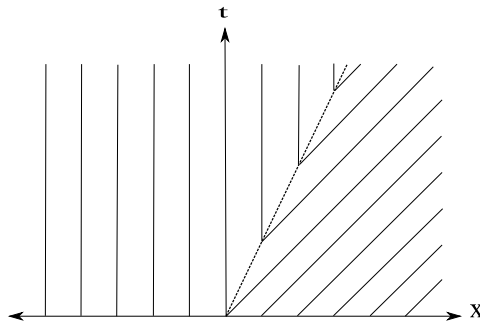


Figure 3.3.2: Case Two

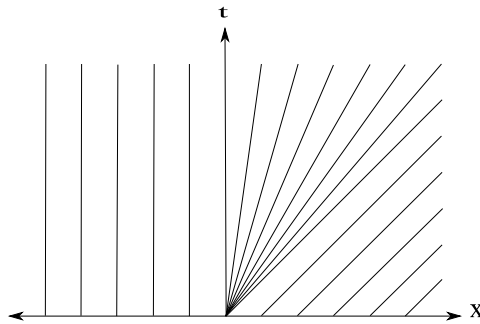


Figure 3.3.3: Another valid solution - wave fan

By weakening the definition of a solution, we have introduced the issue of non-uniqueness. Which of the previous two solutions is the correct one? Weak solutions can take pathological forms which are of no interest to us at all. We are interested in smooth solutions except at a finite number of jump discontinuities. This consideration will ensure that when there is a shock front it is required to be of a particular form in order to be acceptable.

3.4 Rankine-Hugoniot

The Rankine-Hugoniot condition expresses the conservation of the quantity u across a discontinuity. This will be particularly relevant to the Buckley-

Leverett equation, since the solution involves a discontinuity. This condition plays an important role in the study of first order conservation equations and it is covered in virtually any book on the subject. Proofs can be found in Evans [55], Smoller [151], Holden and Risebro [77], Thomas [160] and Leveque [104]. Of these, the last reference is the most elementary.

Theorem 3.4.1. Rankine-Hugoniot. *Suppose there is an open region $A \subset \mathcal{R} \times (0, \infty)$ that is divided into A_l and A_r by a smooth curve C of the form $x_C(t)$. In A , u is a weak solution to the initial value problem*

$$u_t + F(u)_x = 0 \quad (3.4.1)$$

$$u(x, 0) = u_0(x) \quad (3.4.2)$$

Suppose also that u and its first derivatives are uniformly continuous in A_l and A_r . Then,

$$\sigma = \frac{[[F(u)]]}{[[u]]} \quad (3.4.3)$$

where $\sigma = \frac{dx_C}{dt}$, $[[u]] = u_l - u_r$ the jump in u across C and $[[F]] = F_l - F_r$.

Proof:

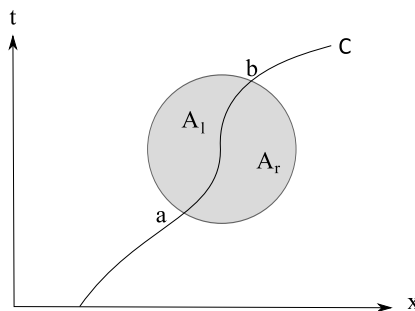


Figure 3.4.1: Jump discontinuity, as described in the theorem.

Let the test function ϕ have compact support in A_l . From the definition of a weak solutions (3.3.2),

$$0 = \int_0^\infty \int_{-\infty}^\infty (u\phi_t + F(u)\phi_x) dx dt \quad (3.4.4)$$

where the second term is omitted because $\phi = 0$ at $t = 0$. Using integration by parts,

$$0 = - \int_0^\infty \int_{-\infty}^\infty (u_t + F(u)_x) \phi dx dt \quad (3.4.5)$$

Since this is true for all test functions with compact support in A_l and u is smooth in A_l , then in A_l

$$u_t + F(u)_x = 0 \quad (3.4.6)$$

This must also be true in A_r . Now take a test function with compact support in A . We are aware that this test function might be non-vanishing along the curve $x_C(t)$, and so we may only deduce that

$$0 = \int_0^\infty \int_{-\infty}^\infty (u\phi_t + F(u)\phi_x) dx dt = \int \int_{A_l} (u\phi_t + F(u)\phi_x) dx dt + \int \int_{A_r} (u\phi_t + F(u)\phi_x) dx dt \quad (3.4.7)$$

In light of (3.4.6) and since u smooth in A_l and A_r , we can we make use of Green's Theorem⁴ to obtain:

$$0 = \int \int_{A_l} (u\phi_t + F(u)\phi_x) dx dt + \int \int_{A_r} (u\phi_t + F(u)\phi_x) dx dt \quad (3.4.8)$$

$$= \int_{\partial A_l} \phi(-udx + F(u)) dt + \int_{\partial A_r} \phi(-udx + F(u)) dt \quad (3.4.9)$$

The test function ϕ vanishes on the boundary of A , therefore we only need concern ourself with integrating along C when we evaluate (3.4.9). Specify u along the curve C by:

⁴Or alternatively the divergence theorem, following Smoller [151] page 248.

$$u_l = \lim_{(x,t) \rightarrow C} u(x,t), \quad (x,t) \in A_l \quad (3.4.10)$$

$$u_r = \lim_{(x,t) \rightarrow C} u(x,t), \quad (x,t) \in A_r \quad (3.4.11)$$

We may now write (3.4.9) as,

$$\int_a^b \phi[-u_l dx + F(u_l) dt] + \int_b^a \phi[-u_r dx + F(u_r) dt] = 0 \quad (3.4.12)$$

and by reversing the integrand of the second term (the line integrals in A_l and A_r pass along C in opposite directions),

$$\int_a^b \phi[-(u_l - u_r) dx + (F(u_l) - F(u_r)) dt] = 0 \quad (3.4.13)$$

We can replace dx with $\frac{dx_C}{dt} dt$, then

$$\int_a^b \phi[-(u_l - u_r) \frac{dx_C}{dt} + (F(u_l) - F(u_r))] dt = 0 \quad (3.4.14)$$

This is true for all test functions ϕ , therefore

$$-(u_l - u_r) \frac{dx_C}{dt} + F(u_l) - F(u_r) = 0 \quad (3.4.15)$$

and the result follows. **End of proof.**

3.5 Entropy Conditions

The Rankine-Hugoniot must be satisfied by a weak solution across a discontinuity. However, these may include weak solutions that are not physically acceptable. We will need to consider additional conditions that pick out the correct solution. These are usually referred to as entropy conditions. The versions included in this section are based on the requirement that characteristics must go into a shock as time advances, because when characteristics come out of the shock the solution is unstable to perturbations. *Either smearing out the initial profile a little, or adding some viscosity to the system, will*

cause this to be replaced by a rarefaction wave of characteristics.⁵

Lax E-condition⁶

A discontinuity propagating with speed $\sigma = \frac{[[F]]}{[[u]]}$ satisfies the entropy condition if $F'(u_l) > \sigma > F'(u_r)$.

The following condition is due to Oleinik [128]. This version applies to all discontinuities, and is true for both convex and nonconvex scalar functions F .

Oleinik E-condition

$u(x,t)$ is the entropy solution if all discontinuities have the property that:

$$\frac{F(u) - F(u_l)}{u - u_l} \geq \sigma \geq \frac{F(u) - F(u_r)}{u - u_r}$$

for all u between u_l and u_r .

These conditions are found in Leveque [104] and Thomas [160] and in both cases are stated without proof. The interested reader is referred to Smoller [151] for a full treatment of this subject. There are a great many other entropy conditions or functions. The underlying motivation and principles for these conditions often is not straightforward. The reader may prefer to gain insight into these ideas by instead consulting Holden and Risebro [77] section 2.1 where the viscous regulation condition is explained in a straightforward but rigorous manner. In short, if the scalar first order conservation equation $u_t + f(u)_t = 0$ is replaced by,

$$u_t^\varepsilon + f(u^\varepsilon)_t = \varepsilon u_{xx}^\varepsilon \tag{3.5.1}$$

then as $\varepsilon \rightarrow 0$ (that is the diffusion is small) we would expect the solution to converge to the solution of the first order conservation equation. If $u(x,t)$

⁵Leveque [104] page 36.

⁶Lax [102].

has a solution consisting of constant states on either side of a discontinuity, then it satisfies a *traveling wave entropy condition*⁷ if it is the pointwise limit almost everywhere of some $u^\varepsilon(x, t) = U((x - st)/\varepsilon)$ as $\varepsilon \rightarrow 0$. It turns out that the traveling wave entropy condition is then equivalent to,

$$s|k - u_l| < \text{sign}(k - u_l)(f(k) - f(u_l)) \quad (3.5.2)$$

for all k strictly between u_l and u_r . This is given as equation (2.9) of Holden and Risebro [77].

3.6 Solving Buckley-Leverett

Recall from (2.4.1) that the Buckley-Leverett equation and initial conditions are given by:

$$\frac{\partial S}{\partial t} + \frac{u}{\phi} \frac{df}{dS} \frac{\partial S}{\partial x} = 0$$

$$S(x, 0) = S_r$$

$$S(0, t) = S_l$$

were S is the saturation of the displacing fluid. Consider this problem in the context of what we know about first order conservation equations. This is Riemann problem, so the method of characteristics together with the Rankine-Hugoniot condition and an appropriate entropy condition should be up to the task of determining the solution. We need to specify the fractional flow term f of the displacing fluid. This is usually determined experimentally and is found to have the form shown in Figure 3.6.1.

Evidently, the flux function is not convex. When the flux function is convex or concave, the solution is either a shock or a rarefaction wave. When it is

⁷[77] page xx

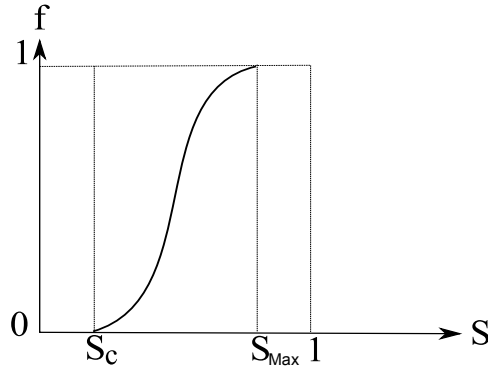


Figure 3.6.1: Flux Function

not convex, the solution may involve both shocks and rarefaction waves.

Characteristics, which are lines of fixed saturation, are given by:

$$\frac{dx}{dt} = \frac{u}{\phi} \frac{\partial f(S(x(t), t))}{\partial S(x(t), t)} \quad (3.6.1)$$

because, by the Buckley-Leverett equation,

$$\frac{\partial S(x(t), t)}{\partial t} + \frac{u}{\phi} \frac{df(S(x(t), t))}{dx} = 0 \quad (3.6.2)$$

$$\frac{\partial S(x(t), t)}{\partial t} + \frac{u}{\phi} \frac{\partial f(S(x(t), t))}{\partial S(x(t), t)} \frac{\partial S(x(t), t)}{\partial x} = 0 \quad (3.6.3)$$

$$\frac{\partial S(x(t), t)}{\partial t} + \frac{dx}{dt} \frac{\partial S(x(t), t)}{\partial x} = 0 \quad (3.6.4)$$

$$\frac{dS(x(t), t)}{dt} = 0 \quad (3.6.5)$$

That is, the saturation is constant along lines given by (3.6.1).

Suppose at some point (x_0, t_0) the water saturation is $S(x(t), t) = S$. Then at time and position given by:

$$t = t_0 + \Delta t \quad (3.6.6)$$

$$x = \Delta t \frac{u}{\phi} \frac{\partial f(S(x(t), t))}{\partial S(x(t), t)} \Big|_S + x_0 \quad (3.6.7)$$

the saturation will also be S . The velocity of a fixed plane of water with saturation S is therefore,

$$v(S) = \frac{u}{\phi} \frac{\partial f(S(x(t), t))}{\partial S(x(t), t)} \Big|_S \quad (3.6.8)$$

Consequently, the saturation profile is determined by (3.6.8). The displacement profile will be given by $v(S)$ turned sideways. A typical example is shown in Figure 3.6.2 at some fixed point in time. Quantitatively, the velocity of saturation values close to $S_r = S_c$ and $S_l = S_{Max}$ will be low, and higher for middle saturations where $f'(S(x(t), t))$ is greatest.

However, the saturation profile given by Figure 3.6.2 is not a physically acceptable solution, because at some values of x three saturation values co-exist. This can be fixed by discarding the assumption of the continuity of variables and introducing a discontinuity that results in a weak solution, which was the approach of Buckley and Leverett. Finding the correct location of the shock to replace the triple valued solution is achieved through a conservation argument. The saturation profile for the triple valued solution, found using the method of characteristics, and the saturation value using a discontinuity, must both satisfy the condition of material balance for the injected fluid. The Rankine-Hugoniot condition ensures material conservation.

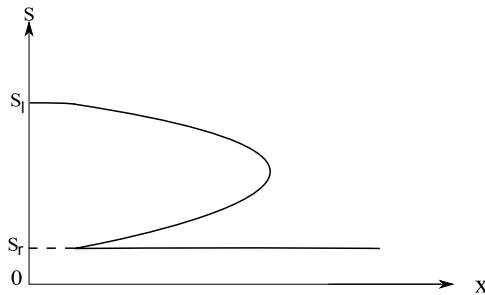


Figure 3.6.2: Uncorrected Profile

3.7 Welge Tangent Method

If S^+ is the saturation ahead of the shock and S^- is the water saturation behind the shock (the origin side), we can use Rankine-Hugoniot to find the shock velocity.

$$\sigma = \frac{u}{\phi} \left(\frac{f(S^+) - f(S^-)}{S^+ - S^-} \right) \quad (3.7.1)$$

This leads to a graphical interpretation, the *Welge Tangent Method*, for determining the location of the shock front. If we are including a shock front

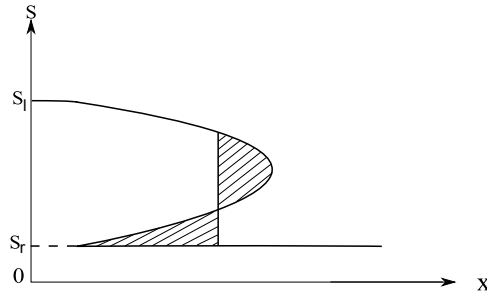


Figure 3.7.1: Material Balance

in the solution then there must be a point that will divide the continuous region behind the front and the region where the shock begins. Denote this by S^* . Using the method of characteristics, we have already determined that the velocity of the saturation front, for the triple valued solution, is given by $\frac{u}{\phi} \frac{df}{dS}$. The velocity of the shock front is given by (3.7.1). If we equate these two velocities at S^* we obtain the equation:

$$\left. \frac{df}{dS} \right|_{S^*} = \frac{f(S_r) - f(S^*)}{S_r - S^*} \quad (3.7.2)$$

where S^+ has been replaced by S_r , which is the initial downstream saturation before that waterflood takes place, and the term $\frac{u}{\phi}$ has been cancelled from both sides. The slope of a line passing through $(S^*, f(S^*))$ and also $(S_r, 0)$

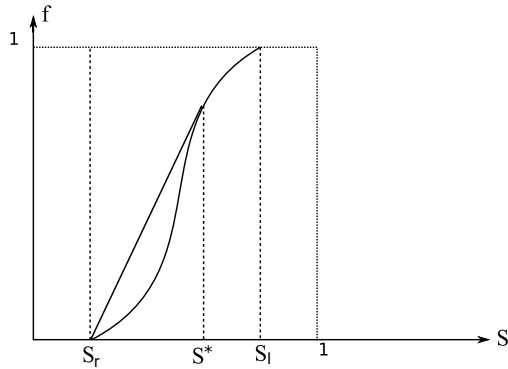


Figure 3.7.2: Welge Tangent Method

is given by

$$m = \frac{f(S^*) - f(S_r)}{S^* - S_r} \quad (3.7.3)$$

which is the same as (3.7.2). Therefore, if we draw a tangent line from $(S_r, 0)$ (the initial saturation value in the reservoir) to the curve $f(S)$, then the point of tangency gives the shock front saturation value S^* . This is the saturation at which the net difference in area between the mathematical and the physical solution is zero. This requires that the material balance is preserved, along the lines of Figure 3.7.1.

That this discontinuity is also admissible can be understood by considering Figure 3.7.2. If the shock was connected at some saturation less than S^* we would have a physically impossible triple valued solution. If the shock saturation was at some point above S^* then (3.5.2), (or indeed the Oleinik E-condition), is violated. This can be seen by drawing a line from S_l to a point on f with a saturation greater than S^* . This line has a slope greater than the slope of any arc between S^* and S_l . The shock front saturation given by Welge satisfies both Rankine-Hugoniot and the entropy condition, and is therefore acceptable.

The solution can be visualized in terms of characteristics in $x-t$ space, shown in Figure 3.7.3. The saturation is S_l on the t -axis and decreases smoothly

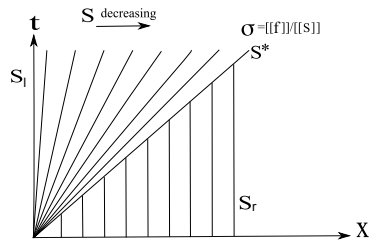


Figure 3.7.3: The characteristics of the solution.

in a rarefaction wave to the shock front saturation S^* , where the speed of the discontinuity is given by the Rankine-Hugoniot condition. To the right of the discontinuity, the initial right-side saturation of S_r (original reservoir state) remains constant for all x until the arrival of the shock front, at which point it abruptly changes.

Important Note

We will always assume that the initial saturation of the displacing fluid (the right state) is the same as the connate saturation. The situation of the initial saturation being equal to the connate saturation is how the problem is usually presented. If they are different the calculations can be readily modified.

3.8 Conclusion

The purpose of this chapter was to firmly place the Buckley-Leverett equation within the context of first order conservation equations. The mathematics for solving first order conservation equations was covered, in particular the concepts of characteristics, weak solutions, and the Rankine-Hugoniot and entropy conditions were examined. The Buckley-Leverett equation was then solved in a deterministic setting for Riemann initial condition. The form of the flux function was only examined in a cursory manner and needs to be

considered in greater detail. More attention will be given to this deficiency in the next chapter.

Chapter 4

Relative Permeability

“The ease with which a phase can flow can therefore be visualised as depending on two factors: the size and number of pores which are occupied by the phase and the probability that those pores are hydraulically interconnected” - M. R. Wyllie¹

Relative permeability, via the fractional flow equation, is the mechanism through which reservoir conditions enter the Buckley-Leverett model. The purpose of this chapter is to justify a stochastic approach to relative permeability and fractional flow. In this chapter we will:

- account for the many factors known to influence relative permeability, together with the inherent errors and uncertainty;
- discuss some of the more commonly used analytical expressions used to describe relative permeability; and,
- by the end of the chapter, be in a position to propose a probabilistic model.

¹Petroleum Production Handbook [61] vol II Ch. 24, page 3

4.1 Introduction

Since the concept of relative permeability was introduced by Wyckoff and Botset [174], there has been an almost continuous investigation into the measurement and properties of relative permeability. The number of publications has even been described as excessive.² We will not attempt to review every paper written on this subject, since that would be a thesis in itself or a book such as Honarpour et al. [80]. However, we need to have a comprehensive understanding of the factors that influence relative permeability curves before a stochastic version of Buckley-Leverett is proposed.

We will cover the factors that affect relative permeability, and review the significant papers that have contributed to our understanding of this subject. While these investigations have attempted to describe in minute detail the many and varied factors in order to describe flow behavior with great accuracy, here the emphasis will be placed more on the variation and errors. It is the inherent uncertainty in the system that provides the motivation for considering a stochastic formulation.

Darcy's law was developed for a porous medium fully saturated by a single, homogeneous fluid. As has already been seen, Darcy's law can be generalized to handle the simultaneous flow of several fluid. This is done by introducing the concept of effective permeability, and the closely related and more useful concept of relative permeability. Relative permeability is the single most important element of petroleum engineering. Within the Buckley-Leverett model, properties of the fluids and the porous medium are captured by the fractional flow equation. Since fractional flow is a function of relative permeability, the ability of the model to capture reality is inseparably tied to the choice and accuracy of the relative permeability curves.

²Marle [112] page 32

4.2 Wettability

Before discussing relative permeability, it is necessary to first understand wettability. Several different definitions of wettability exist. Dandekar [45] includes seven versions of this concept. Wettability may be defined as *the relative adhesion of two fluids to a solid surface*³. Whatever the differences, all texts treat wettability as a fundamental concept which strongly influences relative permeability. According to Dandekar, of all the factors that affect relative permeability, wettability is the most dominant.⁴ Quoting from Honarpour et al. [80]: *It is the main factor responsible for the microscopic fluid distribution in porous media and it determines to a great extent the amount of residual oil saturation and the ability of a particular phase to flow.*⁵

Contact Angle

The relative spreading of the two fluids on the rock surface can be quantified using adhesion tension, A_T , and Young's equation.⁶ In Figure 4.2.1, σ_{SO} , σ_{SW} and σ_{WO} are respectively the interfacial tension between the surface and oil, between the surface and water and between the water and oil. In terms of force balance,

$$A_T = \sigma_{SO} - \sigma_{SW} \quad (4.2.1)$$

so that

$$\cos \alpha = \frac{\sigma_{SO} - \sigma_{SW}}{\sigma_{WO}} \quad (4.2.2)$$

³Tiab and Donaldson [161], page 360

⁴Dandekar [45], page 223.

⁵page 54.

⁶This material is drawn from Amyx[8], Tiab and Donaldson [161], Christiansen [32] and Dandekar [45]. The figure appears in all texts.

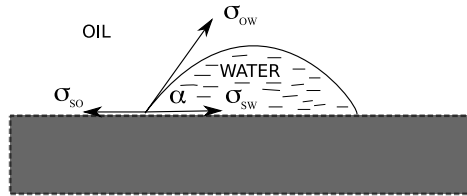


Figure 4.2.1: Contact Angle

Although σ_{SO} and σ_{SW} cannot be measured, σ_{WO} and the angle α are measurable. The adhesion tension is then given by,

$$A_T = \sigma_{WO} \cos \alpha \quad (4.2.3)$$

It follows that wettability can be measured by the angle α . If $\cos \alpha$ is positive the system is defined as water-wet, if $\cos \alpha$ is negative the system is defined as oil-wet, and if $\cos \alpha$ is 0 it has intermediate wettability. This corresponds to $\alpha < 90^\circ$, $\alpha > 90^\circ$ and $\alpha = 90^\circ$.

4.3 Permeability: Absolute, Effective and Relative

Darcy's law applies to the case of a single-phase fluid moving through a porous material when the fluid is at 100% saturation. In this case, the capacity of the material to transmit fluid is called the **absolute permeability** and given the symbol k . The unit of measurement is the *darcy*. A porous material with a permeability of 1 darcy allows flow of 1 centimetre per second (cm/s) for a fluid under a pressure gradient of 1 atmosphere per centimetre (atm/cm) and a viscosity of 1 centipoise (cP). In reservoir engineering, mill-

idarcies are used, since flow rates through rocks are generally low. Absolute permeability is a fundamental property of the rock, and in most cases it is constant, for a range of the fluids.

Petroleum reservoirs are rarely so simple that Darcy's laws is applicable. The simultaneous flow of two or more fluids is the norm. This leads to the concept of effective permeability and the more ubiquitous concept of relative permeability.

When more than one fluid is flowing simultaneously, each fluid has its own **effective permeability**. Effective permeability is a measure of the capacity of the porous material to transmit one fluid in the presence of another. Since the presence of a second fluid will tend to retard the flow of the first, effective permeability must evidently depend on the saturation of each fluid. Through experimentation, effective permeability has been found primarily to be a function of rock geometry, wetting characteristics and the existing fluid saturation. For every saturation value, the effective permeability will be different. When specifying k_w and k_{nw} , the effective permeability of the wetting and non-wetting fluid, it is therefore necessary to specify the saturations S_w and S_{nw} also. Effective permeability is stated as a numerical value given the existing state, so that $k_{w(80,20)}$ would be the wetting fluid permeability when saturation is made up of 80 per cent oil and 20 per cent water.

Relative permeability is a comparative expression of the relative capacity of several fluids to flow simultaneously. It is most commonly given as the ratio of effective and absolute permeability.⁷ Mathematically this is written,

$$k_{rw} = \frac{k_w}{k} \quad (4.3.1)$$

⁷Effective permeability is sometimes normalised using the non-wetting permeability value at the irreducible wetting saturation, see Dake [44] page 123.

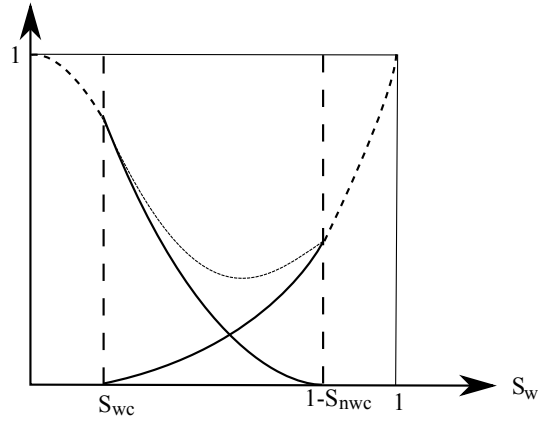


Figure 4.3.1: Typical Relative Permeability Curves

$$k_{rnw} = \frac{k_{nw}}{k} \quad (4.3.2)$$

The information is usually presented in graphical form for convenience, with the wetting saturation as the independent variable, and the non-wetting saturation given by $1 - S_w$ (using the relationship $S_w + S_{nw} = 1$). Figure 4.3.1, drawn from Wyckoff and Botset [174], shows a typical relative permeability curve for a gas water system.⁸

Basic Characteristics

Two-phase relative permeability curves are plotted as functions of the wetting saturation. There are a number of characteristics common to these curves that have been apparent almost from the time such curves were first described. These characteristics are best understood by considering the following three saturation intervals, where S_{wc} and S_{nwc} are the connate wetting saturation and critical non-wetting saturations respectively:

⁸An example for a water-oil system, which looks distinctly similar, can be found in Ahmed [2] page 306.

$0 \leq S \leq S_{wc}$: On this interval only the non-wetting phase is mobile, since the wetting relative permeability curve is zero at or below the connate wetting saturation S_{wc} . The wetting phase occupies the small pore spaces that do not contribute to flow, even if a large pressure differential is applied. At the same time, the non-wetting phase occupies the large, interconnected pore space and is free to flow almost unhindered. Hence, an increase in the wetting saturation has a small effect on the non-wetting permeability.

$S_{wc} \leq S \leq 1 - S_{nwc}$: As the saturation increases beyond the connate saturation, the wetting fluid begins to flow more freely, while the flow capacity of the non-wetting phase decreases. Above the point where the two curves intersect, the combined permeability of the two phases is less than unity, as is clearly evident from Figure 4.3.1. There are a number of reasons for this. The two fluids compete for flow channels, and interfere along shared paths. Large globules can also be isolated and block flow paths where capillary forces are too great or the pressure differential is insufficient to force a path.

$1 - S_{nwc} \leq S \leq 1$: On this interval the non-wetting phase is immobile. Increasing the saturation of the non-wetting fluid significantly reduces the wetting fluid permeability. The non-wetting phase occupies the larger pore space, therefore an increase in the volume of the non-wetting fluid principally reduces the better flow channels.

It should be noted that saturations outside the interval between the connate wetting saturation and $1 - S_{nwc}$ only exist in the laboratory. The relative permeability curves are often only plotted between S_{wc} and $1 - S_{nwc}$, since saturation values outside these are not found under reservoir conditions.

4.4 Laboratory Measurements

Relative permeabilities are determined experimentally. As discussed comprehensively in Amyx [8],⁹ the data can be obtained by (1) measurement in the laboratory by a steady-state fluid flow process (2) measurement in the laboratory by an unsteady state process (3) through capillary-pressure data or (4) calculations from field-performance data. In almost all cases, relative permeabilities are determined through laboratory displacement tests,¹⁰ using (1) or (2). Only the two laboratory displacement methods will be discussed here.

4.4.1 Steady-state experiments

There are a number of steady state procedures for measuring relative permeability. The methods are listed in Honarpour et al. [80] as: *Penn-State*, *Single-Sample Dynamic*, *Stationary Fluid*, *Hassler*, *Hafford* and *Dispersed Feed*¹¹. The differences relate to how the end effects caused by capillary forces are handled in each method. All these methods follow the same basic format which is fundamentally the technique first reported by Leverett [105] in 1939.

In the steady state method, a small core sample is mounted in some kind of sleeve and a fixed volumetric ratio of fluids is forced through the sample. This continues until both the pressure differential across the sample and/or the in-flow and out-flow volumetric ratio achieve equilibrium.¹² The saturations are then determined. The relative permeabilities for each fluid at the specific saturation can be calculated by applying Darcy's Law: at a given wetting

⁹page 184.

¹⁰Dandekar [45] page 187.

¹¹page 1-6.

¹²Dullien [53] page 269.

saturation the effective wetting permeability is,

$$k_w = \frac{q_w \mu_w L}{A \Delta p_w} \quad (4.4.1)$$

with the non-wetting effective permeability similarly defined. To determine the relative permeabilities, the effective permeability at irreducible wetting saturation is calculated and used as a normalising term.

Since the steady state procedure only determines the wetting and non-wetting permeabilities at a single, fixed saturation, the steps must be repeated a number of times to generate data across the full spectrum of saturation values. This whole process is time consuming due to the large number of measurements and the long period required for steady state to be achieved. From the smooth, continuous relative permeability curves, one has the impression that the process is smooth and continuous across the entire saturation domain. This is clearly not the case, and some type of curve fitting is invariably employed. While the process appears straightforward, obtaining accurate and repeatable measurements is a far from trivial task and many sources of variation and error can influence the results. [45] [80] [53] [161]

4.4.2 Unsteady-state experiments

The mathematics for unsteady state methods is more complicated than it is for the steady state case. On the positive side, unsteady state methods are less time consuming. The process commences with the core at the irreducible non-displacing phase saturation. The effective permeability for both phases are calculated at the irreducible displacing saturation, as per the steady state method. From this point, the core is progressively flooded with the displacing fluid at a constant flow rate. The changes in pressure and volume firstly of the displaced fluid, and then the displacing fluid after breakthrough, are measured. From this data, the relative permeabilities can be calculated. The various experimental steps for unsteady state methods are given in Dandekar [45] section 9.4.8.

The method for interpreting the unsteady state results was developed by Johnson, Bossler and Naumann [84], and is widely referred to as the JBN method. The analysis employed to calculate the relative permeability curves relies upon Buckley-Leverett displacement theory. In particular, it uses the extension of Welge [169] that allows for the calculation of average wetting saturation.¹³ For a specific production, injection and pressure drop, the wetting saturation at the production end of a core of length L is given by

$$S_{wL} = \bar{S}_w - Q_i \frac{d\bar{S}_w}{dQ_i} \quad (4.4.2)$$

where \bar{S}_w is the average water saturation and Q_i are the injected pore volumes of wetting fluid. The relative permeabilities (at the production end) are given by:¹⁴

$$k_{ro} = f_o \frac{d[\frac{1}{Q_i I_r}]}{d[\frac{1}{Q_i}]} \quad (4.4.3)$$

$$k_{rw} = k_o \frac{\mu_w(1 - f_o)}{\mu_o f_o} \quad (4.4.4)$$

The term I_r , which comes from Rapoport and Leas [141], is a dimensionless function of cumulative fluid injection called the *relative injectivity*:

“From a physical viewpoint, the relative injectivity may be defined as the ratio of the intake capacity at any given flood stage to the intake capacity of the system at the very initiation of the flood (at which moment practically only oil is flowing through the system).”¹⁵

Although there are a number of alternative methods, JBN is probably the most common inversion method for determining relative permeabilities.¹⁶

¹³See Chapter Seven.

¹⁴Equations 8a and 9 of [84].

¹⁵Rapoport and Leas [141]

¹⁶Dandekar [45] page 215.

4.5 Other Factors Influencing Relative Permeability Measurements - of which there are many.

Relative permeability curves are plotted as a function of fluid saturation only. However, there is copious and detailed published evidence that a number of other parameters effect relative permeability apart from saturation. Leverett [105] notably identified some of these factors in his early study of a two-fluid oil-water system. These factors are given different emphasis by the authors that have reviewed the subject and the list varies slightly from one source to the next.¹⁷ The following may be considered a comprehensive summary, and each will be covered in turn:

- Pore Geometry and Structure
- Wettability
- Core Recovery, Preservation and Restoration
- Testing Conditions
- Testing Fluids
- History
- Interfacial Tension
- Viscosity
- Initial Saturations
- Overburden Pressure
- Temperature

¹⁷See Honarpour et al. [80], Dandekar [45] or Tiab and Donaldson [161] for example.

- Clay and Fines Content
- Displacement Rate

Pore Geometry and Structure

Pore size distribution is mentioned by Leverett [105] as a factor affecting relative permeability.¹⁸ Morgan and Gordon [116] specifically consider the influence of pore geometry on water-oil relative permeability and note that if this factor is ignored *laboratory measurements for predicting fluid flow may be misleading*.¹⁹ Grain size, shape, sorting and packing are listed as properties that affect pore geometry and therefore relative permeability.²⁰ The shape of the curves is also influenced by rock type, homogeneity and heterogeneity. Rocks with large pore spaces tend to have low irreducible water saturations and relatively large flow channels. Similarly, rocks with small pore spaces and large surface areas have larger irreducible water saturations and restricted flow channels. The level of cementation and the various effects of mineralization and post-depositional alteration are noted by Morgan and Gordon [116] as factors that can significantly influence flow properties.

The interconnectivity of pores is noted by Muskat and Meres [121], Botset [18], [58], Dodd and Kiel [48], and Wyllie [175] as effecting relative permeability. It is shown in Bulnes and Fitting [24] and Stone [153] that the flow behavior is similar in uniform porosity carbonates and consolidated sandstone, but as the heterogeneity increases so do the differences in the flow properties. The effects of stratification is discussed in Corey and Rathjens [35], where the directional effects of flow, whether perpendicular or parallel to bedding, are clearly observable. The influence of rock type, homogeneity, heterogeneity and cementation are considered in Arps and Roberts [10]. The influence of cementation is further considered in Naar et al. [123] and Nind

¹⁸page 169

¹⁹Morgan and Gordon [116] page 1199.

²⁰Ibid. page 1200.

NOTE:
This figure is included on page 67 of the print copy of
the thesis held in the University of Adelaide Library.

Figure 4.5.1: Wettability variation, Geffen et al. [130] page 105.

[124]. Authors including Huppler [82], Gorring [66], Leverett and Lewis [106], Wyckoff and Botset [174], Pathak et al. [134] and Land and Baptist [99] have all examined the behavior of relative permeability for gas-oil and oil-water systems for different rock formations and drawn a number of conclusions that reinforce the view that rock properties have a significant influence on relative permeability.

Wettability

Figure (4.5.1) is taken from Geffen et al. [130] and illustrates the change in relative permeability on a single core under three different wettability regimes: 1) untreated 2) treated with a chemical agent to leave the surface preferentially oil wet and initially saturated with brine 3) treated with a chemical agent to leave the surface preferentially oil wet and initially saturated with oil.

A comprehensive study of the effect of wettability on relative permeability was undertaken by Anderson [9]. Results consistent with Geffen et al. [130] are reported in Donaldson and Thomas [49], Owens and Archer [131] and Morrow et al. [117].

Classification of Wettability

The idea that reservoirs are either water-wet or oil-wet is simplistic. At first it was believed all reservoirs were water-wet since water was assumed to be the original fluid. Gradually, more reservoirs were classified as oil-wet. It is now known reservoirs run from water-wet to oil-wet, with many cases lying between the two extremes. This is verified by Cuiec [40], where the wettability of a 20 reservoirs is examined.

Wettability is an average characteristic of a rock-fluid system²¹. There can be considerable variation within a reservoir and new terms have arisen to describe this heterogeneous behavior. *Fractional wettability* is used in Tiab and Donaldson when *scattered areas throughout the rock are strongly wet by oil*²² while the remainder is water-wet. According to Dandekar this occurs when the many minerals that make up rock have different chemical properties.²³ The term *dalmation wetting* is used by Brown and Fatt [21] to describe this phenomenon.

Schmidt [145] showed that fine pores could be water-wet, while the larger pores are oil-wet, a situation referred to as *mixed wettability*. If the oil is located in continuous paths, displacement can occur at very low oil saturation. This case is described in detail by Tiab:

*The water film between the rock and the oil in the pore is stabilized by a double layer of electrostatic forces. As the thickness of the film is diminished by the invading oil, the electrostatic force balance is destroyed and the film ruptures, allowing the polar organic compounds to displace the remaining water and react directly with the rock surface.*²⁴

²¹Tiab and Donaldson [161] page 361.

²²ibid. page 360.

²³Dandekar [45] page 123.

²⁴Tiab and Donaldson [161], page 361.

Quite so! The complexity involved in mixed-wettability is clearly evident. This raises the question of how accurately we can hope to model this system, and supports the case for considering the system within a stochastic setting.

Measuring Wettability

Since wettability has a strong influence on the characterization of a reservoir, obtaining accurate measurements is important. Methods of quantifying wettability can be classified as 1) the direct analysis of contact angles or 2) indirect methods. The indirect methods make use of imbibition (Amott [7]), capillary pressure curves (USBM²⁵), imbibition and capillary data (Amott-USBM) or imbibition rate [110]. Full treatments of wettability evaluation are given in Tiab and Donaldson [161], Honarpour et al. [80] and Dandekar [45]. A large amount of work has been carried out on this subject since the 1930's, with considerable research ongoing. However, *there is no satisfactory method to determine in situ wettability*, so that laboratory evaluation should be related to reservoir conditions *using a great deal of caution*.²⁶

Core Recovery and Preservation, Restoration, and Testing Fluids

Laboratory measurement of relative permeability, particularly the effects of fluids and handling on results, are examined in Geffen et al. [130], Richardson et al. [129] and [144], Caudle et al. [29], Morgan and Gordon [116] and Mugen [119]. Since wettability is primarily determined by fluid characteristics and lithology,²⁷ core recovery, preservation, restoration, and testing fluids principally effect relative permeability through the alteration of wettability. Figure 4.5.2 shows experimental differences is preserved versus fresh cores, with different testing fluids.

²⁵The is known as the United States Bureau of Mines method, although it was developed by Donaldson et al. [50].

²⁶Honarpour [80] page 58.

²⁷Dandekar [45] page 133.

Core Recovery and Preservation

One of the factors that can influence rock wettability is core recovery and preservation. The reduction in pressure and temperature from reservoir conditions may cause components of crude oil to precipitate as a waxy solid, altering the surface characteristics of the core.²⁸ Native cores under reservoir condition are evidently preferable, and techniques that employ a pressure core barrel can help to ensure changes are minimised. However, as Dandekar [45] notes, *the majority of available data on wettability of the oil-water-rock system are for atmospheric pressure and room conditions.*²⁹ Exposure to air can pose problems as oxidation is known to alter wettability.³⁰ Contamination from drilling fluids can also change wettability characteristics, sometimes dramatically.³¹

Core Restoration

Cores in a naturally preserved state are not always available. For example, cleaning may be required to determine other parameters such as porosity and permeability before conducting further tests. The most common practice is cleaning with toluene in a Soxhlet extractor, followed by ethanol to remove the toluene.³² This will invariably alter the wettability by removing the original coating on the grain surface. Several methods are available for restoring cores to their natural state, one of which is found in McGhee et al.[114]. However, there is no way of being completely sure the cores have been properly returned to their native state. As Honarpour et al. succinctly explain, it may be the case that *restored state cores are not.*³³

²⁸Paulya [136] page 71.

²⁹Dandekar [45] page 126.

³⁰Amott [7].

³¹Kyte et al. [95].

³²Tiab and Donaldson [161] page 397.

³³Honarpour et al. [80] page 69.

NOTE:
This figure is included on page 71 of the print copy of
the thesis held in the University of Adelaide Library.

Figure 4.5.2: Fresh and preserved cores, Mugen [119] page 401.

Testing Fluids

The evaluation of wettability and relative permeability is naturally influenced by the fluid used. It is not a simple matter of using reservoir oil or brine, since they are not always available. A wide range of fluids can be used including air, nitrogen, synthetic oils, reservoir oils (in various modified states), formation or reconstituted brine, and pure water.³⁴ Apart from the issue of not perfectly matching the fluids to reservoir condition, core surfaces may be altered by compounds within the fluids. For example, carbonates are sensitive to sulfur and oxygen, while asphaltenes can react with the acid type surfaces of sandstones containing silica.³⁵

Hysteresis

Relative permeability is influenced by how the test is performed, whether the wetting phase is increasing (imbibition) or decreasing (drainage) in the displacement experiment. The displacement of oil by water, if water is the

³⁴Dandekar [45] page 196.

³⁵Honarpour et al. [80] page 70.

wetting phase, is an imbibition process. If gas is injected to displace oil the process is drainage. The alteration of relative permeability through hysteresis is documented in Land [98] and [99], Geffen et al. [130], Richardson et al. [129] and [144], Levine [107], Josendale et al. [85] and Terwilliger et al. [158]. While the wetting fluid relative permeability is largely unchanged, the non-wetting fluid is noticeably less during imbibition than drainage.³⁶ To minimize the influence of hysteresis, the process corresponding to the reservoir condition must be duplicated in testing.

Interfacial Tension

In describe the properties of multiphase systems, we need to consider the effect of forces at the interface of immiscible fluids. *Interfacial tension* is the force per unit length that exists between two immiscible fluids.³⁷ *Surface tension* is the equivalent force at a liquid and gas boundary.

NOTE:
This figure is included on page 72 of the print copy of
the thesis held in the University of Adelaide Library.

Figure 4.5.3: Changing interfacial tension, Leverett [105] page 162.

Figure 4.5, taken from Leverett [105], is the outcome of measuring the relative permeability of two liquid pairs of *widely different interfacial tension*.³⁸ Over the less extreme range 27 to 72 dyne/cm, Wyckoff [174] recorded a small but notable change in relative permeability as a result of altering interfacial

³⁶Marle [112] page 28.

³⁷Bradley [19] 22-I.

³⁸Leverett [105] page 162.

tension. Over the range 27 to 72 dyne/cm Muskat [120] asserted the effect on relative permeability was negligible. Pirson [138] claims that only imbibition relative permeability is sensitive to interfacial tension.

Viscosity

A number of authors have found relative permeability to be essentially independent of fluid viscosity. These include Leverett [105], Leverett and Lewis [106], Wyckoff and Botset [174], Richardson [143], Johnson et al. [84], Levine [107], Lorenz et al. [109], and Parish et al. [65]. While a small degree of variation was in some cases observed, nowhere was it deemed significant.

When the viscosity ratio is varied, the picture is not clear. Several authors including Yuster [177], and Odeh [125] have reported that relative permeability is effected by changing the viscosity ratio. However, Baker [12] rebutted these findings. Morse [118] supported the influence of viscosity ratio on relative permeability. Downie and Crane [51] give qualified affirmation. At the end of the article by Downie and Crane, there is a healthy discussion and response with Odeh on the interpretation of results. Pirson [138] states the effect of viscosity ratio is a second order influence. Figure 2.4.1 of Willhite [135] indicates the viscosity ratio has a noticeable effect on relative permeability.

The influence on relative permeability of changing viscosity (including altering the viscosity ratio) is not firmly established. There is a degree of variation amongst the reported results. This has led Honarpour et al. to conclude *it seems best to conduct laboratory relative permeability experiments with fluids which do not differ greatly in viscosity from the reserve fluids.*³⁹

³⁹Honarpour [80] page 88.

Initial Saturations

Initial water saturation is known to alter the shape and location of the relative permeability curves. Henderson et al. [72] recorded a lateral shift in the curves towards increasing oil saturation. Caudle et al. [29] also verified that the initial water saturation altered relative permeability. Craig [39] proposed that the relative permeability of water-wet rocks was sensitive to initial water saturation but the effect on oil-wet rocks was negligible up to initial saturation of 20%.

Overburden Pressure

Laboratory measurements of relative permeability are frequently taken at atmospheric conditions.⁴⁰ The permeability and porosity of reservoir rocks is reduced by the application of sufficient overburden pressure. This effect, as it applies to sandstones, was examined in Fatt and Davis [59], in which permeability was reduced by 50% using pressure of 10,000 psi. The effect of overburden pressure on relative permeability was studied by Fatt [57] for the case of a gas-oil system. At pressures likely to be found in reservoirs (3000 psi), Fatt observed that *the difference between laboratory and reservoir conditions is not enough to affect the results.*⁴¹ However, at greater pressures or where high accuracy was required, Fatt concluded reservoir overburden pressure conditions may be warranted during testing. Wilson [173] tested at 5000 psi, and recorded only a moderate change in relative permeability.

Temperature

The effect of temperature on relative permeability is not clear. Akin et al. [3] conducted a literature review on the effect of temperature on heavy oil-water relative permeability, covering room temperature to 260 degrees Celcius. While various temperature effects could be observed, there were no

⁴⁰Dandekar [45] page 227.

⁴¹Fatt [57] page 326.

conclusive results. Donaldson et al. [50] report that the system becomes more water-wet as temperature increases. An increase in the irreducible water saturation and a decrease in the residual oil saturation is reported in [54], Poston et al. [139], Davidson [47], Sinnokrot et al. [150] and Weinbrandt et al. [168].

Clay and Fines Content

Laboratory measurements of relative permeability can be adversely altered by the movement of fines that comprise the rock sample. One side effect of the higher flow rates typically employed to minimise capillary end effects is fines can be mobilized that alter the characteristic of the rock-fluid system. Clay swelling occurs *if the injected brine is incompatible with the clay or not in ionic equilibrium with the rock.*⁴² This can also affect relative permeability. Both these issues are examined in Amaefule et al. [6].

Summary

From this section it should be clear that there is considerable debate concerning the many factors that affect relative permeability. Factors that are deemed negligible by one author are seen as significant by another. Pore structure and wettability are generally believed to have the strongest influence on the shapes of the relative permeability curves, but there is a long list of secondary effects. The numerous sources of variation and error provides the motivation for considering the problem within a stochastic setting.

4.6 Two-Phase Analytical Models

Although relative permeability curves are generally determined experimentally, a number of analytical models have been proposed either for examining solutions mathematically or for use in reservoir simulators.

⁴²Dandekar [45] page 228.

4.6.1 Corey and Brooks

Based on the work of Burdine [25], Kozeny [92], and Carman [28], Corey [35] suggested a simple but useful approximation for relative permeability.

$$k_{r1} \propto S_e^4 \quad (4.6.1)$$

$$k_{r2} \propto (1 - S_e)^2(1 - S_e^2) \quad (4.6.2)$$

where $S_e = (S_1 - S_{1c})/(1 - S_{1c})$ is the effective saturation: since the wetting fluid is immobile below its irreducible level, one can assume that values in the irreducible range are part of the solid structure. In effect, the irreducible saturation becomes zero. These equations have been used by petroleum engineers because of their simplicity, despite having limited validity. Brooks and Corey [20] developed an alternative, more general description that could be applied to a wider range of materials. The effective saturation was specified by

$$S_e = \left(\frac{P_d}{P_c} \right)^\lambda \quad (4.6.3)$$

where P_d is the entry pressure, P_c is capillary pressure and λ is the pore size distribution index. They then proposed the following functions to describe relative permeability:

$$k_{r1} = (S_e)^{\frac{2+\lambda}{\lambda}} \quad (4.6.4)$$

$$k_{r2} = (1 - S_e)^2 \left(1 - S_e^{\frac{2+\lambda}{\lambda}} \right) \quad (4.6.5)$$

4.6.2 MBC

The most common model in petroleum engineering is the modified Brooks and Corey model (MBC). As Lake [96] explains, these give an analytical form

that fits most experimental data for oil-water flow:

$$k_{r1} = k_{r1}^0 \left(\frac{S_1 - S_{1c}}{1 - S_{1c} - S_{2c}} \right)^{n_1} \quad (4.6.6)$$

$$(4.6.7)$$

$$k_{r2} = k_{r2}^0 \left(\frac{1 - S_1 - S_{2c}}{1 - S_{1c} - S_{2c}} \right)^{n_2}$$

where k_{r1} and k_{r2} are the relative permeabilities of water and oil respectively, k_{r1}^0 and k_{r2}^0 are the endpoint permeabilities of each fluid, S_1 is the saturation of fluid 1 (water), S_{1c} and S_{2c} are the connate water and critical oil saturations and n_1 and n_2 are constants. Using this formulation, the fractional flow will be given by:

$$f_1 = \frac{1}{1 + \frac{(1-S)^{n_2}}{MS^{n_1}}} \quad (4.6.8)$$

where

$$S = \frac{S_1 - S_{1c}}{1 - S_{2c} - S_{1c}} \quad (4.6.9)$$

is the reduced water saturation and

$$M = \frac{k_{r1}^0 \mu_2}{\mu_1 k_{r2}^0} \quad (4.6.10)$$

is the endpoint water-oil mobility ration. M has an important interpretation, which is:

$$\frac{\text{maximum velocity of the displacing fluid}}{\text{maximum velocity of the displaced fluid}}$$

4.6.3 Carman-Kozeny

Kozeny [92] and later Carman [28], interpreted reservoir rock as a bundle of capillary tubes. Utilizing the concept of mean hydraulic unit radius, they

developed a single phase relationship between permeability and porosity.

$$k = \frac{\phi_e r_{mh}^2}{2\tau^2} \quad (4.6.11)$$

where ϕ_e is the effective porosity (fraction bulk volume), the constant τ is called the tortuosity, and the hydraulic unit radius is given by

$$r_{mh} = \frac{\text{Volume Open to Flow}}{\text{Wetted Surface Area}} \quad (4.6.12)$$

The general form, known as the Kozeny-Carman equation is:

$$k = \frac{\phi_e^3}{(1 - \phi_e)^2} \left(\frac{1}{F_s \tau^2 S_{gv}^2} \right) \quad (4.6.13)$$

where S_{gv} is surface area per unit grain volume and is given by:

$$S_{gv} = \frac{1}{r_{mh}} \left(\frac{\phi_e}{1 - \phi_e} \right) \quad (4.6.14)$$

In the generalised form, F_s is the shape factor. The group $F_s \tau^2$, known as the Kozeny constant, varies between hydraulic units but is constant within a single unit.

Alpak et al. [4] developed expressions for relative permeability based on the ideas of the Carman-Kozeny model, proposing

$$k_{rw} = S_w^3 \frac{\tau}{\tau_w} \frac{A_T^2}{(A_{ow} + A_{ws})^2} \quad (4.6.15)$$

$$k_{ro} = S_{nw}^3 \frac{\tau}{\tau_{nw}} \frac{A_T^2}{(A_{ow} + A_{os})^2} \quad (4.6.16)$$

where A_T is the total surface area of the solid, and A_{wo} , A_{sw} and A_{so} are the interfacial areas between water-oil, solid-water and solid-oil respectively.

Amaefule et al. [5] have developed a method for separating different hydraulic units, within which $F_s \tau^2$ is constant. Dividing both sides of the Carman-Kozeny equation by the effective porosity and taking square roots gives,

$$\sqrt{\frac{k}{\phi_e}} = \frac{\phi_e}{(1 - \phi_e)} \left(\frac{1}{\sqrt{F_s \tau S_{gv}}} \right) \quad (4.6.17)$$

A number of quantities are then defined:

$$RQI = 0.0314 \sqrt{\frac{k}{\phi_e}}$$

is the *reservoir quality index*,

$$\phi_z = \frac{\phi_e}{(1 - \phi_e)}$$

is the *porosity group* and,

$$FZI = \frac{1}{\sqrt{F_s \tau S_{gz}}} = \frac{RQI}{\phi_z}$$

is the *flow zone indicator*. The parameters FZI , RQI and ϕ_z are now substituted into (4.6.17), and taking logarithms yields

$$\log RQI = \log \phi_z + \log FZI \quad (4.6.18)$$

Quoting from Amaefule et al. [5] page 3, *On a log-log plot of RQI versus ϕ_z , all samples with similar FZI values will lie on a straight line with unit slope...Samples that lie on the same straight line have similar pore throat attributes and, thereby, constitute a hydraulic unit.*

The approach of Amaefule et al. [5] to defining a single hydraulic unit has been extended by Behrenbruch and Goda⁴³ [15]. It was found that relative permeabilities from the same hydraulic unit form a straight line in the modified two phase Carman-Kozeny space. Formulas for relative permeability for

⁴³The method is credited to another paper by Behrenbruch, P., *Two-Phase Relative Permeability Prediction: A New Semi-Empirical Model Based on a Modified Carman-Kozeny Equation*, which was unpublished at the time of [15].

oil-water are given by:

$$k_{rw} = \frac{1014m_w^2\phi_e^3S_w}{k} \left[\frac{S_w}{1 - \phi_e S_w} - \frac{S_{wir}}{1 - \phi_e S_{wir}} \right] \quad (4.6.19)$$

$$k_{ro} = \frac{1014m_o^2\phi_e^3(1 - S_w)}{k} \left[\frac{1 - S_w}{1 - \phi_e(1 - S_w)} - \frac{S_{oc}}{1 - \phi_e S_{oc}} \right] \quad (4.6.20)$$

where m_w and m_o are the slopes of the straight line relationships in the Carman-Kozeny space.⁴⁴

4.6.4 Other Models

Although MBC are the most widely used expressions, there are a large number of other analytical relative permeability models. Siddiqui et al. [148] make a comparison of ten two-phase relative permeability models. The authors group them into models that require the use of capillary pressure (Burdine [25], Fatt and Dykstra [60], Gates and Lietz [64], Purcell [140], Timmerman [162], and Wyllie and Gardner [176]), and those that do not (Corey [35], Fulcher et al. [62], Honarpour et al. [79], Naar and Henderson [122], and Pirson [138]). For modeling water-oil relative permeabilities, Chierici [31] suggested the following exponential forms for an oil-water system (water is the wetting phase):

$$k_{rw} = k_{rw}^{max} \text{Exp}[-AS_{wN}^{-p}] \quad (4.6.21)$$

$$k_{ro} = k_{ro}^{max} \text{Exp}[-BS_{wN}^q] \quad (4.6.22)$$

where the normalized wetting saturation is given by $S_{wN} = \frac{S_w - S_{wc}}{1 - S_{oc} - S_w}$. Models that account for hysteresis effects, which can be significant, have been developed by Killough [88] and Carlson [26].

4.7 The Relative Permeability Ratio

More often than not, we are interested in the ratio of the relative permeabilities. It so happens that the plot of saturation versus the logarithm of the

⁴⁴[15] page 3.

relative permeability ratio is frequently linear. This is clearly demonstrated in Figure 4.7.1, which is a worked example taken from Ahmed [2]. Other

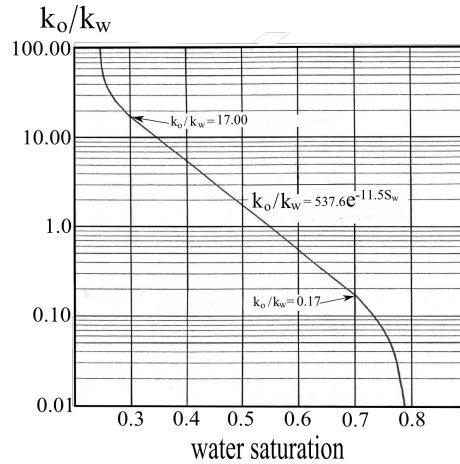


Figure 4.7.1: Relative permeability ratio, Ahmed [2] Figure 14-22.

examples can be found in Craft and Hawkins [38],⁴⁵ or the Malay Basin data used in Chapter Six. It is *common usage*⁴⁶ to describe the central straight part of the relationship by $\frac{\mu_w}{\mu_o} \alpha e^{bS}$, where $\alpha = e^a$. This leads to a convenient expression for the fractional flow function:

$$f(S) = \frac{1}{1 + \frac{\mu_w}{\mu_o} \alpha e^{-bS}} \quad (4.7.1)$$

Like the MBC model, the fraction flow expression (4.7.1) is determined by two parameters. In this case, the parameters can be estimated using linear regression on the plot of saturation versus the logarithm of the relative permeability ratio. The fractional flow curve that results has the expected S shape and possesses sufficient flexibility to cover a wide range of experimental data for two-phase flow. We will make use of this expression when we consider a stochastic version of the Buckley-Leverett equation.

⁴⁵page 341.

⁴⁶Ahmed [2], page 309.

4.8 Conclusion

There are several circumstances in which one might consider using a stochastic differential equation. In the first instance, there is insufficient information to understand the system completely. With respect to petroleum engineering, it is only possible to take measurements at a relatively small number of places, with no guarantee such measurements are fully representational. In the second instance, the system might be known quite well, but accurate measurement is not possible due to physical or technological problems in measurement. In the third instance, the system is all together too complex to fully capture; the many and various individual parts are well understood, there are too many components and interactions to grasp the system with full confidence. Each of these three types of uncertainty are applicable where relative permeability is concerned, but a thorough review the literature indicates the third limitation is especially relevant.

In this chapter, we have examined the many factors known to influence relative permeability, together with the inherent errors, variation and uncertainty. Perhaps the entire subject could have brushed over with a simple statement that uncertainty is a core feature of petroleum engineering - but that would be unprofessional. The relative permeability curves are the mechanism through which reservoir conditions enter the Buckley-Leverett model via the fractional flow curve, and a comprehensive understanding of this input is required before any alteration of the model to include a stochastic input can be proposed.

The more commonly employed analytical expressions used to describe relative permeability were examined. In the following chapters we will investigate a stochastic version of the Buckley-Leverett model. In order to obtain a stochastic differential equation, we need an analytical expression for the fractional flow curve, which is itself, dominated by the relative permeability curves. Without an analytical expression for fractional flow, we will be con-

demned to numerical approximations, possibly involving Monte Carlo methods, rather than a family of closed form solutions. Obtaining closed form solutions is our ambitious goal.

PART II - Something New

Chapter 5

A Stochastic Version

“As far as the laws of mathematics refer to reality, they are not certain; and as far as they are certain, they do not refer to reality.” (Albert Einstein)

In this chapter we will discuss the motivation for considering the Buckley-Leverett equation within a stochastic setting. We will consider one possible way of introducing uncertainty into the model. This will lead to a clearly defined problem, complete with assumptions. Given this formulation, mathematical expectation will be used to calculate the shock front saturation and the position and velocity of the shock front under conditions of uncertainty.

5.1 Introduction

Flow in porous media, as it applies to the modeling of petroleum reservoirs, occurs under conditions of uncertainty. Stochastic differential equations, where one modifies a deterministic equation with a stochastic perturbation, or where there are stochastic initial conditions, offers one possible way of accounting for this uncertainty in order to make the model more realistic. The great benefit of examining a stochastic differential equation is that mathematically rigorous results can be obtained concerning issues such

as the physical characteristics of shock waves and the asymptotic behavior of solutions.

Over the last thirty years there have been enormous developments in stochastic differential equations. The list of applications of this branch of mathematics is almost endless - finance, optimal control and population growth being a few typical examples (see Øksendale [126] or Karatzas and Shreve [87]). However, these uses have mostly involved second order equation with relatively well behaved solutions. First order conservation equations, in comparison, often are not well behaved, as the solutions may involve discontinuities.

The Buckley-Leverett equation is a good approximation for a homogeneous core plug. On this scale, fluid velocities, absolute permeability, injection rates and pressure differentials can be accurately determined. However, factors which are more prominent for larger formations, like dispersion, capillary effects and local heterogeneities, will naturally be more difficult to evaluate. To this add the issue of sampling error. The areal extent of a reservoir is invariably very large and it is only possible to sample at a few selected points, which may turn out not to be representative. Or perhaps only limited sample data is available, due to the high cost of collection. Then there is the problem of averaging information pertaining to different scales. Over a reservoir, or part of a reservoir, there are a number of different rock behaviors, and this will be reflected in the samples brought to the surface. To derive breakthrough time, or one of the other results of interest, a representative element volume must be selected. Thus, the spread of values is discarded in favor of a value that is more representative. It should be clear that there are many avenues for errors to enter the model. It is therefore reasonable to state that there is an intrinsic uncertainty in quantifying the model inputs.

By modeling a stochastic version of the Buckley-Leverett equation, we aim to draw conclusions about the uncertainty associated with the flow proper-

ties of an immiscible two-phase system, generally taken as oil-water. In this enterprise, we are faced with a trade-off between validity and tractability. The way in which uncertainty is introduced into the model must be physically relevant. However the equation, which is already particularly difficult to solve, will be made even more difficult by introducing a non-deterministic term.

5.2 Incorporating Uncertainty

The Input

Relative permeability curves are fundamental to reservoir engineering and central to Buckley Leverett theory. The specific characteristics of the porous media and of the fluids are introduced into the model through the choice of these curves. The relative permeability curves substitute directly into the fractional flow formula, and how they effect the fractional flow curve determines the solution. One could argue that the fractional flow curve is more fundamental than relative permeability, particularly when we consider the process of water-drive in a reservoir, the theoretical mechanics of which are underpinned by Buckley-Leverett displacement theory. This is the view of Dake 2001 [43],¹ who supports this view by writing,

- *it is a single function, the shape of which reveals all about the efficiency of the flood where as the two relative permeability curves do not*
- *when applied in the description of flooding in the reservoir, it incorporates the correct, in situ oil and water viscosities, which is not the case in most relative permeability measurements.*

The fractional flow expression will be used to introduce uncertainty into the models via the fractional flow. This is done for the following reasons:

¹page 342.

- The fractional flow curve is the input mechanism for different physical situations, and therefore the mechanism through which uncertainty enters the model.
- This has a clear and logical physical interpretation.
- We capture the uncertainty inherent in the system in an appropriate but relatively simple way, while ensuring the problem remains tractable.

What form should the fractional flow expression take? Generally, relative permeability curves are derived experimentally, and no general theoretical expression exists. However, in order to derive closed form solutions, we need some kind of analytical expression. Recall from the previous chapter that an analytical form of the fractional flow expression (4.6.8) is given by:

$$f(S) = \frac{1}{1 + \frac{\mu_d}{\mu_{nd}} \alpha e^{-bS}}$$

This function is applicable in a wide range of situations, and it ensures the fractional flow curve has the expected S -shape. The parameters $\alpha = e^a$ and b are set by conducting linear regression on the logarithm of the relative permeability curves. Given this choice, we now have the following problem to solve.

5.3 The Problem

$$\frac{\partial S}{\partial t} + \frac{q_t}{A\phi} \frac{df(S)}{dS} \frac{\partial S}{\partial x} = 0 \quad (5.3.1)$$

$$S(x, 0) = \begin{cases} S_l & \text{if } x \leq 0 \\ S_r & \text{if } x > 0 \end{cases} \quad (5.3.2)$$

$$f(S) = \frac{1}{1 + \frac{\mu_d}{\mu_{nd}} \alpha e^{(-bS+\varepsilon)}} \quad (5.3.3)$$

$$\varepsilon \sim N(\mu, \sigma^2) \quad (5.3.4)$$

where ε is a normally distributed random variable representing the error. The properties of the normal distribution are given in Annex A. Equation (5.3.3) can be written in the form:

$$f(S) = \frac{1}{1 + Z \frac{\mu_d}{\mu_{nd}} \alpha e^{-bS}} \quad (5.3.5)$$

In this expression Z is a random variable equal to e^ε . The distribution and properties of Z can be calculated in a straightforward manner. We are not restricted to using the normal distribution, the family of beta distributions, noteworthy for its flexibility, could equally be used.² However, the normal distribution is closely linked to the analysis of error in regression and appears to be the best choice.

Why do we use a random variable of this form? The parameters a and b are determined by linear regression of saturations versus the logarithm of the ratio of relative permeabilities. The use of linear regression to generate relative permeabilities was employed in Mohamad Ibrahim and Koederitz [115]. Performing regression on the semi-log ratio of relative permeability is less difficult than deriving separate relative permeability curves because the semi-log relationship is usually monotonic and either linear or near linear. An example was given in section 4.7. As with any linear regression, there is an error term. The size of the error is determined through standard techniques of regression analysis. It is assumed that the error ε has a normal distribution. If there is no uncertainty we return to the purely deterministic case. In taking this approach, we are not guessing the degree of uncertainty, or choosing a convenient value, rather it comes from the analysis of the ratio of permeabilities. It does, however, depend on the ratio of relative permeabilities being

²The properties and application of the beta distribution are given a comprehensive treatment in Gupta and Nadarajah [68].

log linear against the saturation. Later we will relax this condition to only requiring that there is a semi-log relationship that can be determined using regression. The method will be difficult to follow as it is, without moving to a general regression function. However, there is little additional difficulty by taking the general case.

Given this formulation, we are interested in questions such as:

- How will the shock front propagate?
- What is the velocity of the shock front?
- What is the location of the shock front?
- What is the time to break-through?
- What is the asymptotic behavior of the solution?
- How does the degree of uncertainty change under different fractional flow curves?

5.3.1 Assumptions

To solve this system, we will make two assumptions:

- **A1** We restrict the model to the situation in which (5.3.3) is appropriate, that is, there is a clear relationship between saturation and the logarithm of the permeability ratio. We will start with a linear relationship.
- **A2** The initial conditions (saturations) are non-random.

We make these assumptions for a number of reasons. The first is that any stochastic model is based upon an underlying deterministic model. Where the underlying deterministic equation does not model reality well, it is no surprise that the stochastic version also fails. This model for the fractional flow is

accepted in the literature and sufficiently general to be useful. Clearly, if (5.3.3) is not appropriate, the stochastic form chosen here should not be used. Regarding the second assumption, it is justified on the following grounds:

- several mechanisms through which uncertainty enter the model are unnecessary; one input that captures the majority of uncertainty inherent in the system is sufficient.
- the connate water saturation is often chosen as the initial state and there is less uncertainty in specifying the connate saturation than the shock front saturation. The shock front saturation is affected by the variation of two curves, while the connate saturation is a property of the solid and the non-wetting fluid only (sorting and wettability are the most significant factors influencing the connate saturation).
- in modeling stochastic first order conservation equations, either stochastic flux or stochastic initial conditions are considered, but not both; the second assumption/limitation keeps the problem solvable.

5.4 Analytical Solution

The *Welge Tangent Method* gives a geometric solution to the Buckley-Leverett equation, and this will motivate us in finding the solution to the stochastic problem. We would expect that the new solution will be the old solution plus a perturbation. We might therefore look for some kind of distribution around the original, non-stochastic solution.

For the flux function under consideration, the concave hull has two components: the straight line tangent to the curve and the component of the hull that follows the original function at saturation values greater than the shock front value. First we will obtain the closed form solution to the shock front value. This is found by solving:

$$\frac{f(S^*)}{S^* - s_c} = f'(S^*) \quad (5.4.1)$$

where s_c is the connate water saturation and S^* is the shock front saturation, which is a random variable. We are restricted to the concave section of f in order to avoid physically impossible triple valued solutions.

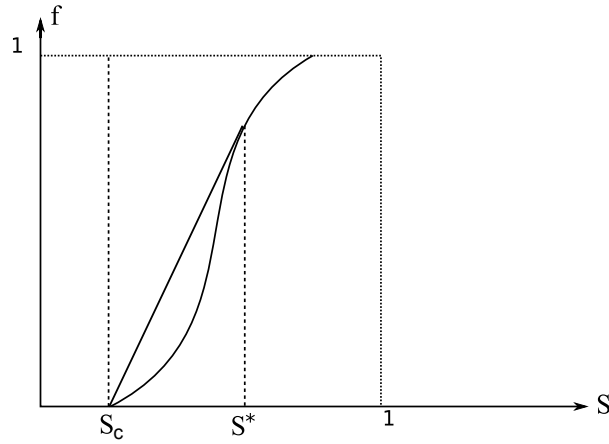


Figure 5.4.1: Welge tangent method - again.

Equation (5.4.1) can be more conveniently written as,

$$\frac{f'(S^*)}{f(S^*)} = \frac{1}{S^* - s_c} \quad (5.4.2)$$

$$f(S^*) = \frac{1}{1 + Z \frac{\mu_d}{\mu_{nd}} \alpha e^{-bS^*}} \quad (5.4.3)$$

$$\ln f(S^*) = -\ln \left(1 + Z \frac{\mu_d}{\mu_{nd}} \alpha e^{-bS^*} \right) \quad (5.4.4)$$

$$\frac{f'(S^*)}{f(S^*)} = \frac{Z \frac{\mu_w}{\mu_{nw}} \alpha b e^{-bS^*}}{1 + Z \frac{\mu_d}{\mu_{nd}} \alpha e^{-bS^*}} \quad (5.4.5)$$

Using (5.4.2),

$$\frac{1}{S^* - s_c} = \frac{Z \frac{\mu_d}{\mu_{nd}} \alpha b e^{-bS^*}}{1 + Z \frac{\mu_d}{\mu_{nd}} \alpha e^{-bS^*}}$$

This leads to,

$$Z = \xi(S^*) = \frac{1}{(b(S^* - s_c) - 1)^{\frac{\mu_d}{\mu_{nd}}} \alpha e^{-bS^*}} \quad (5.4.6)$$

on saturation values such that f is concave. Just why this expression is useful will soon become clear.

5.4.1 Distribution of a Function of a Random Variable

Knowing the distribution of ε , we can find the distribution of Z . We will look at this issue in generality before evaluating the specific example above. Such standard results concerning distributions and expectations can be found in almost any comprehensive text on probability, such as Shiryaev [147].

Suppose X is a random variable with probability distribution function (pdf) $f_X(x)$, and $Y = h(X)$. We want to find the pdf of Y , which we will denote by $f_Y(y)$. Suppose the inverse h exists and is denoted h^{-1} . We recall that X has pdf f_X if and only if for any bounded Borel (or continuous) measurable function on \mathcal{R} ,

$$E[h(X)] = \int_{\mathcal{R}} h(x) f_X(x) dx \quad (5.4.7)$$

To find the distribution of Y we write

$$E[Y] = E[h(X)] \quad (5.4.8)$$

$$= \int_{\mathcal{R}} h(x) f_X(x) dx \quad (5.4.9)$$

$$= \int_{\mathcal{R}} y f_X(h^{-1}(y)) \left| \frac{d}{dy} h^{-1}(y) \right| dy \quad (5.4.10)$$

so that

$$f_Y(y) = f_X(h^{-1}(y)) \left| \frac{d}{dy} h^{-1}(y) \right| \quad (5.4.11)$$

Special Case

We shall calculate the distribution of Z .

$$g(X) = e^X$$

$$g^{-1}(X) = \ln X$$

and,

$$g'(x) = e^x$$

Hence,

$$f_Z(z) = \frac{f_X(\ln z)}{|z|} \quad (5.4.12)$$

If $X \sim N(\mu, \sigma^2)$,

$$f_Z(z) = \frac{e^{-\frac{(\ln z - \mu)^2}{2\sigma^2}}}{z\sigma\sqrt{2\pi}} \quad (5.4.13)$$

for $z > 0$, which is the familiar log-normal pdf. The properties of this distribution are given in Annex A.

5.4.2 Expectation

As we have chosen a stochastic flux function, the shock front saturation will now be a distribution. Other quantities of interest, such as the position and velocity of the saturation profile will also have distributions, which we would like to know. Mathematical expectation will provide a mechanism for calculating these results.

For a bounded Borel function $g(x)$, the expectation is given by:

$$E[g(X)] = \int g(x)\psi(x)dx \quad (5.4.14)$$

where ψ is a probability density function of the random variable X . The saturation will be a random variable of the form $S^* \equiv S^*(Z)$, while we know

both $z = \xi(s^*)$ by (5.4.6) and the probability density function $f_Z(z)$ of the random variable Z . Using (5.4.11),

$$f_{S^*}(s^*) = f_Z(\xi(s^*)) \left| \frac{\partial \xi(s^*)}{\partial s^*} \right| \quad (5.4.15)$$

If \mathbf{I} is the indicator function,

$$P[0 \leq S^* \leq \beta] = \int_{-\infty}^{\infty} \mathbf{I}_{[0,\beta]}(\xi(s^*)) f_{S^*}(s^*) ds^* \quad (5.4.16)$$

$$= \int_0^\beta f_{S^*}(s^*) ds^* \quad (5.4.17)$$

Using (5.4.6) and (5.4.17),

$$\xi(s^*) = \frac{1}{\frac{\mu_d}{\mu_{nd}} \alpha(b(s^* - s_c) - 1) e^{-bs^*}} \quad (5.4.18)$$

$$\frac{\partial \xi(s^*)}{\partial s^*} = \frac{b(b(s^* - s_c) - 2)}{\frac{\mu_d}{\mu_{nd}} \alpha(b(s^* - s_c) - 1)^2 e^{-bs^*}} \quad (5.4.19)$$

$$f_Z(\xi(s^*)) = \frac{N_{(0,\sigma^2)}(\ln[\xi(s^*)])}{|\xi(s^*)|} \quad (5.4.20)$$

$$P[0 \leq S^* \leq \beta] = \int_0^\beta \frac{e^{-\frac{(\ln[\xi(s^*)] - \mu)^2}{2\sigma^2}}}{|\xi(s^*)| \sigma \sqrt{2\pi}} \left| \frac{b(b(s^* - s_c) - 2)}{\frac{\mu_d}{\mu_{nd}} \alpha(b(s^* - s_c) - 1)^2 e^{-bs^*}} \right| ds^* \quad (5.4.21)$$

where $N_{(\mu,\sigma^2)}(x)$ is the normal probability density function. That is:

$$N_{(\mu,\sigma^2)}(x) = \frac{1}{\sqrt{2\pi\sigma^2}} \exp\left(-\frac{(x - \mu)^2}{2\sigma^2}\right) \quad (5.4.22)$$

Equation (5.4.21) is the distribution for the shock front saturation. Granted, it is not a simple expression that can be worked out by hand. However, many of the terms are known constants. The expression can be evaluated quite easily using a symbolic package like *Mathematica*, which is capable of finding an expression for the integral and plotting the function.

5.4.3 Stochastic Velocity and the Position of the Shock Front

If the flux function is stochastic, then of course the velocity will be stochastic also. We now turn to calculating its distribution. This requires that we invert the expression for velocity. Since this function happens to be quadratic in the random variable Z , this is possible, provided we restrict the solution to that part that is physically feasible. The concave hull of the flux function is given by:

$$\hat{f}(S) = \begin{cases} f(S) & \text{if } S \geq S^* \\ \frac{f(S^*)(S-S_c)}{S^*-S_c} & \text{if } S \leq S^* \end{cases} \quad (5.4.23)$$

The relevance of this is the inverse of the piecewise derivative of the concave hull determines the saturation profile, as covered in Chapter Three. The Buckley-Leverett equation models the velocity of a plane of non-wetting fluid of constant saturation. We will be interested in the non-wetting saturations greater than the S^* , which corresponds to the curved section of the concave hull.

Velocity

The derivative of $f(S)$ is given by,

$$f'(S) = \frac{\frac{\mu_d}{\mu_{nd}} \alpha b e^{-bS}}{\left(1 + \frac{\mu_d}{\mu_{nd}} \alpha e^{-bS}\right)^2} \quad (5.4.24)$$

In this expression b is positive. According to Buckley Leverett theory, the speed of a constant plane of water behind the shock front is given by,

$$\frac{x}{t} = \frac{q_{total}}{A\phi} f'(S) \quad (5.4.25)$$

that is,

$$\frac{x}{t} = \frac{q_{total}}{A\phi} \frac{\frac{\mu_d}{\mu_{nd}} \alpha b e^{-bS}}{\left(1 + \frac{\mu_d}{\mu_{nd}} \alpha e^{-bS}\right)^2} \quad (5.4.26)$$

We have just calculated the distribution of the shock front saturation S^* , equation (5.4.21), and we would now like to find the distribution of (5.4.26) using the shock front saturation distribution. Setting $S^* = \eta$, which is a random variable representing the shock front saturation, and $\nu = x/t$

$$\nu = g(\eta) = \frac{q_{total}}{A\phi} \frac{\frac{\mu_d}{\mu_{nd}} \alpha b e^{-b\eta}}{\left(1 + \frac{\mu_d}{\mu_{nd}} \alpha e^{-b\eta}\right)^2} \quad (5.4.27)$$

Multiplying the numerator and denominator by $e^{2b\eta}$ and setting $R = e^{b\eta}$ results in a quadratic in R :

$$\nu = \frac{q_{total}}{A\phi} \frac{\frac{\mu_d}{\mu_{nd}} \alpha b R}{\left(R + \frac{\mu_d}{\mu_{nd}} \alpha\right)^2} \quad (5.4.28)$$

$$\nu R^2 + \frac{\mu_d}{\mu_{nd}} \alpha \left(2\nu - b \frac{q_{total}}{A\phi}\right) R + \left(\frac{\mu_d}{\mu_{nd}} \alpha\right)^2 = 0 \quad (5.4.29)$$

Using the quadratic formula we have,

$$R(\nu) = \frac{-B \pm \sqrt{B^2 - 4AC}}{2A} \quad (5.4.30)$$

where,

$$A = \nu \quad (5.4.31)$$

$$B = \frac{\mu_d}{\mu_{nd}} \alpha \left(2\nu - b \frac{q_{total}}{A\phi}\right) \quad (5.4.32)$$

$$C = \left(\frac{\mu_d}{\mu_{nd}} \alpha\right)^2 \quad (5.4.33)$$

The inverse function of $\nu = g(\eta)$, which we denote $g^{-1}(\nu)$ is then given by:

$$g^{-1}(\nu) = \log[R(\nu)]/b \quad (5.4.34)$$

Following the approach taken in using expectation to calculate the shock front saturation, we can calculate the distribution of the shock front velocity:

$$P[0 \leq V(t, S, Z) \leq \gamma] = \int_0^\gamma \chi(g^{-1}(\nu)) \left| \frac{\partial g^{-1}(\nu)}{\partial \nu} \right| d\nu \quad (5.4.35)$$

In these calculations $\chi(\eta)$, the probability density function of the shock front saturation, is given by (5.4.17) and (5.4.21). Once again, the expression obtained is not simple, but it can be evaluated quite easily using numerical methods and any symbolic package can evaluate and plot the function. Although the expression looks complicated, it is simpler than first appears, since $A, \alpha, b, q_{total}, \phi, \mu_d, \mu_{nd}, \sigma,$ and μ are known constants.

Why two solutions for R?

We have assumed there is a shock front solution in order to avoid the physically impossible situation of a triple valued solution. Under this assumption, the saturation changes smoothly along the rarefaction wave from the saturation value of S to the shock front value S^* , at which point there is an abrupt change in saturation to the right initial state S_r . This means that saturations between S^* and S_r are not physically valid.

One of the solution $R(\nu)$ of the quadratic corresponds to the lower half of the velocity function, which we discard as non-physical. The other solution is for the half corresponding to the correct values. It is easy to tell which solution is relevant. When we take $\log[R(\nu)]/b$, the appropriate $R(\nu)$ will result in a function that is evidently the inverse of (5.4.27). Generally, it will be visually obvious, but a simple plot of $g(\log[R(\nu)]/b)$ will produce a

straight line of gradient 1 for the correct root, and the other value of $R(\nu)$ will not. A fully worked example is given in the next chapter.

Position

We have calculated the velocity of a plane of wetting fluid with a fixed saturation. The position at time t (we will be especially interested in the position of the shock front) is given by

$$x_{S_w} = vt \tag{5.4.36}$$

If the velocity is a random variable denoted by V , and the position is a random variable denoted X (which we do not yet know), then we can calculate the distribution of X :

$$f_X(x) = \frac{f_V(x/t)}{t} \tag{5.4.37}$$

where f_V is given by (5.4.35). Here f is the probability density function, not to be confused with the flux function. This leads to:

$$P[0 \leq X(t, S, Z) \leq \beta] = \frac{1}{t} \int_0^\beta \chi(g^{-1}(x/t)) \frac{\partial g^{-1}(x/t)}{\partial \nu} dx \tag{5.4.38}$$

5.5 Conclusion

At the start of this chapter, the goal was to calculate the shock front saturation, and the position and velocity of the shock front under conditions of uncertainty. These results are found at (5.4.21), (5.4.35) and (5.4.38). In the next chapter we will work through an example reservoir.

The results are entirely dependent on the assumptions:

- **A1** We restrict the model to this situation in which (5.3.3) is appropriate, that is, there is a linear relationship between saturation and the logarithm of the permeability ratio.
- **A2** The initial conditions (saturations) are non-random.

It is fairly easy to question assumptions in any mathematical work. The simple fact of the matter is we need an expression for the flux function in order to obtain a closed form solution. The flux function chosen is sufficiently general to obtain results that are relevant and interesting. It is clear that even with a relatively simple flux function, the calculations become exceedingly difficult.

Chapter 6

Numerical Results

“The theory of probability is nothing more than good sense, confirmed by calculation.” (Pierre Laplace)

In this chapter we will evaluate the expressions developed in the previous chapter. The calculations will be based upon typical reservoir data.

6.1 Introduction

In Chapter Five we obtained closed form solutions for the distributions of a number of quantities of interest. In this chapter we will calculate the deterministic values of a number of important reservoir quantities, based upon an example reservoir. This will be followed by the equivalent stochastic calculations.

6.2 Example Reservoir

Table (6.1) contains the various values we need in order to apply Buckley-Leverett to the modeling of two-phase flow. It should be obvious that the

example does not pretend to be a real reservoir. We are only considering one dimensional, horizontal flow. The parameters included in the table are generally known to a good degree of accuracy compared to the relative permeability curves. It is upon this basis that we have concentrated on the errors and variation in relative permeability.

Reservoir Length, L	300 m
Cross-sectional area, A	2500 m ²
Porosity, ϕ	25%
Injection rate i_w	100 m ³ /day \equiv 629 bbl/day
Oil viscosity, μ_o	2.0 cp
Water viscosity, μ_w	1.0 cp
Connate water saturation, S_{wc}	26.5%
Initial water saturation, S_{wi}	26.5%
Critical oil saturation S_{oc}	20%
Formation thickness, h	20 m

Table 6.1: Example reservoir.

Table (6.2) shows experimental imbibition relative permeability data for water (increasing) and oil (decreasing) of a sample taken in the Malay Basin.¹ These represent typical water and oil relative permeability curves. It is understood that there is an underlying true model for the data set, but measurement errors prevent us from obtaining an exact picture. In the following, water is the wetting fluid and oil the non-wetting fluid.

Relative permeability are usually shown as smooth and well behaved curves. This gives a false impression of uniformity. In the steady state method (which is how this example was derived), a set of discrete values is obtained. Interpolation is employed between data points to obtain smoothness. The curves

¹Coyne [37] page 7.

S_w	0.265	0.313	0.376	0.430	0.488	0.560	0.628	0.700	0.800
k_{rw}	0.000	0.006	0.025	0.075	0.180	0.280	0.400	0.520	0.750
k_{ro}	1.000	0.650	0.350	0.230	0.150	0.070	0.021	0.004	0

Table 6.2: Saturation values

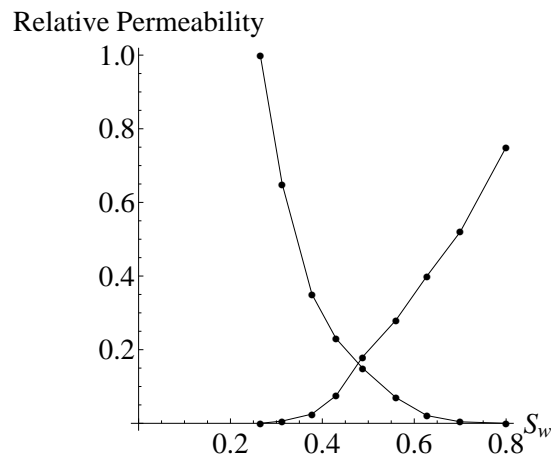


Figure 6.2.1: Malay Basin example

shown in Figure (6.2.1) are in their natural, non-smoothed state. The reader may consult Carlson [27] Chapter Seven (pages 182-189 in particular) for examples of individual, unadulterated relative permeability curves.

Following the approach of Ahmed [2] or Craft and Hawkins [38] amongst others, we form the ratio k_{ro}/k_{rw} and make a semi-log plot against saturation, as shown in Figure (6.2.1). The linear relationship on the interval $[0.3, 0.7]$ is clearly very strong. We are limited in making any claims outside this interval if we wish to use a linear (or possibly higher polynomial) approximation for the data. Fortunately the saturation values outside the linear region play a small part in the calculation we wish to make. This corresponds to the regions of the lower values of the derivatives, and the error has a small effect on

the calculations². When we do need to look outside this region, for example when considering recovery, we shall take a different approach.

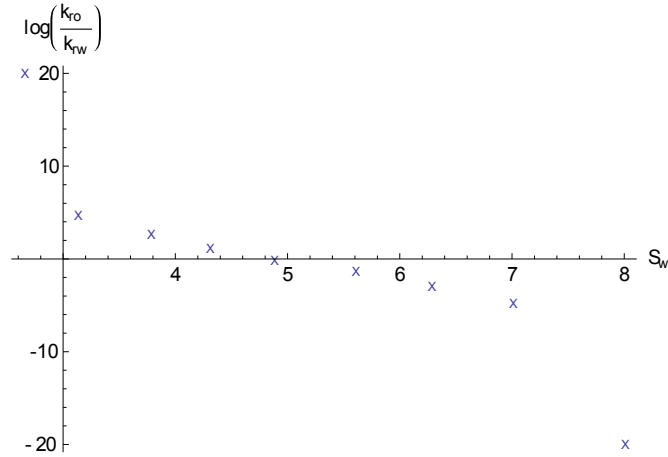


Figure 6.2.2: Semi-log plot.

We can calculate the coefficients of the fractional flow curve by performing linear regression on $y = S_w$ against $x = \log\left(\frac{k_{ro}}{k_{rw}}\right)$. The coefficients are given by:³

$$b = \frac{\sum_{i=1}^n (x_i - \bar{x})(y_i - \bar{y})}{\sum_{i=1}^n (x_i - \bar{x})^2} \quad (6.2.1)$$

$$a = \bar{y} - b\bar{x} \quad (6.2.2)$$

and the mean square error is,

$$s^2 = \frac{\sum_{i=1}^n (y_i - \bar{y})^2}{n - 2} \quad (6.2.3)$$

Tables (6.3) and (6.4) summarise the regression calculations.

²Craft and Hawkins [38] page 351.

³Draper and Smith [52] page 22-25.

	Estimate	SE	TStat	PValue
1	10.9078	0.4352	25.0624	0.0000
x	-22.3313	0.8030	-27.8086	0.000

Table 6.3: Parameter values.

	DF	SumOfSq	MeanSq	FRatio	PValue
Model	1	37.0861	37.0861	773.32	0.0000
Error	4	0.1918	0.0480		
Total	5	37.2779			

Table 6.4: ANOVA

This results in the fitted model:

$$y = -22.3313S_w + 10.9078 \quad (6.2.4)$$

The estimated variance is 0.048 and R^2 is 0.99, indicating a very good fit. It is common practice with regression analysis to assume the errors are normal independent and identically distributed random variables with zero mean and some variance σ^2 . Provided the model chosen is the correct model, then using s^2 as an estimate of σ^2 is appropriate.⁴ If we have chosen the incorrect

⁴[52] page 35.

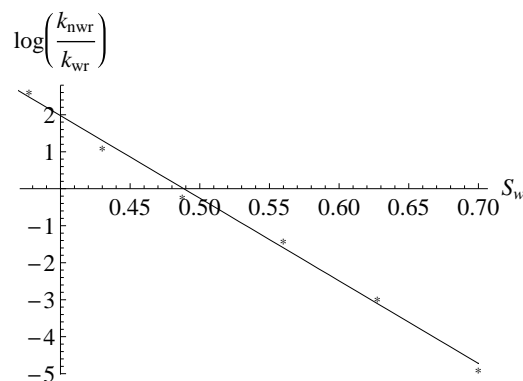


Figure 6.2.3: Fitted line.

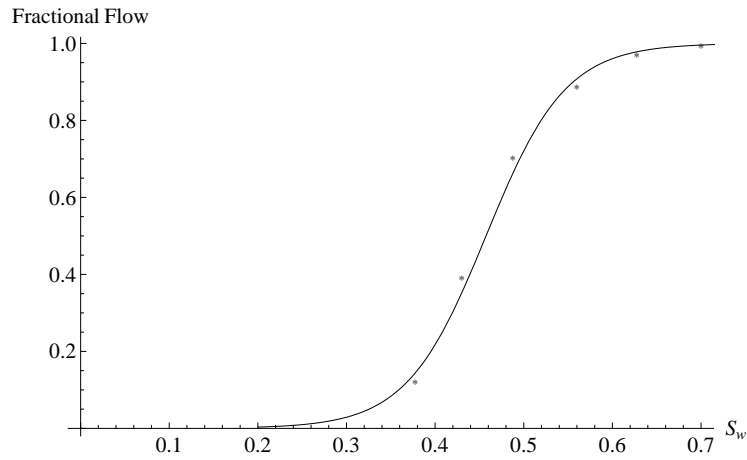


Figure 6.2.4: Fractional Flow

model (in this case that the ratio of relative permeabilites are semi-log linear) then we cannot use s^2 for the variance.

With the calculated values of a and b , and the viscosities of each fluid, we obtain an analytical expression for the fractional flow equation:

$$f_w = \frac{1}{1 + 0.5e^{-22.3313S_w + 10.9078}} \quad (6.2.5)$$

The curve in Figure 6.2.4 is the graph of equation (6.2.5) and the points are the fractional flow calculated using the now familiar form:

$$f_w = \frac{1}{1 + \frac{k_{ro}\mu_w}{k_{rw}\mu_o}} \quad (6.2.6)$$

As is evident from the figure above, the fractional flow approximation is very good for middle saturation value.

There are at least four different kinds of error that afflict this model, the first two of which we have captured with a degree of success. Modeling error is the difference between the fitted model and the true values. Estimation error incorporates the non-exact measurement of the apparatus used to determine

data values (this is examined in Tao and Watson [155][154]). Closely related to this is the error introduced by incorrect procedure, for example, how were the cores prepared, whether the testing fluids are truly indicative reality. Finally, and most significant of all, there is error due to variation between core samples. This last source of error will generally be greater than the others.

Accounting for Variation

Relative permeability curves are often averaged. This may be done to describe a multilayer reservoir where each layer is described by a number of curves⁵. Reducing a multilayer problem to a single layer is a simplifying assumption that can help in the simulation of a large field that cannot be solved otherwise.⁶ Methods for obtaining pseudo relative permeability and upscaling is discussed at length in Carlson [27] Chapter Eight. Averaging may also be performed because the results of permeability measurements on several core samples will almost certainly vary, however, a single set of curves is required for calculations.

Dake 2001 [43] notes that averaging is a questionable practice (even though widespread) as it has no theoretical basis, and he gives an example where employing averaging clearly gives the incorrect result. Despite the theoretical concerns, it is also true that there is no viable alternative.⁷ Without joining the debate, the techniques employed in the last two chapters are amenable to a form of averaging. This procedure is less ad-hoc because it would be performed within the framework of regression on the combined values from several curves, with the added flexibility of fitting the curve and analysing the errors. A general method for normalizing relative permeability curves (to remove the influence of different initial water and critical oil saturations), averaging, and finally de-normalizing, is given in Ahmed [2] Chapter Five. We

⁵Ahmed [2] page 311.

⁶Carlson [27] page 205.

⁷Carlson [27] page 180.

S_w	0.10	0.20	0.30	0.40	0.50	0.60	0.70	0.80	0.90
k_{rw1}	0.035	0.100	0.170	0.255	0.360	0.415	0.585	0.700	0.840
k_{ro1}	0.910	0.810	0.720	0.630	0.540	0.440	0.330	0.230	0.120
k_{rw2}	0.075	0.148	0.230	0.315	0.405	0.515	0.650	0.745	0.870
k_{ro2}	0.880	0.780	0.670	0.510	0.460	0.370	0.270	0.170	0.070
k_{rw3}	0.020	0.066	0.134	0.215	0.310	0.420	0.550	0.680	0.825
k_{ro3}	0.930	0.850	0.780	0.700	0.610	0.520	0.420	0.320	0.180

Table 6.5: Values for three cores.

will use this example as a means to account for variability. Rather than trying to create an averaged curve, we are only interested in the combined error.

Consider the normalized data value for three different cores in Table (6.5).⁸ The semi-log plot of the relative permeability ratio is shown in Figure 6.2.5. In this example, the cores are distributionally similar, and averaging to obtain a combined total error appears to make sense. In this case, the estimated variance is 0.091. It is proposed that the samples could then be de-normalized following the direction of Ahmed [2], and the error term applied to each sample. In this way, the variation between samples is accounted for, without attempting to obtain an averaged curve.

The papers of Amaefule et al. [5] and Behrenbruch and Goda [15], which were discussed in section 4.6.3, provide some interesting ideas with regards to accounting for core variation. These papers discuss methods for determining samples that come from a single hydraulic unit: *Samples that lie on the same straight line [on a log-log plot of RQI versus ϕ_z] have similar pore throat attributes.*⁹ Attempting to average in any way samples that belong to different flow units will of course always produce a nonsense result. Averaging can

⁸These are taken from the normalization example in Ahmed [2] page 319.

⁹Amaefule et al. [5] page 3.

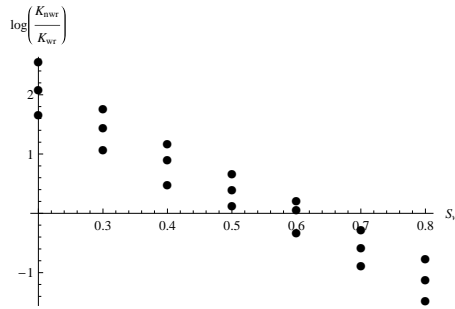


Figure 6.2.5: Three cores, plotted values.

only make sense if there is some kind of distributional similarity between the samples. This is a topic for future discussion.

While it is understood error and variation is an inherent quantity of all relative permeability curves, how it is quantified is an open issue and certainly not a simple matter. Our immediate goal is to work through the mathematics. For the following calculations we will only focus on the modeling error and estimation error, since there is a procedure for deriving this through regression. It is assumed the correct preparation procedures were used, and although sample variation is not incorporated into the model, a way in which this can be done has at least been proposed. We are always free to increase the size of the mean square error at any stage, either because it would be more realistic or simply to determine the consequences.

6.3 Deterministic Calculations

The shock front saturation is found by solving equation (5.4.1), with the flux function given by (6.2.5), which is easily done using *Mathematica*. This results in the shock front saturation,

$$S^* = 0.528 \tag{6.3.1}$$

and front water-cut,

$$f_w|_{s^*} = 0.829 \quad (6.3.2)$$

The position of the shock front is given by equation (5.4.36). For the example reservoir,

$$\begin{aligned} x|_{s^*} &= \left(\frac{100 \text{ m}^3/\text{day}}{2500 \text{ m}^2 \times 0.25} \right) \frac{df}{dS}|_{s=0.528} \times t \\ &= 0.507t \text{ meters} \end{aligned} \quad (6.3.3)$$

where t is in days. The velocity of the shock front is thus 0.507 meters/day. At this rate, the shock front would take 591 days to reach the end of the reservoir. The deterministic calculations in this section are found in any standard textbook on petroleum engineering, including Ahmed [2], Craig [39], Craft and Hawkins [38], Dake [44], Green and Willhite, Lake [96] and Towler [164].

6.4 Stochastic Calculations

To this point, we really have not calculated anything new. We have taken a quite standard approach to using the Buckley-Leverett equation. Where we depart from the past is how we treat the error term. The previous deterministic results will now become distributions. We begin with the expression for the distribution of the shock front, using equations (5.4.18) to (5.4.21).

6.4.1 Stochastic Shock Front Saturation

$$\xi(\eta) = \frac{1}{\frac{1}{2}e^{10.9078}(22.3313(\eta - 0.265) - 1)e^{-22.3313\eta}} \quad (6.4.1)$$

$$\frac{\partial \xi(\eta)}{\partial \eta} = \frac{22.3313(22.3313(\eta - 0.265) - 2)}{\frac{1}{2}e^{10.9078}(22.3313(\eta - 0.265) - 1)^2 e^{-22.3313\eta}} \quad (6.4.2)$$

$$\psi(\xi(\eta)) = \frac{N_{(0,\sigma^2)}(\ln[\xi(\eta)])}{|\xi(\eta)|} \quad (6.4.3)$$

$$P[0 \leq S(t, x, Z) \leq \beta] = \int_0^\beta \frac{N_{(0, \sigma^2)}(\ln[\xi(\eta)])}{|\xi(\eta)|} \frac{22.3313(22.3313(\eta - 0.265) - 2)}{\frac{1}{2}e^{10.9078}(22.3313(\eta - 0.265) - 1)^2 e^{-22.3313\eta}} d\eta \quad (6.4.4)$$

where $N_{(\mu, \sigma^2)}(x)$ is the normal distribution for which in the calculations above the mean μ is zero and the variance σ^2 is set at 0.048, using the expression for s^2 from ANOVA. Equation (6.4.4) appears more complicated than it actually is: the expression is simply a transformation of the normal distribution. It is easy to integrate numerically and is shown at Fig. (6.4.1). The area under the curve and the expected value, both calculated numerically, are 1.000 and 0.528 respectively. The expected value corresponds to (6.3.1).

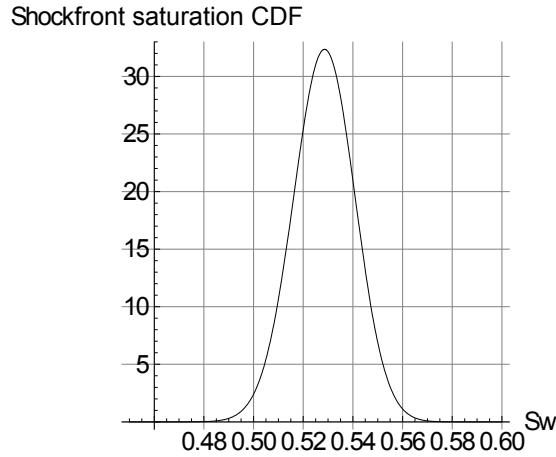


Figure 6.4.1: Shock front distribution, linear case.

6.4.2 Stochastic Velocity

In this section we will evaluate equations (5.4.27) to (5.4.35) in order to find the distribution and expected value of the velocity of the shock front. The first of these equations is for the velocity of a plane of water with constant saturation.

$$\nu = g(\eta) = \frac{97544.2e^{-22.3313\eta}}{(1 + 27300.3e^{-22.3313\eta})^2} \quad (6.4.5)$$

We are only interested in that half of the curve with higher water saturation values so that physically impossible triple valued solutions are avoided. This interval is shown in Fig (6.4.2).

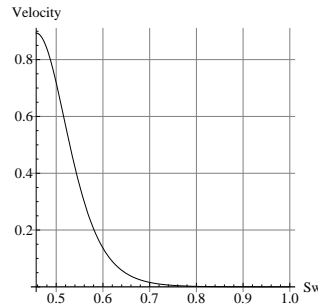


Figure 6.4.2: Velocity values that are physically acceptable.

Multiplying the numerator and denominator by $e^{2 \times 22.3313\eta}$ and setting $R = e^{22.3313\eta}$ results in a quadratic in R :

$$\nu = \frac{97544.2R}{(R + 27300.3)^2} \quad (6.4.6)$$

$$R^2 + \left(54600.6 - \frac{97544.2}{\nu}\right)R + \frac{(27300)^2}{\nu} = 0 \quad (6.4.7)$$

Using the quadratic formula we have,

$$R(\nu) = \frac{1}{2} \left(-54600.6 + \frac{97544.2}{\nu} \pm \sqrt{-2.98123 \times 10^9 + \left(54600.6 - \frac{97544.2}{\nu}\right)^2} \right) \quad (6.4.8)$$

The inverse function of $\nu = g(\eta)$, which we denote $g^{-1}(\nu)$ is then given by:

$$g^{-1}(\nu) = \log[R(\nu)]/22.3323 \quad (6.4.9)$$

The larger root is the correct one for the inverse function and is shown below.

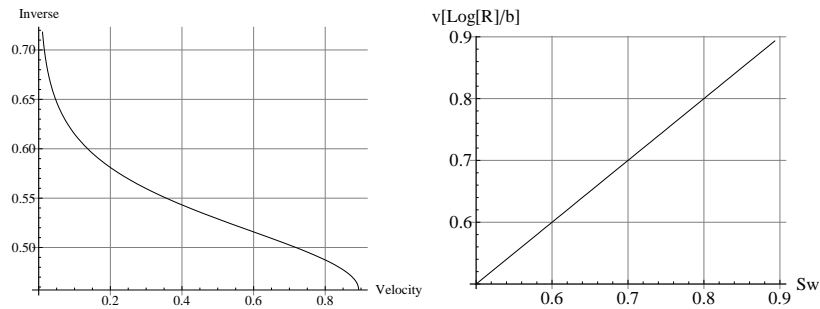


Figure 6.4.3: The inverse, and verification.

The simple test to ensure we have the correct inverse, given the function is one-to-one over the domain of interest, is plotting $g^{-1}(g(\eta))$. This results in a perfectly straight line.

Following the approach taken in using expectation to calculate the shock front saturation, we can calculate the distribution of the shock front velocity:

$$P[0 \leq V(t, x, Z) \leq \gamma] = \int_0^\gamma \chi(g^{-1}(\nu)) \left| \frac{\partial g^{-1}(\nu)}{\partial \nu} \right| d\nu \quad (6.4.10)$$

where the pdf χ comes from (5.4.21). The result is shown in Figure (6.4.4).

Perhaps it is worth pointing out that the distribution shown above is not the spread of velocities for a single saturation value. Rather, there is a spread of shock front saturations that arise because of the uncertainty we are endeavoring to model. For each of these specific saturation values there is a corresponding velocity.

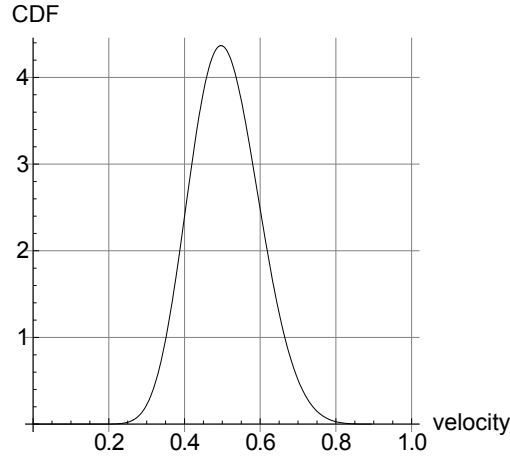


Figure 6.4.4: Distribution of shock front velocities.

6.4.3 Stochastic Position

In this section we will evaluate equations (5.4.37) and (5.4.38) in order to calculate the distribution of the position of the shock front at various points in time. Since we have the distribution for the velocity, we are finding the the function of a distribution we already know.

$$f_X(x) = \frac{f_V(x/t)}{t} \quad (6.4.11)$$

where f_V is given by (5.4.35). This leads to:

$$P[0 \leq X(t, S, Z) \leq \beta] = \frac{1}{t} \int_0^\beta \chi(g^{-1}(x/t)) \left| \frac{\partial g^{-1}(x/t)}{\partial \nu} \right| dx \quad (6.4.12)$$

It was calculated that a fixed plane of water at the shock front saturation of 0.528 would take 591 days to travel 300 meters. Figure (6.4.5) show the movement of the shock front at 100, 200 and 400 days, along with the corresponding position and distribution at each of these times. Over time, the distribution widens, as expected. In each case, it is slightly skewed to the right. Long tailed distributions are not commonly employed in petroleum engineering. We could have used a curtailed normal distribution. Beta distributions, which have a fixed support, are frequently employed in modeling.

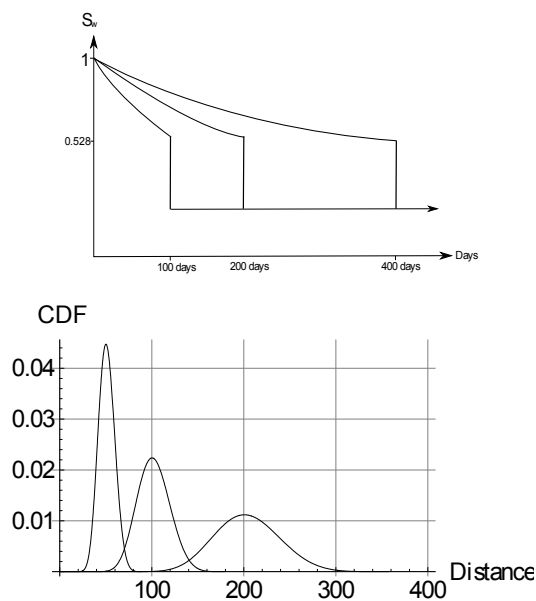


Figure 6.4.5: Shock front position

Mathematically, we are not restricted, and are free to use whatever distribution is most appropriate. Since we are dealing with error, the normal distribution, curtailed or otherwise, is the natural choice.

6.5 Extensions and Considerations

6.5.1 Non-Linear Semi-Log Relationships

Although the case in which the ratio of relative permeabilities forms a semi-log relationship covers a wide range of cases, we are not restricted to the linear case, because regardless of the regression function the error term can still be written $Z = e^\varepsilon$. Of course, some calculations will be easier than others. A significant benefit of the approach we have taken is there is a wealth of information on regression and analysis of errors. Rather than simply approximate the fractional flow equation and the errors, the error term is at the center of all the calculation we have made.

Using the Malay Basin data, we can fit a cubic to the logarithm of the permeability ratio, as was done for the linear case. Once again, the end data values for low and high saturations have been omitted since they are irrelevant for calculations. The model is:

$$g(S) = 4.02S^3 - 7.34S^2 - 17.98S + 10.08 \quad (6.5.1)$$

To calculate the distribution of the shock front, we must repeat 5.4.18 to 5.4.21, modified for a general regression function $g(S)$,

$$\xi(\eta) = \frac{-1}{\frac{\mu_d}{\mu_{nd}}(1 + g'(\eta)(\eta - S_c))e^{g(\eta)}} \quad (6.5.2)$$

$$\frac{\partial \xi(\eta)}{\partial \eta} = \frac{g'(\eta)[2 + g'(\eta)(\eta - S_c)] + g''(\eta)(\eta - S_c)}{\frac{\mu_d}{\mu_{nd}}(1 + g'(\eta)(\eta - S_c))^2 e^{g(\eta)}} \quad (6.5.3)$$

$$\psi(\xi(\eta)) = \frac{N_{(0,\sigma^2)}(\ln[\xi(\eta)])}{|\xi(\eta)|} \quad (6.5.4)$$

$$P[0 \leq S^*(t, x, Z) \leq \beta] = \int_0^\beta \psi(\xi(\eta)) \left| \frac{\partial \xi(\eta)}{\partial \eta} \right| d\eta \quad (6.5.5)$$

Evaluating these expressions results in Figure 6.5.1. Comparison with Figure 6.4.1 shows the two graphs are distinctly similar. The expectation for the cubic case is 0.529 and for the linear case 0.528. Otherwise, it is difficult to distinguish between the two distributions. In the context of probability models, a difference of this order is negligible and the extra computational difficulty is hard to justify.

Determining the velocity distribution adds an extra layer of complexity compared to the linear case. This arises because it will be necessary to calculate the distribution of the regression expression as a function of the shock front distribution previously calculated. Section (5.4.1) explains how to determine the distribution of the function of a known distribution. We have used this technique a number of times over the last two chapters. The cases of linear,

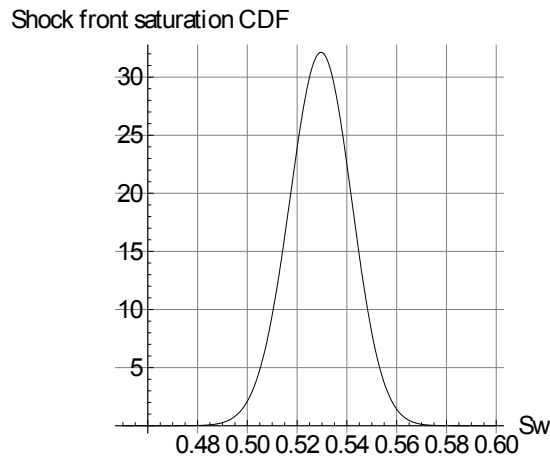


Figure 6.5.1: Shock front position, cubic regression.

quadratic and cubic semi-log relationships would likely be more than enough for modeling any realistic fractional flow curve. For the Malay Basin, the additional accuracy is not worth the computational effort - but it can be done.

6.5.2 Generalized and Weighted Least Squares

How might we handle the case where some observation are less reliable than others? Generalized least square applies when the error covariance matrix is not diagonal. When it is diagonal, but the variance terms are not equal, weighted least squares applies.¹⁰ The easiest way to determine if heteroscedacity exists is by examining the residual plot. Virtually all symbolic and numerical computer packages can perform weighted regression. In *Mathematica* it is an option under the *Regress* command, as part of the *LinearRegression* package.

For the calculation in this chapter, we are interested in the fractional flow curve only in the neighborhood of the shock front saturation. Over a small

¹⁰Draper and Smith [52] page 223

interval of saturation values, we do not expect the variance to change greatly. On this basis, there would seem to be little benefit in complicating the model still further. It is simply noted that the tools of regression analysis are more than capable of dealing with this situation if required. Heteroscedacity is more likely to pose a problem when examining recovery efficiency. Recovery calculations are made over the saturation interval between the shock front saturation and the critical oil saturation. We shall revisit this issue later.

6.5.3 Uncertainty is an Open Issue

It is well and good to derive a stochastic version of the Buckley-Leverett equation, and make a number of calculations based on this model, but how exactly is the level of uncertainty quantified? We have endeavored to cover modeling error within a sample, and determining the standard error through averaging for the multi-core case was proposed. What about the errors introduced through using inappropriate fluids or preservation techniques, for example? There is no simple answer - certainly not one that will be provided here. The problem is not unlike the problem faced in using the Black-Scholes formula.¹¹ Black-Scholes is an elegant and highly successful model for determining the price of options. However, the accuracy of Black-Scholes is limited by the determination of the volatility. This has not stopped the model being useful.

6.6 Conclusion

In this chapter we have calculated everything we set out to determine from the expressions that were derived in Chapter Five. It was assumed that the experimental fractional flow curve is a noisy representation of the true, underlying curve that we are attempting to model. Regression would appear

¹¹Black and Scholes [17].

to be a sound method for modeling the true curve.

At no point are we trying to model a particular realization of reality. The approach taken involved modeling the fractional flow curve, while cognisant of the errors in measurements. What separates the method we have used from previous work is the specific interest in how the errors propagate. The reward from taking this approach is we have obtained distribution and expected values of the quantities of interest such as the:

- shock front saturation;
- shock front velocity; and,
- position over time of the shock front.

The method we have used is not a simple one, but difficult problems generally do not have simple solutions. These kinds of problems are difficult to solve because they are non-linear and the solutions involve discontinuities. By adding a stochastic terms there is now a further level of complexity that makes the problem almost intractable. The solution we have obtained are certainly not trivial. A number of extensions were also discussed, although each would make the model even more complicated.

Chapter 7

Break Through and Beyond

“There’s a whole ocean of oil under our feet! No one can get at it except for me!” (from the film *There Will Be Blood*)

This chapter examines production from the time the shock front reaches the end of the reservoir. The distribution of the breakthrough time is calculated. Distributions and expectations for recovery are then calculated. This completes the model, as all quantities of interest have been determined within a stochastic setting.

7.1 Introduction

All the quantities we have calculated to this point only depend upon modeling the fractional flow function in the vicinity of a single point of the curve, corresponding to the point of tangency of a line drawn from the initial water saturation to the fractional flow curve. It has been important that we were able to describe the behavior of the fractional flow function f_w in the neighborhood of the point of tangency, but the other points of the flux function have been essentially irrelevant to the solution. In order to describe recovery efficiency we need to accurately model the flux function on an interval above

the shock front saturation S^* .

It is relatively easy to obtain good approximation for fractional flow in the vicinity of the shock front saturation - in this region the logarithm of the relative permeability ratio often forms a linear relationship. The analytical expression we use so far is less effective for low saturation values and very high saturation values. This deficiency does not significantly impact on the calculations we wish to make. The low saturation values are irrelevant to recovery calculations, and high saturations correspond to the circulation of a large number of pore volumes of the displacing fluid, which is also of limited relevance. If it is likely to be a problem, we are free to switch to a function that can provide a better approximation to fractional flow over an extended range. We can still use regression to find a suitable function, but more terms may be involved.

A distribution for the breakthrough time can be calculated, following the methods employed in previous two chapters. To calculate recovery efficiency it is necessary to first model the fractional flow curve for high saturation values. Oil recovery was first calculated by Welge in 1952 [169] by determining the average water saturation behind the shock front. We will look at the expression Welge used, along with his method of integration. We will then consider a stochastic model in order to obtain equivalent results. The total oil recovery and the number of injected pore volumes of water required to achieve this result will be calculated, but the solution will be in terms of probability distributions. At the end of Chapter Eight, an alternative approach is suggested, along the lines of stochastic splines. This is entirely ancillary to the previous work, and merely points the way to one possible avenue of future research.

7.2 Breakthrough Time

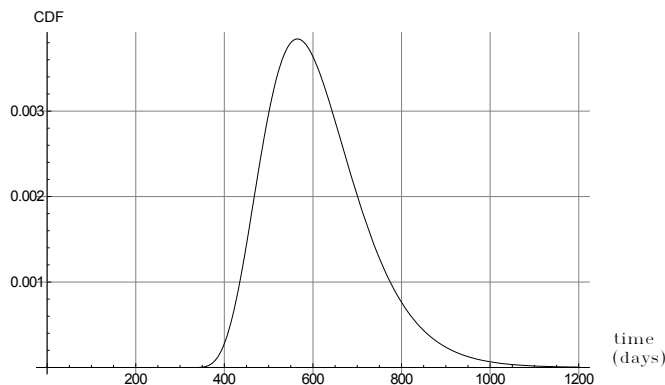


Figure 7.2.1: Breakthrough Time

We previously calculated the velocity distribution of the shock front. This can be used to derive a distribution for the breakthrough time. If the reservoir has length L , then the relationship between velocity and breakthrough time is,

$$t_{bt}(v) = L/v \quad (7.2.1)$$

We have a simple functional relationship between breakthrough time and velocity, and there is a straight forward derivative and inverse function. The derivative is given by,

$$t'_{bt}(v) = \frac{-L}{v^2} \quad (7.2.2)$$

and since (7.2.1) is self-inverse,

$$t_{bt}^{-1}(v) = L/v \quad (7.2.3)$$

If the velocity distribution density is given by $f_V(v)$, then the distribution density of the breakthrough time will be:

$$f_{bt}(y) = \frac{L f_V(L/y)}{y^2} \quad (7.2.4)$$

Employing the velocity probability density function within the integrand of (5.4.35) and the parameters of the example reservoir, we obtain Figure 7.2.1.

The expected value of the distribution (7.2.4) is 610 days and the mode is 565 days. The deterministic value for this calculation based on zero error was 591 days. The distribution is mildly right skewed, which is evident visually as well as from the difference in the mode and expected value. Some degree of skewing is to be expected since there is an abrupt limit to how fast the front can move.

7.3 Average Saturation and Recovery

Extending the Buckley-Leverett model to encompass average saturation and oil recovery was first proposed by Welge [169]. To calculate recovery, it is necessary to determine the average water saturation behind the shock front. We will look at the expression Welge used, and directly follow his method of integration. Welge obtained an elegant graphical solution for obtaining both the shock front saturation and the average saturation. After deriving the key equations, we will examine a stochastic version of recovery efficiency.

The situation before water breakthrough has occurred is shown graphically in Figure 7.3.1.¹ It was noted in Craig [39] that the value of f' at the maximum displacing fluid is not zero, as proposed by Welge, but has a finite value. This necessitates a slight modification to the approach in [169] but does not alter the final result. At the moment the snap-shot is taken, an amount of displacing fluid equal to Q_i has been injected into the block of porous media. In the following, S is the displacing fluid saturation (understood to be water) and S_{max} is the maximum saturation of the displacing fluid (equal to $1 - S_{ndc}$). The initial displacing saturation is the connate saturation S_c . The average displacing saturation can be calculated by integrating over the saturation profile from 0 to x_2 .

$$\bar{S} = \frac{(S_{max})x_1 + \int_{x_1}^{x_2} S dx}{x_2} \quad (7.3.1)$$

¹After Craig [39] Annex E or Dake [44] page 360.

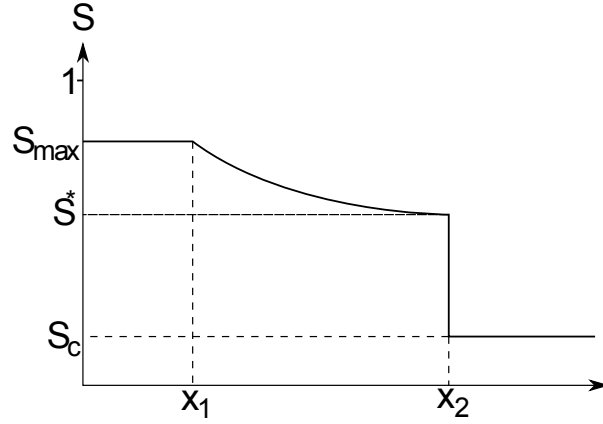


Figure 7.3.1: Profile of Shock Front

Welge observed that since $x \propto f'$ for saturation values behind the shock front, equation (7.3.1) can be written,

$$\bar{S} = \frac{S_{max} \frac{df(S_{max})}{dS} + \int_{x_1}^{x_2} S d\left\{\frac{df(S)}{dS}\right\}}{\frac{df(S^*)}{dS}} \quad (7.3.2)$$

The second term of the numerator can be evaluated using integration by parts,

$$\int_{S_{max}}^{S^*} S d\left\{\frac{df(S)}{dS}\right\} = \left[S \frac{df(S)}{dS} \right]_{x_1}^{x_2} - [f(S)]_{x_1}^{x_2} \quad (7.3.3)$$

$$= S^* \frac{df(S^*)}{dS} - S_{max} \frac{df(S_{max})}{dS} - (f(S^*) - 1) \quad (7.3.4)$$

where S^* is the saturation at the shock front (located at x_2) and the saturation at x_1 has the value S_{max} , so that equation (7.3.2) becomes,

$$\bar{S} = S^* + \frac{(1 - f(S^*))}{\frac{df(S^*)}{dS}} \quad (7.3.5)$$

This is equation (7) of Welge [169].

Turning to the quantity of injected water, from the Buckley-Leverett equation, we know that the velocity of a plane of constant water is given by,

$$v = \frac{q_{total}}{A\phi} \frac{df(S)}{dS} \quad (7.3.6)$$

where q_{total} , the total flow rate, is the sum of flow rate of oil and water ($q_0 + q_w$). Integrating this with respect to time yields,

$$x = \frac{1}{A\phi} \frac{df(S)}{dS} \int_0^t q_{total} dt \quad (7.3.7)$$

If Q_i is the quantity of injected water, then assuming that $Q_i = 0$ at $t = 0$, we have,

$$x = \frac{Q_i}{A\phi} \frac{df(S)}{dS} \quad (7.3.8)$$

At x_2 , which is the location of the shock front (where the saturation is S^*), we then have,

$$\frac{x_2 A\phi}{Q_i} = \frac{df(S^*)}{dS} \quad (7.3.9)$$

At the production end, where $x = L$,

$$\frac{Q_i}{LA\phi} = \frac{1}{\frac{df(S_L)}{dS}} = Q_{dim} \quad (7.3.10)$$

In this last equation, S_L refers to the saturation of water at the end of the porous block having length L . Since the total void space of the block is given by $LA\phi$, it follows that dividing the injected fluid Q_i by the total void space gives the cumulative water injection expressed in terms of the number of pore volumes, denoted by Q_{dim} . In other words, if the entire space available for

fluid is given the value 1 then the cumulative water injected in pore volumes is the fraction of that total space.

Prior to breakthrough, the amount of oil recovered at the production end will be equal to the volume of injected water. At breakthrough, the water saturation will immediately rise to the shock front saturation value, since breakthrough is the instant at which the shock front arrives. After breakthrough, equation (7.3.5) can be rewritten at the production end as:

$$\bar{S} = S_L + \frac{1 - f(S_L)}{\frac{df(S_L)}{dS}} \quad (7.3.11)$$

Since the amount of oil produced, denoted P is the difference between the average and the initial water saturation, that is $\bar{S} - S_c$, subtracting S_c from (7.3.11) gives us the desired recovery equation (expressed in dimensionless pore volumes):

$$P = S_L - S_c + \frac{1 - f(S_L)}{\frac{df(S_L)}{dS}} \quad (7.3.12)$$

To use (7.3.12), we take S_L as the independent variable and using (7.3.10),

$$Q_{dim} = \frac{1}{\frac{df(S_L)}{dS}} \quad (7.3.13)$$

we can calculate Q_{dim} and hence P by incrementally increasing S_L from the breakthrough (shock front) value S^* to the maximum displacing fluid saturation level S_{max} . This is standard fare within the literature, and examples of such calculations can be found in Ahmed [2], Craig [39], Craft and Hawkins [38], Dake [44], Green and Willhite [67], Lake [96] and Towler [164], indeed almost any modern book on petroleum engineering.

Geometric Interpretation

There is a simple geometric means of finding the average saturation behind the shock front. If the tangent line to the fractional flow curve from the initial

wetting saturation to an ordinate of 1 (100% wetting fractional flow), then the abscissa is the average wetting saturation. This is included at Appendix B for completeness. The interested reader may also refer to Dake [44] page 360-362.

7.4 Production with Uncertainty

How is (7.3.12) affected by uncertainty? In previous calculations we made use of the semi-log linear relationship often found for the ratio of relative permeabilities. It was made clear that other relationships could be modeled using the same method.

$$f = \frac{1}{1 + \frac{\mu_d}{\mu_{nd}} e^{g(S)+\varepsilon}} \quad (7.4.1)$$

For the moment, let us assume that the regression has been performed and $g(S)$ is known. From the process of regression, the error term will also be known. Once again the regression error term e^ε can be replaced with the random variable Z . The derivative of f is given by,

$$\frac{\partial f}{\partial S} = \frac{-Z \frac{\mu_d}{\mu_{nd}} g'(S) e^{g(S)}}{(1 + Z \frac{\mu_d}{\mu_{nd}} e^{g(S)})^2} \quad (7.4.2)$$

Both f and its derivative can be substituted into (7.3.12) to give,

$$\begin{aligned} P &= S_L - S_c + (1 - f(S_L)) \frac{1}{\frac{df(S_L)}{dS}} \\ &= S_L - S_c + \left(1 - \frac{1}{1 + Z \frac{\mu_w}{\mu_{nd}} e^{g(S)}}\right) \frac{(1 + Z \frac{\mu_d}{\mu_{nd}} e^{g(S)})^2}{-Z \frac{\mu_d}{\mu_{nd}} g'(S) e^{g(S)}} \\ &= S_L - S_c - \frac{1 + Z \frac{\mu_d}{\mu_{nd}} e^{g(S_d)}}{g'(S_d)} \end{aligned} \quad (7.4.3)$$

Following the approach of Chapter Five, we rearrange (7.4.3) to make Z the subject,

$$Z = \frac{(S_L - S_c - P)g'(S_L) - 1}{\frac{\mu_d}{\mu_{nd}} e^{g(S_L)}} \quad (7.4.4)$$

Setting $Z = \xi$, $P = \varrho$, we have

$$\xi(\varrho) = \frac{(S_L - S_c - \varrho)g'(S_L) - 1}{\frac{\mu_d}{\mu_{nd}} e^{g(S_L)}} \quad (7.4.5)$$

$$\frac{\partial \xi(\varrho)}{\partial \varrho} = \frac{-g'(S_L)}{\frac{\mu_d}{\mu_{nd}} e^{g(S_L)}} \quad (7.4.6)$$

$$\psi(\xi(\varrho)) = \frac{e^{\frac{(\ln[\xi(\varrho)] - \mu)^2}{2\sigma^2}}}{|\xi(\varrho)|\sigma\sqrt{2\pi}} \quad (7.4.7)$$

The distribution for oil recovery at a given endpoint water saturation S_{wL} is then given by:

$$Pr[0 \leq P \leq \beta] \Big|_{S_c} = \int_0^\beta \frac{e^{\frac{(\ln[\xi_\eta(\varrho)] - \mu)^2}{2\sigma^2}}}{|\xi_\eta(\varrho)|\sigma\sqrt{2\pi}} \left| \frac{-g'(S_L)}{\frac{\mu_d}{\mu_{nd}} e^{g(S_L)}} \right| d\varrho$$

Example Calculations

Using the example reservoir and relative permeability curves given at the beginning of Chapter Six, we will calculate recovery efficiency. The first step is to obtain an appropriate regression function for water saturation above the shock front value. This was calculated in Chapter Six as,

$$g(S) = -22.3313S + 10.9078 \quad (7.4.8)$$

Applying the reservoir parameters and (7.4.8) to equations (7.4.5) through to (7.4.8),

$$\xi(\varrho) = e^{22.3313S_L}(0.000180137 + 0.000817987\varrho - 0.000817987S_L) \quad (7.4.9)$$

$$\frac{\partial \xi(\varrho)}{\partial \varrho} = 0.000817987e^{22.3313S_L} \quad (7.4.10)$$

Injected Water (pore vol.)	0.5	1	2	3	10
End Saturation	0.556	0.592	0.625	0.644	0.700
Fractional Flow	0.900	0.953	0.978	0.985	.996
Expected Production (pore vol.)	0.340	0.374	0.406	0.424	0.480

Table 7.1: Production values.

$$\psi(\xi(\varrho)) = \frac{e^{\frac{(\ln[\xi(\varrho)])^2}{2\sigma^2}}}{|\xi(\varrho)|0.219\sqrt{2\pi}} \quad (7.4.11)$$

using $\sigma^2 = .048$ and $\mu = 0$. The distribution for oil recovery at a given end point water saturation S_L is then given by:

$$Pr[0 \leq P \leq \beta]_{S_L} = \int_0^\beta \frac{e^{\frac{(\ln[\xi(\varrho)])^2}{2\sigma^2}}}{|\xi(\varrho)|0.219\sqrt{2\pi}} (0.000817987e^{22.3313S_L}) d\varrho \quad (7.4.12)$$

The recovery results are captured in Table (7.1). The injected water volume (in dimensionless pore volumes) is calculated using equation (7.3.13). Deterministic calculations like this may be found in Craig [39] appendix E. However, the expected production (in a probability sense) and distribution curves for recovery at various saturation values, as shown below, will not be found there or elsewhere.

Recovery

The distributions for production with the value $\sigma = 0.657$ were calculated. This standard deviation is three times greater than that used in the previous calculations we have made. It should be noted that this is *not* based on any sound physical considerations, apart from the understanding that the amount of error in the system must be greater at the relatively late stage of calculating oil recovery, compared to the very beginning of our calculation when we are first determining the shock front saturation. The criticism must be accepted that precisely determining the degree of error is an open issue,

without a simple answer. For the moment we are just interested in working through the mathematics, and showing the progression of recovery over time. We are free to change the amount of error in the system at any time, provided it is justifiable.

The results for oil recovery are shown in Figures (7.4.1) to (7.4.3), for different injected pore volumes. The distribution for Figure (7.4.1) is significantly skewed, with the result that the expected value for oil production in pore volumes is different to the value calculated without a stochastic terms. It is also evident from these plots that the variance diminishes significantly for higher saturation values. This is consistent with Fig. 23.21 of Latil [100] which shows production for two different displacement scenarios: the graph forms a lens shape between slow displacement and rapid displacement curves. The diminished variance is only to be expected. The fractional flow equation is given by (2.4.3), that is

$$f_d = \frac{1}{1 + \frac{\mu_d}{\mu_{nd}} \frac{k_{rnd}}{k_{rd}}}$$

As k_{rnd} approaches zero, f_d approaches unity. This corresponds to a large number of pore volumes circulating through the reservoir (in the order of 10 or more). Probability wise, it is hard to draw any meaningful conclusions about this portion of the curve. Recovery efficiency approaches a limiting value, and regardless of any variation, the dominant factor is how rapidly k_{rnd} approaches zero. It is well understood that recovery efficiency is very sensitive to the shape of the fractional flow curve at higher saturation values. Thus even a small variation in the shape of the curve will strongly effect the number of injected pore volumes required to further alter recovery.

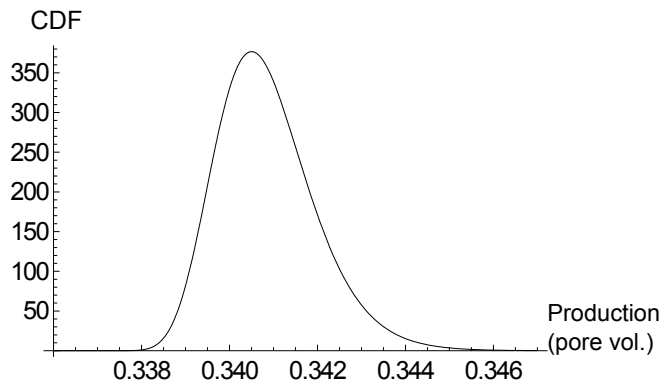


Figure 7.4.1: $Q_{dim} = 0.5$

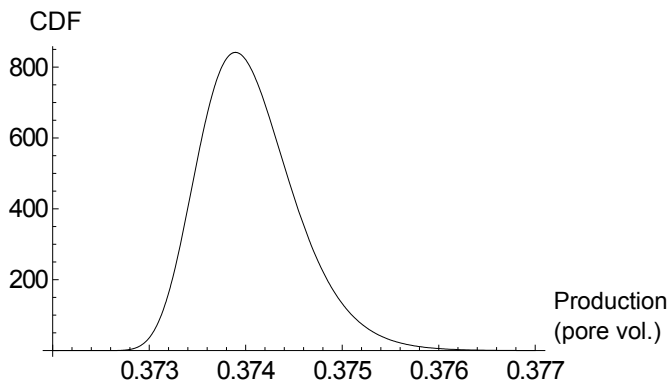


Figure 7.4.2: $Q_{dim} = 1$

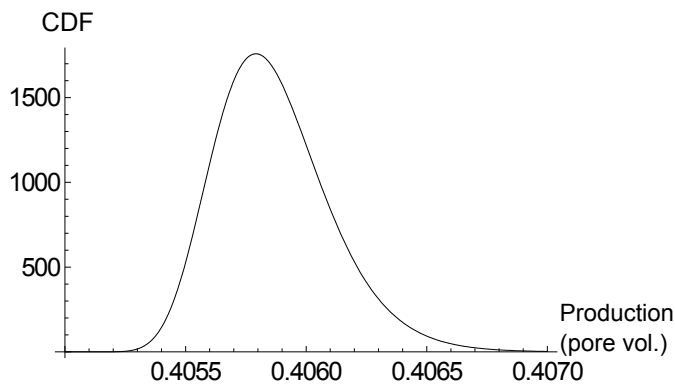


Figure 7.4.3: $Q_{dim} = 2$

7.5 Conclusion

In this chapter, the focus was production from the moment the shock front reached the end of the reservoir, the so called breakthrough time, and followed the asymptotic decline in recovery. The distributions and expectations for breakthrough time and recovery were obtained. The approach taken in this chapter was conceptually the same as the approach taken previously. However, recovery was examined over a large segment of the fractional flow curve, rather than the neighborhood of a single point. Computationally, a valid and meaningful approximation is more difficult to achieve since we need to accurately model the flux function from the shock front saturation S^* to the critical oil saturation S_{or} . As mentioned previously, it is relatively easy to obtain good approximation for fractional flow in the vicinity of the shock front saturation - in this region the logarithm of the relative permeability ratio often forms a linear relationship, although a more complicated relationship can be employed if required.

We might have considered a piecewise approximation to the fractional flow curve, but the question is, will this approach bring a significant improvement in the results? One of the noticeable positives of the last three chapters is that a “family” of results has been obtained that is quite easy to interpret, without being either a gross approximation or too specific. It appears to be true that most realistic situation could be modeled with the approach we have taken. In the next chapter, we will consider an alternative method, along the lines of stochastic splines. This is entirely ancillary to the previous work, and merely points the way to one possible avenue of future research.

Chapter 8

Achievements, Future Research and Concluding Comments

“In mathematics you don’t understand things. You just get used to them.”
(Johann von Neumann)

In this chapter, we will discuss the success and limitations of the approach taken and point to areas of future research.

8.1 Overview

We appear to have achieved as much as one could reasonably expect from taking an analytical approach in which closed form solutions were sought. It was noted at the start that the problem was a particularly difficult one: a first order conservation equation, with a discontinuity, complicated still further by the addition of a stochastic term. Despite the difficulties, a number of results not found elsewhere were obtained. We have produced distributions and expected values for a number of quantities of interest such as the:

- shock front saturation;

- shock front velocity;
- position over time of the shock front; and,
- recovery efficiency.

In summary, we have obtained a well rounded description of the displacement process within a stochastic setting. Other descriptions are possible, and for a number of reasons may even be preferable. However, in light of the mathematical issues, what has been achieved is significant.

Buckley-Leverett is a mathematical model which is useful because it gives insight into the physical processes behind oil recovery. Any claim that the proposed model is also useful rests upon the manner in which the uncertainty inherent in petroleum engineering is translated into the solutions, and helps us to understand the nature of the problem. The material in this thesis is not about to end reservoir simulation and replace it with a stochastic model. We have taken an analytical approach because closed form solutions can provide insight into the physical situation that simulation cannot provide, and on this basis the approach is valid. Such concerns no doubt prompted the plea by Dake, quoted in the Preface, for a revival of displacement modeling based upon fractional flow.

8.2 Limitations and Improvements

Any model lives and dies by the assumptions upon which it is based. Two basic assumptions were made in section 5.3.1. The first restricted the model to the situation in which a clear relationship between saturation and the logarithm of the permeability ratio exists, while the second specified that the initial conditions (saturations) were non-random.

A decision was made to use the fractional flow curve as the vehicle for incorporating the stochastic term. Since this curve is the fundamental input into the Buckley-Leverett model, focusing on fractional flow (rather than relative permeability) is reasonable and supported by at least one prominent author - the one quoted in the Preface. The issue is whether the particular form chosen is too limiting or, for some other reason, inappropriate. The fractional flow curve was given by:

$$f(s) = \frac{1}{1 + \frac{\mu_d}{\mu_{nd}} e^{g(s)}}$$

where $g(s)$ models the logarithm of the ratio of the relative permeability curves and is determined by regression. Any physical situation likely to be faced can be adequately approximated; the accuracy of the approximation depends on the number of terms in $g(s)$. Provided there are enough data points, a high order polynomial or any other suitable function can be fitted. There are many published examples of a linear model being used, and several prominent authors believe this is sufficient for acceptable, although possibly restricted, calculations to be made. By taking the more general approach, we are free to cover a wider range of examples.

The solutions we have generated over the last three chapters depend upon a surprisingly small section of the fractional flow curve. The shock front saturation without a stochastic term was 0.528. Recovery calculations were only relevant up to a saturation of 0.7 and even at this level, 10 pore volumes of water must be injected through the reservoir. In short, the interval [0.5,0.7] is used for calculations, and needs to be modeled effectively - the rest is largely irrelevant. This goes some way to explaining why a semi-log linear model is so effective. Accurately obtaining relative permeability curves across all saturation values is very difficult. Determining the fractional flow over an interval like [0.5,0.7] is significantly simpler. We are also faced with only one uncertainty term, rather than two, which is the case if separate relative

permeability curves are used.

The approach we took involved approximating the data points with smooth curves. Smooth curves for relative permeability and fractional flow are expected by petroleum engineers. ‘Kinked data’ is viewed as bad from a modeling perspective.¹ This is grounds for not considering some kind of solution to the problem in terms of Brownian motion, more common to the methods employed in mathematical finance. This would not be physically appropriate for the Buckley-Leverett model.

Regarding the second assumption, requiring that the initial state is deterministic, this is not the same as insisting the irreducible wetting saturation is deterministic. There is clearly a level of variation in S_{wc} , but since our focus is on middle to high wetting saturations, we have side-stepped the issue to a degree. It would be worthwhile extension of the model if random initial conditions could be included, but that might be hoping for too much mathematically. There is nothing preventing any of the formulas being used with a spread of different initial saturations. This suggests making S_i a independent random variable, which would result in double integrals to calculate distributions and expectations. Perhaps that is something for the future.

The way in which errors have been modeled has features that are good and also not so good. On the positive side, we have obtained a raft of results that otherwise might have proved illusive. We have avoided an ad-hoc approach by providing a mechanism for quantifying degree of error via regression. This approach is flexible since the treasure chest of mathematical tools found in regression analysis is available to interpreting both the input and the output.

When it comes to possible improvement, it is easier to obtain a solution that is locally correct, as opposed to finding a global solution. Everything in

¹Carlson [27] page 199.

Chapter Five, Chapter Six and the first part of Chapter Seven, is firmly focussed on the neighborhood of the shock front, therefore the results are more robust. The stochastic modeling of recovery efficiency is by necessity more problematic because the solution is over all saturation between the shock front and $1 - S_{ndc}$. Heteroscedacity is likely to be a problem for recovery calculations, although limiting this weakness by employing weighted regression was discussed at the end of Chapter Six.

The Buckley-Leverett equation is a first order conservation equation. That is, it takes the form,

$$u_t + f(u)_x = 0$$

In finding and manipulating the solution of a first order conservation equation, we must be alert to the existence of discontinuities and shock fronts, and how they propagate. By contrast, the equation for recovery efficiency is not a first order conservation equation. There is no need to be troubled by discontinuities and weak solutions, the solution is continuous and increasing. Depending on how the problem is formulated, many of the more common tools of stochastic partial differential equations, as found in say Øksendal [126], where continuity is generally assumed, could be used to examine the problem. Once again, this is something for the future.

8.3 Further Work

There are a number of extensions to the work in this thesis and ideas that have arisen from studying this subject. There are many alternative ways of looking at first order conservation equations in general and the Buckley-Leverett equation in particular, within a stochastic setting. The following points are worthy of further consideration.

- We only considered horizontal flow. The addition of a gravity term

does not alter the approach.

- The initial saturation state was taken as given. A more general approach might take this as non-deterministic.
- The distributions calculated in chapters five to seven were left in integral form. It may be possible to evaluate these further if, instead of the normal distribution, the triangular distribution² or even the beta distribution was used. The triangular distribution may seem a gross simplification, but cumulative probability function of comparable triangular and normal distribution are quite similar, and the difference between the two may be unimportant for modeling purposes.
- Recovery efficiency only has continuous solutions, and the problem is open to more general methods.
- The manner in which the error, variation and uncertainty interact with the model needs to be better understood.
- Two-phase, three component models exist for tertiary miscible displacements. Like the Buckley-Leverett model this can be solved analytically. The alternative model has a rich solution structure, and it appears that the ideas covered in this thesis could be extended to the more advanced model in a straightforward fashion.³

8.4 One Alternative Approach

In this section we will consider an alternative approach to finding the distribution of the equation for oil production as a function of the random variable representing saturation. We will not explore this subject fully. Rather, this

²See Kotz and van Dorp [91] for the properties of this distribution.

³This final point was suggested by one of the thesis examiners. Since the examiner is unknown to the writer, it is not possible to correctly attribute this contribution.

is included to show that the problem is open many avenues of attack.

The relative permeabilities are determined at a finite number of discrete points. This motivates us to consider stochastic splines in modeling the fractional flow curve for high water saturation values. We might only be blessed with a handful of data points and must endeavor to obtain the best curve through these point and also obtain a measure of the uncertainty associated with the underlying problem.

We would like to calculate the production recovery efficiency, using (7.3.12). This could be done by:

- representing the flux function by a cubic spline;
- substituting this flux function into the oil production equation P , to obtain a piecewise function;
- inverting the production equation piecewise by solving the resulting cubic or by using Lagrange Inversion; and finally,
- determine the distribution of P by calculating the Expectation.

Recall recovery (production) efficiency is given by (7.3.12):

$$P(S_L) = S_L - S_c + \frac{1 - f(S_L)}{f'(S_L)}$$

There are a number of considerations that will make our task easier. Firstly, f is concave for saturation values greater than the shock front saturation. Better still, it is monotonically increasing on this interval. Our task is to calculate the distribution of P if S_L is a random variable. Fortunately, we no longer have to worry about a discontinuous solution. Recovery efficiency is calculated after the shock front has reached the production end of the reservoir. From that point, there will be a continuous and steady increase in the production level as an ever increasing quantity of water is injected into the

system. We are therefore only concerned with solutions that are continuous.

Since we only have a finite number of known water-cut values f_i , it is natural to consider some kind of piecewise interpolation. Cubic splines are the most common interpolation procedure for fitting approximating polynomials to data, since they are a good compromise between accuracy and complexity. Suppose we have a table of data points on an interval $[0, T]$.

x	t_0	t_1	t_2	\cdots	t_n
y	f_0	f_1	f_2	\cdots	0

Table 8.1: Data points.

Using these values, we can to obtain a set of n piecewise cubic polynomial of the form,

$$m_i(t) = a_i + b_it + c_it^2 + d_it^3, \quad t_i \leq t \leq t_{i+1} \quad (8.4.1)$$

for $i = 0, 1, 2, \dots, n$ and $0 = t_0 < t_1 < t_2 \dots t_{n-1} < t_n = T$. The t_i are called **knots**. References van der Hoek and Elliot [165] Annex F or Hoffman [73] chapter four provide information on how this system is obtained. As an example, consider the following data points in Table (8.2).

A natural cubic spline is:

$$3.3 - 20.2x + 45.x^2 - 30x^3 \quad \text{on } [0.5, 0.6) \quad (8.4.2)$$

$$-8.58 + 39.2x - 54.x^2 + 25.x^3 \quad \text{on } [0.6, 0.7) \quad (8.4.3)$$

$$-1.72 + 9.8x - 12.x^2 + 5.x^3 \quad \text{on } [0.7, 0.8] \quad (8.4.4)$$

x	0.5	0.6	0.7	0.8
y	0.7	0.9	0.975	1

Table 8.2: Example.

Substituting the spline form of the flux function into the expression (8.4.1), gives a piecewise production curve.

$$P(x) = \begin{cases} \frac{-0.0193333+0.2x-0.7x^2+0.666667x^3}{0.224444-x+x^2} & \text{on } [0.5, 0.6) \\ \frac{1.74+21.6x-69.x^2+50x^3}{39.2-108x+75.x^2} & \text{on } [0.6, 0.7) \\ \frac{0.76+4.8x-15x^2+10x^3}{9.8-24x+15x^2} & \text{on } [0.7, 0.8] \end{cases}$$

We are now in a position to find an expression for the inverse of the production function. Ordinarily, this function would not be invertible, but using the piecewise representation we have chosen, the problem of finding an inverse reduces to solving a cubic. The production function is given by (8.4.1). If the flux function is represented by a cubic spline, then on a given interval, (8.4.1) will take the form,

$$P(S_L) = S_L - S_c + \frac{1 - (aS_L^3 + bS_L^2 + cS_L + d)}{3aS_L^2 + 2bS_L + c} \quad (8.4.5)$$

This can be re-arranged to give the cubic

$$S_L^3 + \frac{S_L^2}{2} \left(\frac{b}{a} - 3P - 3S_c \right) + S_L \left(-\frac{bp}{a} - \frac{bS_c}{a} \right) + \frac{1}{2a} (1 - d - cP - cS_c) = 0 \quad (8.4.6)$$

This equation is invertible (although possibly only on a restricted domain) since closed form solutions of the cubic equation exist. The interested reader is referred to Oldham and Spanier [127] or Abramowitz and Stegun [1]. The formulas are significantly more complex than for the quadratic case. Solutions may be all real and distinct, repeated, or one real and a pair of complex conjugates may exist. Alternatively, the *Lagrange* Inversion Theorem could be used directly on (8.4.6). This theorem gives the inverse of any function that can be represented by a Taylor Series. This theorem can be found in Markushevich⁴, Whittaker and Watson [172] or Kranz [93]. Whichever method is used, the inverse piecewise cubic function for P can be obtained. Having obtained the inverse, we can use mathematical expectation to find the distribution of (8.4.1). This technique has been used many times already

⁴Markushevich [111] vol. 2, page 86.

in this thesis and there is no need to repeat it here. Stochastic splines are gaining traction within the study of interest rate models, and it appears such methods might be useful in examining the recovery equation.

8.5 Concluding Comments

In the Forward to Bedrikovetsky [14], which is a book that deals entirely with analytical models, Professor John Archer writes: *“the appropriateness of particular representations of relative permeability relationships and partition coefficients are not the primary concern. Rather, it is the way such information could be used, if it were available, that is of importance in this analytical mathematical approach.”* While we accept that accurately specifying the nature and level of variation and error is still an open issue, we are permitted to hope that this will become a better defined quantity in the future.

Since the paper by Holden and Risebro [75], it is unfortunate that the study of the stochastic Buckley-Leverett equation has not been taken up by a larger number of researchers. The problem is evidently difficult, but it is an interesting problem that is becoming more relevant by the day with the ever increasing dependence on enhanced oil recovery to meet the worlds energy needs. It is unquestionably a problem worthy of further consideration.

Appendix A

Properties of the Normal and Log-Normal Distribution

The standard results found in this annex are drawn from Patel, Kapadia and Owen, *Handbook of Statistical Distributions* [132] and *Handbook of the Normal Distribution* [133].

The **normal distribution** with mean μ and variance σ^2 is a continuous probability distribution with unbounded support in \Re that has a probability density function given by,

$$f(x)_{\mu,\sigma^2} = \frac{1}{\sigma\sqrt{2\pi}} \exp\left(-\frac{(x-\mu)^2}{2\sigma^2}\right) \quad (\text{A.0.1})$$

The median and mode are also μ . The cumulative density function is given by,

$$\Phi(x)_{\mu,\sigma^2} = \frac{1}{\sigma\sqrt{2\pi}} \int_{-\infty}^x \exp\left(-\frac{(z-\mu)^2}{2\sigma^2}\right) dz \quad (\text{A.0.2})$$

$$= \frac{1}{2} \left\{ 1 + \operatorname{erf}\left(\frac{x-\mu}{\sigma\sqrt{2}}\right) \right\} \quad (\text{A.0.3})$$

The error function **erf** must be calculated numerically or approximated. For example, it can be defined by the Maclaurin series,

$$\operatorname{erf}(x) = \frac{2}{\pi} \sum_{k=0}^{\infty} \frac{(-1)^k x^{2k+1}}{k!(2k+1)} \quad (\text{A.0.4})$$

The moment generating function is,

$$M_X(t) = E[\exp(tX)] \quad (\text{A.0.5})$$

$$= \exp\left(\mu t + \frac{t^2 \sigma^2}{2}\right) \quad (\text{A.0.6})$$

The **lognormal distribution** is the probability distribution of the random variable Y whose logarithm is normally distributed. That is to say, $Y = \exp(X)$, where X is a normally distributed random variable. The lognormal distribution is single tailed, with support in \mathfrak{R}^+ . The probability density function is given by,

$$f(x)_{\mu, \sigma^2} = \frac{1}{x\sigma\sqrt{2\pi}} \exp\left(-\frac{(\ln(x) - \mu)^2}{2\sigma^2}\right) \quad (\text{A.0.7})$$

where μ and σ^2 are the mean and variance of the random variable that is the logarithm of Y . The mean, median and mode of the lognormal distribution are $\exp(\mu + \sigma^2/2)$, $\exp(\mu)$ and $\exp(\mu - \sigma^2)$ respectively. The variance is $(\exp(\sigma^2) - 1) \exp(2\mu + \sigma^2)$ and the cumulative distribution function is,

$$\Phi(x)_{\mu, \sigma^2} = \frac{1}{2} \left\{ 1 + \operatorname{erf}\left(\frac{\ln(x) - \mu}{\sigma\sqrt{2}}\right) \right\} \quad (\text{A.0.8})$$

The moment generating function for the lognormal distribution does not exist.

Appendix B

Geometric Method for Finding Average Saturation

This Appendix follows directly from section 7.3. This is standard material within petroleum engineering ([2] [39] [38] [44] [67] [96] [164]) and is included here for completeness. From the end at which water is injected, at $x = 0$, to the position of the shock front saturation, x_2 , the injected water volume is proportional to the difference between the average saturation and the initial water saturation in the porous medium. That is,

$$Q_i = x_2 A \phi (\bar{S} - S_c) \quad (\text{B.0.1})$$

or by rearranging,

$$\frac{x_2 A \phi}{Q_i} = \frac{1}{\bar{S} - S_c} \quad (\text{B.0.2})$$

Re-arranging (7.3.5)

$$\frac{df(S^*)}{dS} = \frac{(1 - f(S^*))}{\bar{S} - S^*} \quad (\text{B.0.3})$$

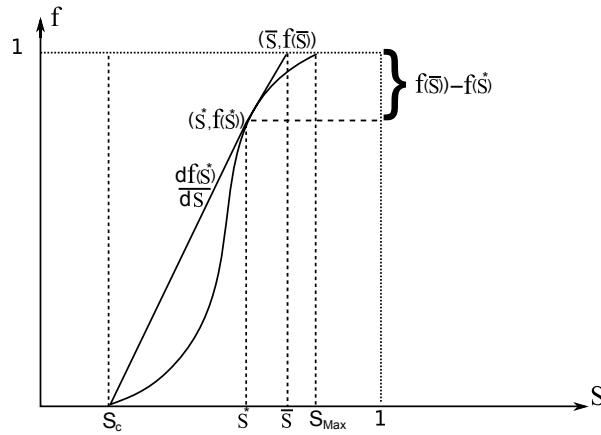
Recall that (7.3.9) gave,

$$\frac{x_2 A \phi}{Q_i} = \frac{df(S^*)}{dS} \quad (\text{B.0.4})$$

Combining (B.0.3), (B.0.2) and (B.0.4) results in,

$$\frac{1}{\bar{S} - S_c} = \frac{1 - f(S^*)}{\bar{S} - S^*} = \frac{df(S^*)}{dS} \quad (\text{B.0.5})$$

What does this mean? The implication is readily seen by considering the following diagram, where the different terms have been marked.



Each term in (B.0.5) is the slope of the same line, calculated as the derivative of f at S^* and over the intervals $\bar{S} - S_c$ and $\bar{S} - S^*$. To find the average water saturation \bar{S} , we simply continue the tangent line at S^* from S_c to the horizontal line $f(S) = 1$. However, for recovery calculation, (7.3.5) is generally used.

Bibliography

- [1] M Abramowitz and I. Stegun, *Handbook of mathematical functions: with formulas, graphs, and mathematical tables*, Dover Publications, 1965.
- [2] T. Ahmed, *Reservoir engineering handbook*, Gulf Professional Publishing, United Kingdom, 2006.
- [3] S. Akin, L. M. Castanier, and W. E. Brigham, *Effect of temperature on heavy-oil/water relative permeabilities*, SPE 49021, presented at the Annual Technical Conference and Exhibition, New Orleans LA, 27-30 September, 1998.
- [4] F. O. Alpak, L. W. Lake, and S. M. Embid, *Validation of a modified Carman-Kozeny equation to model two-phase relative permeabilities*, SPE 56479, presented at the Annual Technical Conference and Exhibition, Houston, 3-6 October, 1999.
- [5] J. Amaefule, M. Altunbay, D. Tiab, D Kersey, and D. Keelan, *Enhanced reservoir description: Using core and log data to identify hydraulic (flow) units and predict permeability in uncored intervals/wells*, SPE 26436, presented at the Annual Technical Conference Exhibition, Houston, 1993.
- [6] J. O. Amaefule, A. Ajufu, E. Peterson, and K. Durst, *Understanding formation damage processes: an essential ingredient for improved mea-*

- surement and interpretation of relative permeability data*, SPE 16232, presented as the Production Operation Symposium, 1986.
- [7] E. Amott, *Observations relating to the wettability of porous rocks*, Trans. AIME **216** (1959), 156.
- [8] A. Amyx, D. Bass, and R. Whiting, *Petroleum reservoir engineering*, McGraw-Hill, New York, 1960.
- [9] W. G. Anderson, *Wettability literature survey - part 5: the effect of wettability on relative permeability*, J. Pet. Technol. (1987), 1453.
- [10] J. Arps and T. Roberts, *The effect of the relative permeability ration, the oil gravity, and the solution gas-oil ratio on the primary recovery from depletion type reservoirs*, Trans. AIME **204** (1955), 120.
- [11] Y. Bachmat and J. Bear, *Macroscopic modelling of transport phenomena in porous media 1: the continuum approach*, Trans. Porous Media **1**, 213.
- [12] P. E. Baker, *Discussion of effect of viscosity ratio on relative permeability*, J. Pet. Technol. **219** (1960), 65.
- [13] J. Bear, *Dynamics of fluids in porous media*, Environmental Science Series. Elsevier, New York, 1972.
- [14] P. Bedrikovetsky, *Mathematical theory of oil and gas recovery*, Kluwer Academic Publishers, 1993.
- [15] P. Behrenbruch and H. M. Goda, *Two-phase relative permeability prediction: A comparison of the modified Brooks-Corey methodology with a new Carman-Kozeny based flow simulation*, SPE 101150, presented at the Asia Pacific Oil and Gas Conference and Exhibition, Adelaide Australia, 11-13 September, 2006.

- [16] A. Bensoussan and Glowinsk R., *Approximation of some stochastic differential equations by the splitting up method*, Appl. Math. Optim. **25** (1992), no. 1, 81.
- [17] F Black and M. Scholes, *The pricing of options and corporate liabilities*, Journal of Political Economy **81** (3) (1973), 637.
- [18] H. G. Botset, *Flow of gas-liquid mixtures through consolidated sands*, Trans. AIME **136** (1940), 91.
- [19] H. B. Bradley, *Petroleum engineering handbook*, Society of Petroleum Engineers, 1987.
- [20] R. H. Brooks and A. T. Corey, *Hydraulic properties of porous media*, Hydrology Papers, Colorado State University, Fort Collins, Colo., 1964.
- [21] R. J. S. Brown and I Fatt, *Measurements of fractional wettability of oil field rocks by the nuclear magnetic relaxation method*, Trans. AIME **207** (1956), 262.
- [22] E. Buckingham, *Studies on the movement of soil moisture*, USDA Bureau of Soils Bul. **38** (1907), 61.
- [23] S.E. Buckley and M. C. Leverett, *Mechanism of fluid displacement in sands*, Petrol. Trans. AIME **146** (1942), 107.
- [24] A. Bulnes and R. Fitting, *An introductory discussion of reservoir performance of limestone transformations*, Trans. AIME **160** (1945), 179.
- [25] N.T. Burdine, *Relative permeability calculations from pore size distribution data*, Trans. AIME **198** (1953), 71.
- [26] M. R. Carlson, *Simulation of relative permeability hysteresis to the non-wetting phase*, SPE paper 10157, presented at the Annual Technical Conference and Exhibition, San Antonio, Texas, 5-7 October, 1981.

- [27] ———, *Practical reservoir simulation: using, assessing and developing results*, PennWell, 2003.
- [28] P. C. Carman, *Fluid flow through granular beds*, AICHE **15** (1937), 150.
- [29] B. H. Caudle, R. L. Slobod, and E. R. Brownscombe, *Further developments in the laboratory determination of relative permeability*, Trans. AIME **192** (1951), 145.
- [30] R. E. Chapman, *Physics for geologists*, second ed., CRC Press, Boca Raton, 2002.
- [31] G. L. Chierici, *Novel relations for drainage and imbibition relative permeabilities*, Soc. Pet. Eng. J. **Jun** (1984), 275.
- [32] R. L. Christiansen, *Petroleum engineering handbook - volume I, general engineering*, ch. Annex I, Relative Permeability and Capillary Pressure, Society of Petroleum Engineers, 2006.
- [33] J. D. Cole, *On a quasilinear parabolic equation occurring in aerodynamics*, Quart. Appl. Math. **9** (1951), 225.
- [34] R. E. Collins, *Flow of fluids through porous materials*, Reinhold Publishing Corporation, New York, 1961.
- [35] A. Corey and C. Rathjens, *Effect of stratification on relative permeability*, Trans. AIME **207** (1956), 69.
- [36] R. Courant and K. O. Friedrichs, *Supersonic flow and shock waves*, Wiley-Interscience, New York, 1948.
- [37] P. L. Coyne, *20 years of laboratory oil-water relative permeability data in the malay basin*, SPE paper 64375, prepared for presentation at the Asia Pacific Oil and Gas Conference and Exhibition in Brisbane, Australia, 16-18 October, 2000.

- [38] B. C. Craft and M. F. Hawkins, *Applied petroleum reservoir engineering*, second ed., Prentice Hall, 1991.
- [39] F. F. Craig, *Reservoir engineering aspects of waterflooding*, H. L. Doherty Memorial Fund of AIME, 1971.
- [40] L. E. Cuiec, *Restoration of the natural state of core samples*, SPE 5634, presented at the Fall Meeting, 28 September-1 October, Dallas, Texas, 1975.
- [41] C. M. Dafermos, *Polygonal approximations of solutions of the initial value problem for a conservation law*, J. Math. Anal. Appl. **38** (1972), 33.
- [42] ———, *Hyperbolic conservation laws in continuum physics*, second ed., Springer-Verlag, 2005.
- [43] L. Dake, *The practice of reservoir engineering*, revised ed., Elsevier, North Holland, 2001.
- [44] L. P. Dake, *Fundamentals of reservoir engineering*, Elsevier, Amsterdam, 1978.
- [45] A. Y. Dandekar, *Petroleum reservoir rock and fluid properties*, CRC Press, Boca Raton, 2006.
- [46] H. Darcy, *Les fontaines publique de la ville de dijon*, Dalmont, Paris, 1856.
- [47] L. B. Davidson, *The effect of temperature on the permeability ratio of different fluid pairs in two phase systems*, J. Pet. Technpl. **8** (1969), 1037.
- [48] C. G. Dodd and O. G. Kiel, *Evaluation of Monte Carlo methods in studying fluid-fluid displacement and wettability in porous rocks.*, J. Phys. Chem. **63** (1959), 1646.

- [49] E. C. Donaldson and R. D. Thomas, *Microscopic observations of oil displacement in water-wet and oil-wet systems.*, SPE paper 3555, presented at the Annual Meetings, New Orleans, LA., 1971.
- [50] E. C. Donaldson, R. D. Thomas, and P. B. Lorenz, *Wettability determination and its effect on recovery efficiency*, Soc. Pet. Eng. J. (1969), 13.
- [51] J. Downie and F. E. Crane, *Effects of viscosity on relative permeability*, Soc. Pet. Eng. J. **6** (1961), 59.
- [52] N.R. Draper and S. Smith, *Applied regression analysis*, John Wiley & Sons, Inc., 1998.
- [53] F. A. L. Dullien, *Porous media fluid transport and pore structure*, Academic Press, New York, 1979.
- [54] T. A. Edmondson, *Effect of temperature on waterflooding.*, Can. J. Pet. Technol. **10** (1965), 236.
- [55] L. C. Evans, *Partial differential equations*, Graduate Studies in Mathematics, vol. 19, American Mathematical Society, 1998.
- [56] J. R. Fanchi, *Principles of applied reservoir simulation*, Gulf Publishing Company, USA, 1997.
- [57] I. Fatt, *The effect of overburden pressure on relative permeability*, Trans. AIME **198** (1953), 325.
- [58] ———, *Network models of porous media*, Trans. AIME **207** (1956), 164.
- [59] I. Fatt and D. H. Davis, *Reduction in permeability with overburden pressure*, Trans. AIME **195** (1952), 329.
- [60] I. Fatt and H. Dykstra, *Relative permeability studies*, Trans. AIME **192** (1951), 249.

- [61] T. C. Frick (ed.), *Petroleum production handbook*, vol. 2, McGraw-Hill Book Company, USA, 1962.
- [62] R. A. Fulcher, T. Ertekin, and C. D. Stahl, *Effect of capillary number and its constituents on two-phase relative permeability curves*, Journal of Petroleum Technology **Feb** (1985), 249.
- [63] W. Gardner, O Israelsen, N Edlefsen, and D Clyde, *The capillary potential function and its relation to irrigation practice*, Phys. Rev. **20** (1922), 196.
- [64] J. I. Gates and W. T. Lietz, *Relative permeabilities of Californian cores by the capillary-pressure method*, Drilling and Production Practices., American Petroleum Institute, 1950.
- [65] T. M. Geffen, D. R. Parish, and G. W Morse, R. A. and Hayes, *Efficiency of gas displacement from porous media by liquid flooding*, Trans. AIME **195** (1952), 29.
- [66] R. L. Gorring, *Multiphase flow of immiscible fluids in porous media*, Ph.D. thesis, University of Michigan, Ann Arbour, 1962.
- [67] D. W. Green and P. G. Willhite, *Enhanced oil recovery*, Society of Petroleum Engineers Textbook Series, 1998.
- [68] A. K. Gupta and S. Nadarajah, *Handbook of beta distribution and its applications*, Marcel Dekker, Inc, 2004.
- [69] R. E. Guzmán and F. Fayers, *Solutions to the three-phase Buckley-Leverett problem*, Soc. Pet. Eng. J. **2** (1997), 301–311.
- [70] M. Hassanizadeh and W. Gray, *General conservation equations for multiphase systems: 1. averaging procedure.*, Adv. Water Resour. **2** (1979), no. 3, 131.

- [71] G. L. Hassler, R. R. Rice, and E. H. Leeman, *Investigation on the recovery of oil from sandstone by gas-drive*, Trans. AIME **118** (1936), 116.
- [72] J. H. Henderson and S. T. Yuster, *Relative permeability study*, World Oil **3** (1948), 139.
- [73] J. D. Hoffman, *Numerical methods for engineers and scientists*, Marcel Dekker, Inc., 2001.
- [74] H. Holden, L. Holden, and R. Høegh-Krohn, *A numerical method for first order nonlinear scalar conservation laws in one-dimension*, Comput. Math. Appl. **15** (1988), 595.
- [75] H. Holden and N. H. Risebro, *Stochastic properties of the scalar Buckley-Leverett equation*, SIAM J. Appl. Math. **51** (1991), no. 5, 1472.
- [76] ———, *Conservation laws with a random source*, Appl. Math. Optim. **36** (1997), no. 2, 229.
- [77] ———, *Front tracking for hyperbolic conservation laws*, Springer-Verlag, 2002.
- [78] L. Holden, *The Buckley-Leverett equation with spatially stochastic flux function*, SIAM J. Appl. Math. **57** (1997), no. 5, 1443.
- [79] M. Honarpour, L. Koederitz, and A. H. Harvey, *Empirical equations for estimating two-phase relative permeability in consolidated rock*, Journal of Petroleum Technology **Dec** (1982), 2905.
- [80] ———, *Relative permeability of petroleum reservoirs*, CRC Press, Inc., Boca Raton, 1986.
- [81] E. Hopf, *The partial differential equation $u_t + uu_x = \nu u_{xx}$* , Commun. Pure Appl. Math. **3** (1950), 201.

- [82] J. D. Huppler, *Numerical investigation of the effect of core heterogeneity on waterflood relative permeability*, Soc. Pet. Eng. J. **10** (1970), 381.
- [83] F. John, *Partial differential equations*, fourth ed., Applied Mathematical Sciences, vol. 1, Springer-Verlag, New York, 1991.
- [84] C. E. Johnson and S. A. Sweeney, *Quantitative measurements of flow heterogeneity in laboratory core samples and its effect on fluid flow characteristics*, SPE 3610, presented at the SPE 46th Annual Meeting, New Orleans., 1971.
- [85] V. A. Josendale, B. B. Sandford, and J. W. Wilson, *Improved multiphase flow studies employing radioactive tracers*, Trans. AIME **216** (1959), 65.
- [86] E. F. Kaasschieter, *Solving the Buckley-Leverett equation with gravity in a heterogeneous porous medium*, Comput. Geosci. **3** (1999), no. 1, 23.
- [87] I. Karatzas and S. Shreve, *Brownian motion and stochastic calculus*, Springer, 2nd edition, 2008.
- [88] J. H. Killough, *Reservoir simulation with history-dependant saturation functions*, Soc. Pet. Eng. J. **Feb** (1976).
- [89] M. F. King, *Numerical simulation in oil recovery*, ch. Viscous fingering and probabalistic suimulation, p. 161, Springer-Verlag, Berlin, New York, 1988.
- [90] M. F. King and H. Scher, *Probability approach to multiphase and multicomponent fluid flow in porous media*, Phys. Rev. A **35** (1987), 929.
- [91] S. Kotz and J. van Dorp, *Beyond beta: Other continuous distributions with bounded support and applications*, World Scientific Publishing, 2004.

- [92] J. Kozeny, *Über kapillare leitung des wasser im boden sitzungberichte*, Royal Academy of Science, Vienna (1927).
- [93] S. G. Krantz and H. R. Parkes, *The implicit function theorem: History, theory and applications*, second ed., Birkhäuser Boston, 2003.
- [94] W. C. Krumbein and G. D. Monk, *Permeability as a function of the size parameters of unconsolidated sands*, Trans. AIME **151** (1943), 153.
- [95] J. R. Kyte, V. O. Naumann, and C. C. Mattax, *Effect of reservoir environment on water-oil displacement*, J. Pet. Technol. **6** (1961), 579.
- [96] L. W. Lake, *Enhanced oil recovery*, Prentice-Hall, Englewood Cliffs, NY, 1989.
- [97] L. W. Lake and J. R. Franchi (eds.), *Petroleum engineering handbook volume 1: General engineering*, Society of Petroleum Engineers, 2006.
- [98] C. S. Land, *Calculation of imbibition relative permeability for two- and three-phase flow from rock properties*, Soc. Pet. Eng. J. **6** (1968), 149.
- [99] ———, *Comparison of calculated with experimental imbibition imbibition relative permeability*, Trans. AIME **251** (1971), 419.
- [100] M. Latil, *Enhanced oil recovery*, Editions Technip, Paris, 1980.
- [101] P. D. Lax, *Weak solutions of nonlinear hyperbolic equations and their numerical computation*, Comm. Pure Appl. Math. **7** (1954), 159.
- [102] ———, *Hyperbolic systems of conservation laws*, Comm. Pure. Appl. Math. **10** (1957), 537.
- [103] ———, *Hyperbolic systems of conservation laws and the mathematical theory of shock waves*, CBMS Regional Conference Series in Mathematics No. 11. Philadelphia. SIAM, 1973.
- [104] R. J. LeVeque, *Numerical methods for conservation laws*, second ed., Lectures in Mathematics ETH Zürich, Birkhäuser Verlag, Basel, 1992.

- [105] M. C. Leverett, *Flow of oil-water mixtures through unconsolidated sands*, Trans. AIME **132** (1939), 149.
- [106] M. C. Leverett and W. B. Lewis, *Steady flow of gas-oil water mixtures through unconsolidated sands*, Trans. AIME **142** (1941), 107.
- [107] J. S. Levine, *Displacement experiments in consolidated porous systems*, Trans. AIME **201** (1954), 57.
- [108] K. Lie and R. Juanes, *A front-tracking method for the simulation of three-phase flow in porous media*, Transport in Porous Media **55** (2004), 47.
- [109] P. B. Lorenz, E. C. Donaldson, and R. D. Thomas, *The effect of viscosity and wettability on oil water relative permeability*, Paper SPE 1562, presented at the SPE annual conference, Dallas, Oct 2-5, 1966.
- [110] S. Ma, N. R. Morrow, and X. Zhang, *Characterization of wettability from spontaneous imbibition measurements*, J. Can. Petrol. Tech. (Special Edition) **38** (1999), no. 13, 56.
- [111] A.I. Markushevish, *Theory of functions of a complex variable*, trans. silverman, r. a. second english edition ed., Chelsea Publishing Company, New York, N.Y., 1977.
- [112] C. M. Marle, *Multiphase flow in porous media*, Editions Technip, Paris, 1981.
- [113] G. Matheron, *Eléments pour une théorie des milieux poreux*, Masson, Paris, 1967.
- [114] J. W. McGhee, M. E. Crocker, and E. C. Donaldson, *Relative wetting properties of crude oils in berea sandstones*, Tech. Report BETC/RI-79/9, Natl. Tech. Inf. Sv, U.S. Dept. Energy, Springfield VA, Jan, 1979.

- [115] M. N. Mohamad Ibrahim and L. F. Koederitz, *Two-phase relative permeability prediction using a linear regression model*, SPE paper 65631, presented at the 2000 SPE Eastern Regional Meeting, Morgantown, West Virginia, 17-19 October, 2000.
- [116] T. J. Morgan and D. T. Gordon, *Influence of pore geometry on water-oil relative permeability*, J. Pet. Technol. **1199** (1970), 407.
- [117] N. R. Morrow, C. P. Cram, and F. G. McCaffery, *Displacement studies in dolomite with wettability controlled by octanoic acid*, Soc. Pet. Eng. J. (1973), 221.
- [118] P. M. Morse and H. Feshbach, *Methods of theoretical physics*, international student ed., vol. 1, McGraw Hill Book Company, 1953.
- [119] N. Mugen, *Relative permeability measurements using reservoir fluids*, SPE Journal of Petroleum Technology **Oct** (1972), 398.
- [120] M. Muskat, *Physical principles of oil production*, McGraw-Hill, New York, 1949.
- [121] M. Muskat and M. W. Meres, *The flow of heterogeneous fluids through porous media*, Physics **7** (1936), 346.
- [122] J. Naar and J. H. Henderson, *An imbibition model - its application to flow behavior and the prediction of oil recovery*, SPEJ **Jun** (1961), 61.
- [123] J. Naar, R. Wygal, and J. Henderson, *Imbibition relative permeability in unconsolidated porous media*, Trans. AIME **225** (1962), 13.
- [124] T. Nind, *Principles of oil production*, McGraw Hill, New York, 1964.
- [125] A. S. Odeh, *Effects of viscosity ratio on relative permeability*, Trans. AIME **216** (1959), 346.
- [126] B. Øksendal, *Stochastic differential equations: an introduction with applications*, sixth ed., Universitext, Springer-Verlag, Berlin, 2007.

- [127] K. B. Oldham and J. Spanier, *An atlas of functions*, second ed., Springer, 1996.
- [128] O. Oleinik, *Discontinuous solutions of non-linear differential equations*, Amer. Math. Soc. Transl. **26** (1963), 95.
- [129] J. S. Osoba, J. G. Richardson, J. K. Kerver, and J.A. Hafford, *Laboratory measurements of relative permeability*, Trans. AIME **192** (1951), 47.
- [130] W. W. Owen, T. M. Geffen, D. R. Parish, and R. A. Morse, *Experimental investigation of factors affecting laboratory relative permeability measurements*, Trans. AIME **192** (1951).
- [131] W. W. Owens and D. Archer, *The effect of rock wettability on oil-water relative permeability relationships*, Trans. AIME **251** (1971), 873.
- [132] J. Patel, C. H. Kapadia, and D. B. Owen, *Handbook of statistical distributions*, Marcel Decker, Inc. New York, 1976.
- [133] ———, *Handbook of the normal distribution*, Marcel Decker, Inc. New York, 1982.
- [134] P. Pathak, O. G. Kiel, and L. E. Scriven, *Dependence of residual non-wetting liquid on pore topology*, SPE 11016, presented at the 57th Annual Fall Meeting, New Orleans, 1982.
- [135] G. Paul Willhite, *Waterflooding*, Society of Petroleum Engineers, 1986.
- [136] J. Paulya, J. Daridon, and J. Coutinho, *Measurement and prediction of temperature and pressure effect on wax content in a partially frozen paraffinic system*, Fluid Phase Equilibria **187** (2001), 71.
- [137] D. W. Peaceman, *Fundamentals of numerical reservoir simulation*, Developments in Petroleum Science, vol. 6, Elsevier, Amsterdam, 1977.
- [138] S. J. Pirson (ed.), *Oil reservoir engineering*, McGraw-Hill, 1958.

- [139] S. W. Poston, S. Ysrael, A. K. Hossain, E. F. Montgomery, and H. R. Ramey, *The effect of temperature on irreducible water saturation and relative permeability of unconsolidated sands*, Soc. Pet. Eng. J. **6** (1970), 171.
- [140] W. R. Purcell, *Capillary pressures - their measures using mercury and calculation of permeability therefrom*, Trans. AIME **186** (1949), 39.
- [141] L. A. Rapoport and W. J. Leas, *Properties of linear waterfloods*, Trans. AIME **198** (1953), 139.
- [142] L. A. Richards, *Capillary conduction of liquids through porous mediums*, Physics **1** (1931), 318.
- [143] J. G. Richardson, *Calculation of waterflood recovery from steady-state relative permeability data*, Trans. AIME **210** (1957), 373.
- [144] J. G. Richardson, J. K. Kerver, J. A. Hafford, and J. S. Osoba, *Laboratory determination of relative permeability*, Trans. AIME **195** (1952).
- [145] C. Schmidt, *The wettability of petroleum rocks and the results of experiments to study the effects of variations in the wettability of core samples*, Erdoel und Hohl-Redgas-Petrochemie **17** (1964), no. 8, 605.
- [146] Z. She, E. Aurell, and U. Frisch, *The inviscid Burgers equation with initial data of Brownian type*, Comm. Math. Phys. **148** (1992), no. 3, 623.
- [147] A. N. Shiriyayev, *Probability*, Springer-Verlag, New York Inc, 1984.
- [148] S. Siddiqui, P. Hicks, and T. Ertekin, *Two-phase relative permeability models in reservoir engineering calculations*, Energy Sources **21** (1999), 145.
- [149] Y. G. Sinai, *Statistics of shocks in solutions of inviscid Burgers equation*, Comm. Math. Phys. **148** (1992), no. 3, 601.

- [150] A. A. Sinnokrot, H. J. Ramey, and S. S. Marsden, *Effect of temperature level upon capillary pressure curves*, Soc. Pet. Eng. J. **3** (1971), 13.
- [151] J. Smoller, *Shock waves and reaction-diffusion equations*, second ed., Springer-Verlag, New York, 1994.
- [152] G. Sposito, *The statistical mechanical theory of water transport through unsaturated soil 1: the conservation laws*, Water Resour. Res. **14**, no. 3, 474.
- [153] H. Stone, *Probability models for estimating three-phase relative permeability*, Trans. AIME **249** (1970), 214.
- [154] T. M. Tao and A. T. Watson, *Accuracy of JBN estimates of relative permeability: Part 1-algorithms*, Soc. Pet. Eng. J. **Apr** (1984), 215.
- [155] ———, *Accuracy of JBN estimates of relative permeability: Part 1-error analysis*, Soc. Pet. Eng. J. **Apr** (1984), 209.
- [156] M. E. Taylor, *Partial differential equations III: non-linear equations*, Springer-Verlag, 1996.
- [157] I. E. Terez and A. Firoozabadi, *Water injection in water-wet fractured porous media: Experiments and a new model with modified buckley-leverett theory*, Soc. Pet. Eng. J. **4** (1999), 134.
- [158] P. L. Terwilliger, L. E. Wilsey, H. N. Hall, P. M. Bridges, and R. A. Morse, *Experimental and theoretical investigation of gravity drainage performance*, Trans. AIME **192** (1951), 285.
- [159] P. L. Terwilliger, S. T. Yuster, and R. A. Morse, *Relative permeability measurements on small core samples*, Oil Gas J. **46** (1947), 109.
- [160] J. W. Thomas, *Numerical partial differential equations: finite difference methods*, Texts in Applied Mathematics, Springer-Verlag, New York, 1995.

- [161] D. Tiab and E. C. Donaldson, *Petrophysics: theory and practice of measuring reservoir rock and fluid transport properties*, second ed., Gulf Professional Publishing, UK, 2004.
- [162] E. H. Timmerman, *Practical reservoir engineering, part i*, Penwell, Tulsa, OK, 1982.
- [163] C. B. Tjølsen, E. Damsleth, and T. Bu, *Stochastic relative permeabilities usually have neglectable effect on reservoir performance*, (1993).
- [164] B. F. Towler, *Fundamental principles of reservoir engineering*, Society of Petroleum Engineers Textbook Series, 2002.
- [165] J. van der Hoek and R. J. Elliot, *Binomial models in finance*, Springer Science and Business Media, Inc., New York, 2006.
- [166] J. Wehr and J. Xin, *White noise perturbation of the viscous shock fronts of the Burgers equation*, Comm. Math. Phys. **181** (1996), no. 1, 183.
- [167] ———, *Front speed in the Burgers equation with a random flux*, J. Statist. Phys. **88** (1997), no. 3-4, 843.
- [168] R. M. Weinbrandt, H. J. Ramey, and F. J. Casse, *The effect of temperature on relative and absolute permeability of sandstones*, Soc. Pet. Eng. J. **10** (1975), 376.
- [169] H. G. Welge, *A simplified method for computing oil recovery by gas or water drive*, Petrol. Trans. AIME **195** (1952), 91.
- [170] S. Whitaker, *Flow through porous media*, p. 35, Amer. Chem. Soc., 1970.
- [171] G. B. Whitham, *Linear and nonlinear waves*, Pure and Applied Mathematics (New York), John Wiley and Sons Inc., New York, 1999.
- [172] E. T. Whittaker and G. N. Watson, *A course of modern analysis*, third ed., Cambridge at the University Press, 1920.

- [173] J. W. Wilson, *Determination of relative permeability under simulated reservoir conditions*, AIChE J. **2**(1) (1956), 94.
- [174] R. D. Wyckoff and H. G. Bosset, *Flow of gas-liquid mixtures through sands*, Physics **7** (1936), 325.
- [175] M. R. Wyllie, *Interrelationships between wetting and non-wetting phase relative permeability*, Trans. AIME **192** (1951), 381.
- [176] M. R. J. Wyllie and G. H. F. Gardner, *The generalized Kozeny-Carman equation: its application to problems of multiphase flow in porous media*, World Oil **Mar-Apr** (1958), 210.
- [177] S. T. Yuster, *Theoretical considerations of multiphase flow in idealized capillary systems*, Proceedings of the Third World Petroleum Congress, Hague, Netherlands **2** (1951), 437.